

## Contents

- Introduction
- Basics
- Synthesis of Nano Materials
- Fabrication of Nano Structure
- Nano Characterization
- Properties and Applications

## 3-1. Synthesis of Nanomaterials in Liquid Media

### □ 0-Dimensional nanomaterials

- (a) Metal nanoparticles
- (b) Semiconductor nanoparticles
- (c) Metal oxides nanoparticles
- (d) Polymeric nanoparticles
- (e) Kinetic confinement

### □ 1-Dimensional nanomaterials

- (a) Dissolution and condensation
- (b) Solution-Liquid-Solid
- (c) Template-based
- (d) Self-assembly
- (e) Electrospinning

### □ 2-Dimensional nanomaterials

- (a) Self-assembly
- (b) Langmuir-Blodgett films
- (c) Electrochemical deposition
- (d) Sol-gel films

# Synthesis of Nano Materials- 0D from liquid (Metal)

## □ Homogeneous Nucleation & Growth

### - Chemical Reductions:

ex1) HAuCl<sub>4</sub> (Chloroauric acid) + Na<sub>3</sub>C<sub>6</sub>H<sub>5</sub>O<sub>7</sub> (sodium citrate) in water at 100 °C  
→ Au nanoparticles (3 ~ 10 nm)

ex2) AgNO<sub>3</sub> in ethylene glycol at 150 °C with PVP → Ag nanoparticles or wires

ex3) RhCl<sub>3</sub> (Rhodium chloride) + methanol + water + PVA (polyvinylalcohol) at 80 °C  
→ Rh nanoparticles (<~5 nm)

ex4) H<sub>2</sub>PtCl<sub>6</sub> + Na<sub>3</sub>C<sub>6</sub>H<sub>5</sub>O<sub>7</sub> in water at 100 °C → 2.5 nm Pt nanoparticles

ex5) Most metal precursors in ethylene glycol at 150 °C → nanoparticles (Polyol Process)

### - Photochemical Reductions:

ex1) AgNO<sub>3</sub> + UV irradiation + ethanol → Ag nanoparticles

ex2) AgClO<sub>4</sub> + UV irradiation + acetone + isopropyl alcohol → Ag nanoparticles

### - Sonochemical Reduction:

ex 1) AgNO<sub>3</sub> + ultrasonication → Hydrogen radical formation → AgNO<sub>3</sub> reduction to Ag NPs

# Synthesis of Nano Materials- 0D from liquid (Metal)

## □ Chemical Reduction

- low concentration of solute and polymeric monolayer- diffusion controlled  
 → uniformly sized nanoparticles

### Precursors

Metal anode	Pd, Ni, Co
Palladium chloride	PdCl <sub>2</sub>
Hydrogen hexachloroplatinate IV	H <sub>2</sub> PtCl <sub>6</sub>
Potassium tetrachloroplatinate II	K <sub>2</sub> PtCl <sub>4</sub>
Silver nitrate	AgNO <sub>3</sub>
Silver tetraoxychlorate	AgClO <sub>4</sub>
Chloroauric acid	HAuCl <sub>4</sub>
Rhodium chloride	RhCl <sub>3</sub>
Selenious acid	H <sub>2</sub> SeO <sub>3</sub>

### Reducing agents

Hydrogen	H <sub>2</sub>
Ethylene glycol at > 120 °C	HOCH <sub>2</sub> CH <sub>2</sub> OH
Sodium citrate	Na <sub>3</sub> C <sub>6</sub> H <sub>5</sub> O <sub>7</sub>
Citric acid	C <sub>6</sub> H <sub>8</sub> O <sub>7</sub>
Carbon monoxide	CO
Phosphorus in ether	P in -O-
Methanol	CH <sub>3</sub> OH
Hydrogen peroxide	H <sub>2</sub> O <sub>2</sub>
Formaldehyde	HCHO
Sodium tetrahydroborate	NaBH <sub>4</sub>
Ammonium	NH <sub>3</sub>
Hydrazine	N <sub>2</sub> H <sub>4</sub>

### Polymer Stabilizer

Poly(vinylpyrrolidone), PVP
Polyvinylalcohol, PVA
Polyethyleneimine
Sodium polyphosphate
Sodium polyacrylate
Tetraalkylammonium halogenides

### 4 Nanomaterials

# Synthesis of Nano Materials- 0D from liquid (Metal)

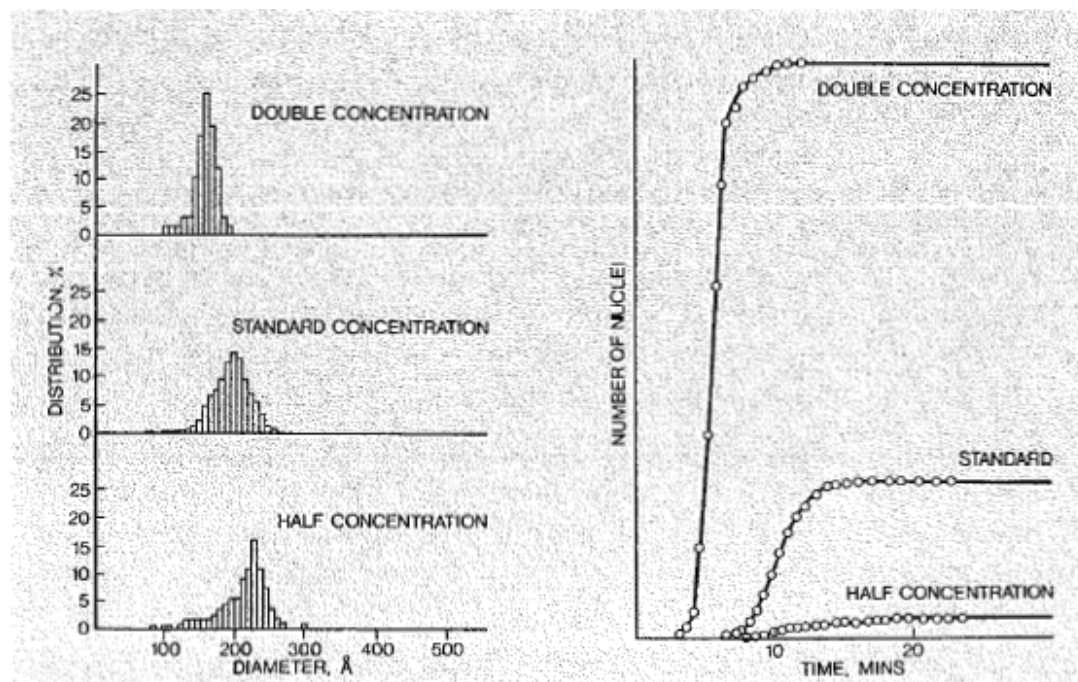
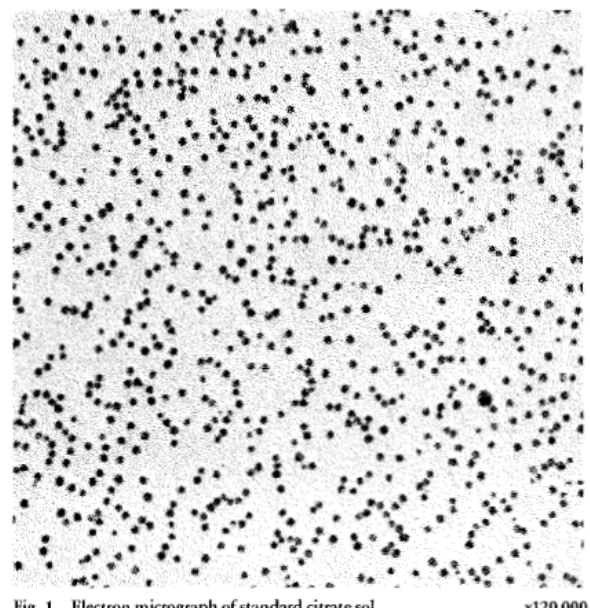
## □ Chemical Reduction

- Ex) Au nanoparticles

$\text{HAuCl}_4$  (chloroauric acid) +  $\text{Na}_3\text{C}_6\text{H}_5\text{O}_7$  (sodium citrate) in water at 100 °C

excellent stability and uniform particle size of ~20 nm

a large number of initial nuclei → a large number of nanoparticles with smaller size and narrow size distribution

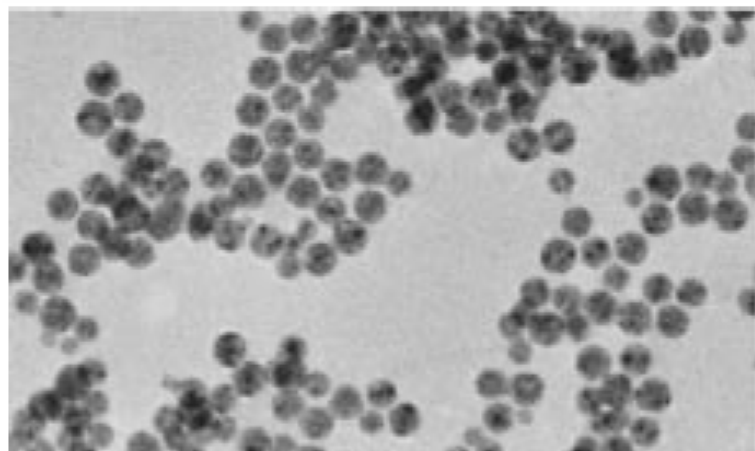
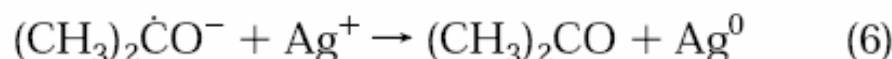
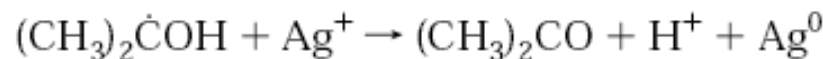
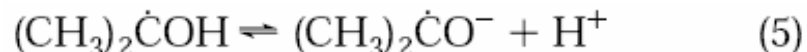


# Synthesis of Nano Materials- 0D from liquid (Metal)

## □ Photochemical Reduction

- Ex) Ag nanoparticles

aqueous solution of  $\text{AgClO}_4$ , acetone, 2-propanol, polymer stabilizer  
UV illumination



**6** **Figure 5.** Electron micrograph of the silver particles formed in a  $4.0 \times 10^{-4}$  M  $\text{AgClO}_4$  solution the presence of  $6.0 \times 10^{-4}$  M polyethylenimine. Mean particle size 7 nm. Standard deviation 5 nm.

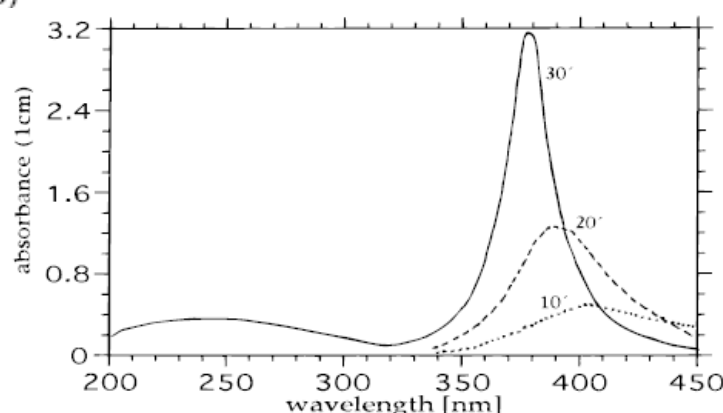


**Figure 1.** Absorption spectrum of a solution containing  $2 \times 10^{-4}$  M polyethylenimine as stabilizer at various minutes of UV illumination.  $[\text{AgClO}_4]$   $1.1 \times 10^{-4}$  M; [2-propanol] 1.0 M; [acetone]  $2.0 \times 10^{-2}$  M. The 260 nm absorption of acetone was compensated by the nonilluminated solution in the reference beam of the spectrophotometer.

# Synthesis of Nano Materials- 0D from liquid (Metal)

## □ Sonochemical Reduction

- Ex) amorphous Ag nanoparticles of ~20 nm  
aqueous  $\text{AgNO}_3$  at 10°C in Ar and  $\text{H}_2$   
sonication

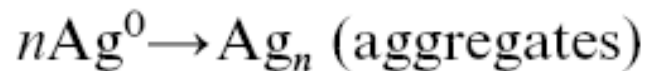


Fig. 1 Transmission electron micrograph of the amorphous silver nanoparticles.

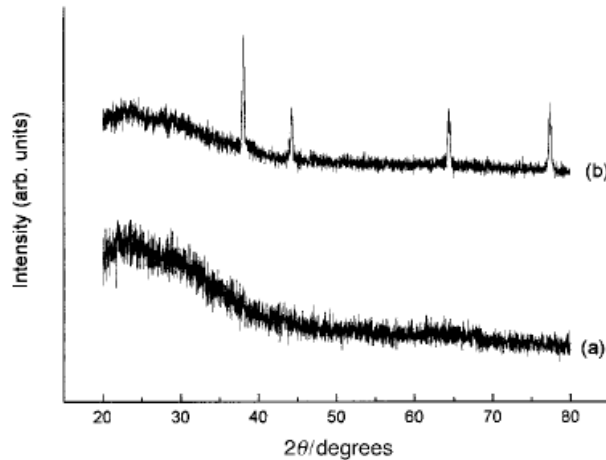


Fig. 2 X-Ray diffraction pattern of as-prepared silver nanoparticles, and silver nanoparticles crystallized at 340°C.

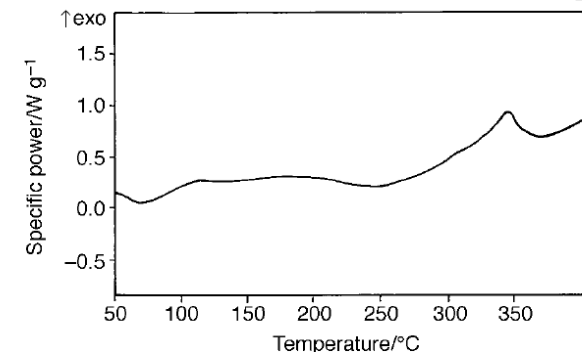
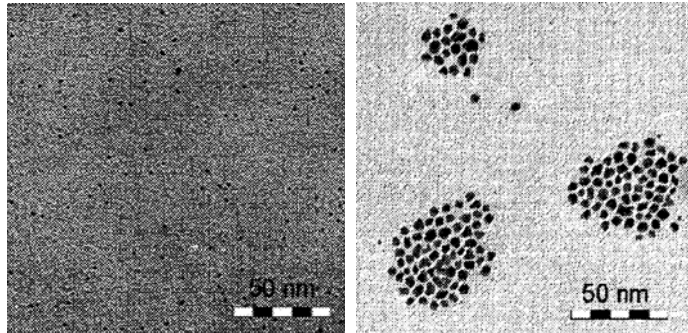
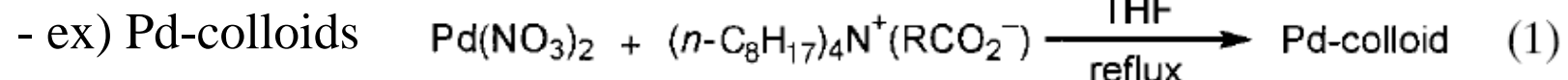


Fig. 3 DSC spectrum of the amorphous silver nanoparticles. The crystallization temperature is indicated by a sharp exotherm at 340°C.

# Synthesis of Nano Materials- 0D from liquid (Metal)

## □ Effect of Reducing Agents (1)

- strong reducing agent → small nanoparticles in a fast reaction



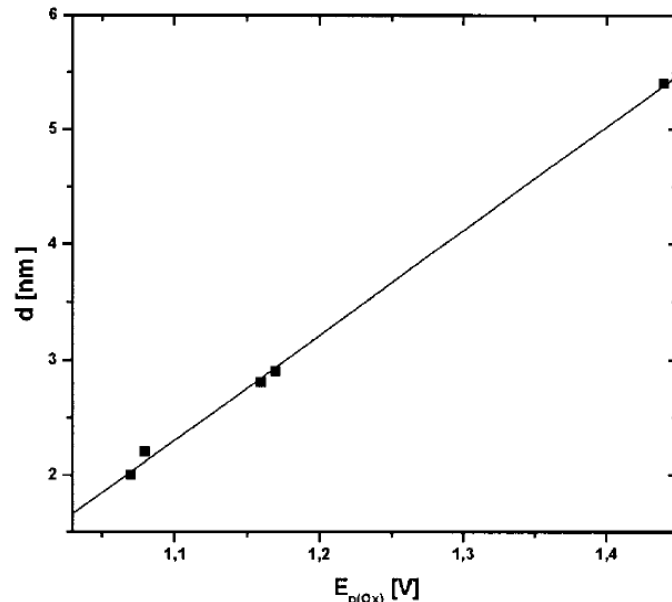
Pivalate  
2.2 nm

Dichloracetate  
5.4 nm

Table 1. Particle size of Pd-colloids,  $pK_a$  values, and peak potentials of the carboxylates studied.

Reductant $(\text{n-C}_8\text{H}_{17})_4\text{N}^+$ -salt	$E_{\text{p(Ox)}}$ [V]	$pK_a$ of the acid	$d$ after 50 min [nm]	$d$ after 4 h [nm]
Dichloracetate	1.44	1.5	5.4	6.8
Lactate	1.16	3.1	2.8	[a]
Glycolate	1.17	3.8	2.9	5.0
Acetate	1.07	4.8	2.0	2.5
<b>8 Pivalate Nanomaterials</b>	<b>1.08</b>	<b>5.0</b>	<b>2.2</b>	<b>2.5</b>

[a] Not determined.



Weak → larger

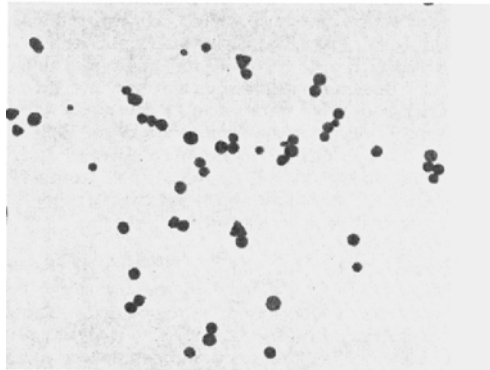
Strong → small

M.T. Reetz and M. Maase, Adv. Mater. 11, 773 (1999).

# Synthesis of Nano Materials- 0D from liquid (Metal)

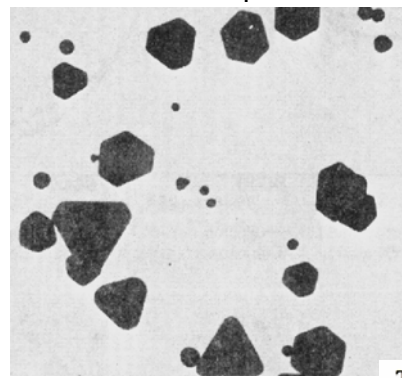
## □ Effect of Reducing Agents (2)

- morphology as well as size and size distribution
- ex) Au colloid       $\text{HAuCl}_4 + \text{reducing agent}$



Sodium citrate- spherical

Hydrogen peroxide- spherical



Hydroxylamine hydrochloride- cubical  
Citric acid- trigon

**Table 3.2.** Comparison of average sizes of Au nanoparticles synthesized using various reduction reagents, all in nanometer.<sup>27</sup>

Reduction reagents	436 nm*	546 nm*	XRD <sup>#</sup>	SEM
Sodium citrate	29.1	28.6	17.5	$17.6 \pm 0.6$
Hydrogen peroxide	25.3	23.1	15.1	$15.7 \pm 1.1$
	31.0	31.3	18.7	$19.7 \pm 2.6$
Hydroxylamine hydrochloride			37.8	$22.8 \pm 4.2$
Citric acid	23.5	22.8		$12.5 \pm 0.6$
Carbon monoxide	9.1	7.4	9.0	$5.0 \pm 0.5$
	15.3	15.3	9.8	$7.5 \pm 0.4$
	18.9	18.3	13.1	$12.2 \pm 0.5$
Phosphorus			13.9	$8.1 \pm 0.5$
			21.0	$15.5 \pm 1.7$
			29.6	$25.6 \pm 2.6$
			36.9	$35.8 \pm 9.7$

\* The particle sizes are determined using light scattering with the indicated wavelengths.

# The particle sizes are determined based on X-ray diffraction line broadening.

## 9 Nanomaterials

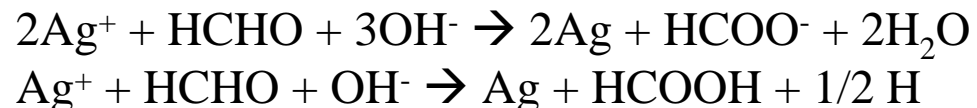
W.O. Miligan, J. Am. Chem. Soc. 86 (1964) 3461.

# Synthesis of Nano Materials- 0D from liquid (Metal)

## □ Effect of Concentration of Reactants

ex) Ag nanoparticles using HCHO (formaldehyde) in aqueous solution

- quantity of reducing agent- negligible effect on particle size distribution
- only formaldehyde was used- reaction rate was too slow due to a low pH
- addition of alkaline solution consisting of NaOH and/or Na<sub>2</sub>CO<sub>3</sub>
- possible reaction mechanism



- strong base (NaOH) addition: fast reduction rate  
→ large particles
- weak base (Na<sub>2</sub>CO<sub>3</sub>) addition  
: diffusion-limited process → fine particles

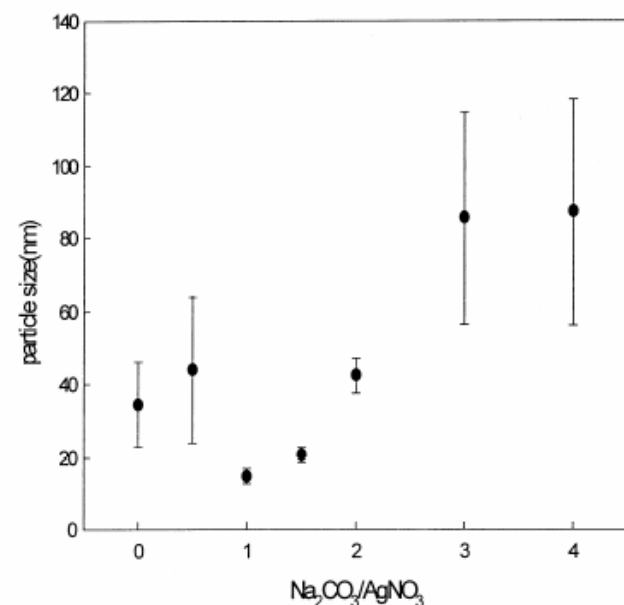


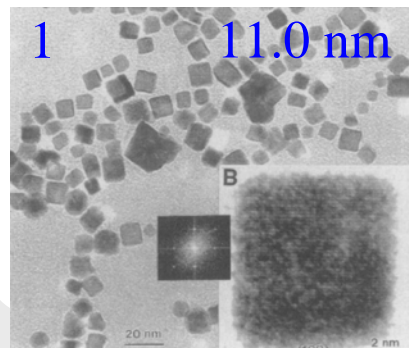
Fig. 2. Effect of [Na<sub>2</sub>CO<sub>3</sub>]/[AgNO<sub>3</sub>] ratio on silver average size and its standard deviation (other conditions: [AgNO<sub>3</sub>]=0.005 M, [HCHO]/[AgNO<sub>3</sub>]=4, [NaOH]/[AgNO<sub>3</sub>]=1, PVP/AgNO<sub>3</sub>=9.27).

# Synthesis of Nano Materials- 0D from liquid (Metal)

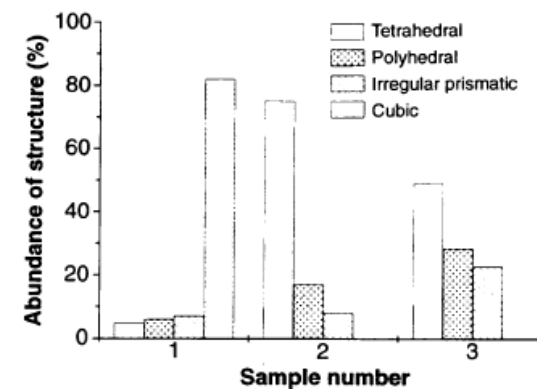
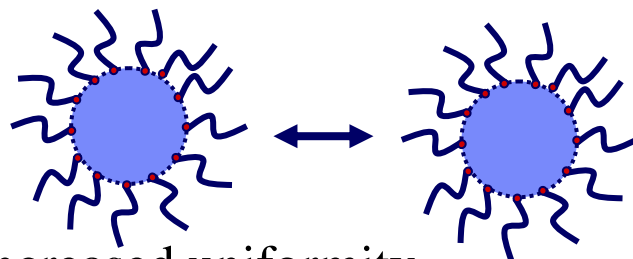
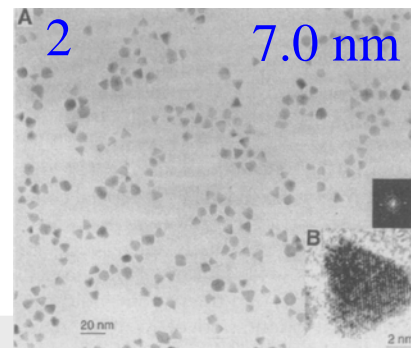
## □ Effect of Polymer Stabilizer

1. Preventing agglomeration of nanoparticles:  
Steric hindrance
2. Diffusion barrier: diffusion-limited N & G → increased uniformity
  - strong adsorption with metal surface → occupy the reaction sites
  - closely-packed polymer layer → slow down the diffusion of elements
3. Shape control: face-selective growth of crystals  
Ex.)  $\text{K}_2\text{PtCl}_4$  aqueous with sodium polyacrylate:  
→ the shape was dependent on the concentration of sodium polyarylate

$[\text{K}_2\text{PtCl}_4]:[\text{surfactants}] = 1:1$   
cubic with {100} faces



$[\text{K}_2\text{PtCl}_4]:[\text{surfactants}] = 1:5$   
tetrahedra with {111} faces

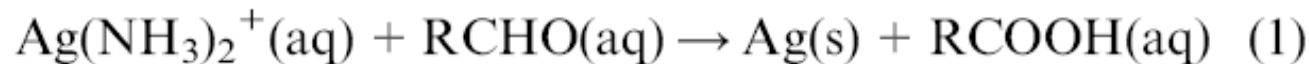


T.S. Ahmadi, Science 272 (1996) 1924.

## Synthesis of Nano Materials- 0D from liquid (Metal)

### □ Effect of Temperature

- Ag nanoparticles- Tollens process



- silver nitrate, sodium hydroxide, (formaldehyde and sorbitol)
- frequency of collision between the small particles increased as the temperature was raised

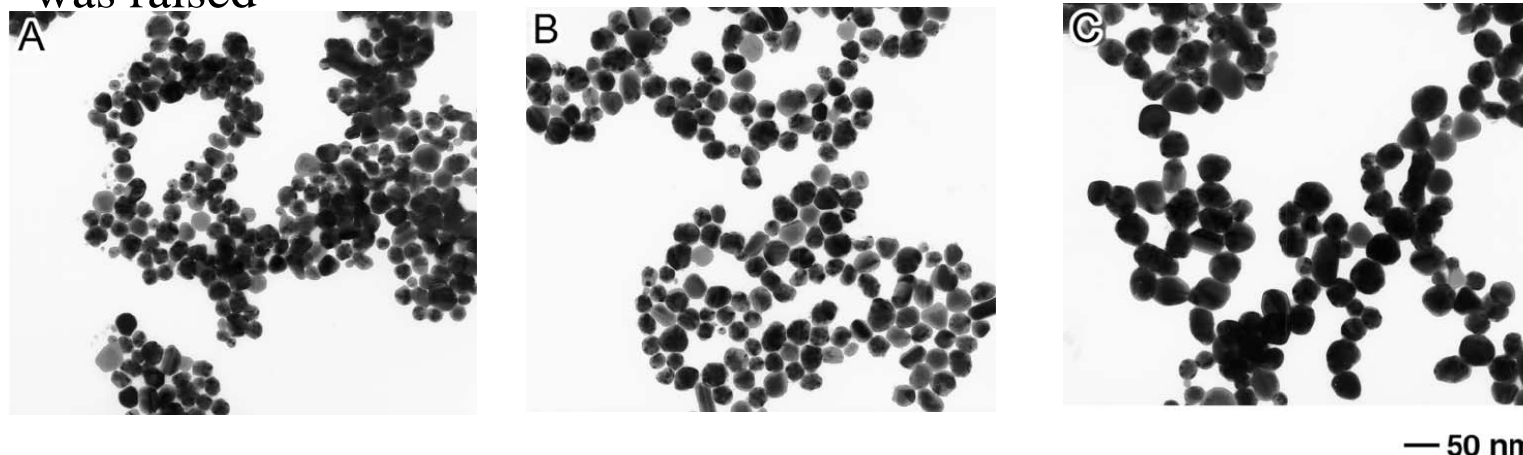


**Fig. 3** The TEM images of silver nanoparticles that were obtained as the final products when the reactions were carried out under nitrogen at (A) 27, (B) 30, and (C) 35 °C, respectively. The mean size of these silver nanoparticles changed from ~20, to ~30 and ~40 nm when the temperature was raised.

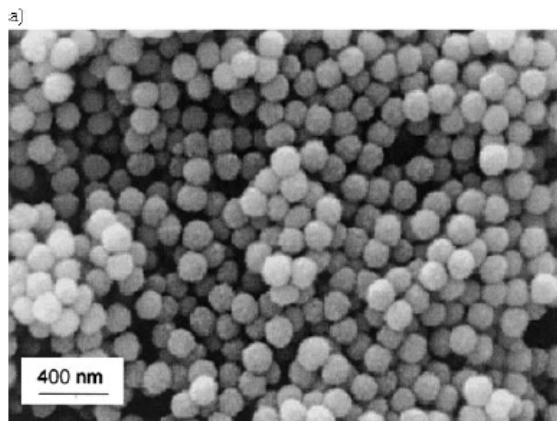
Y. Yin, J. Mater. Chem. 12 (2002) 522.

# Synthesis of Nano Materials- 0D from liquid (Metal)

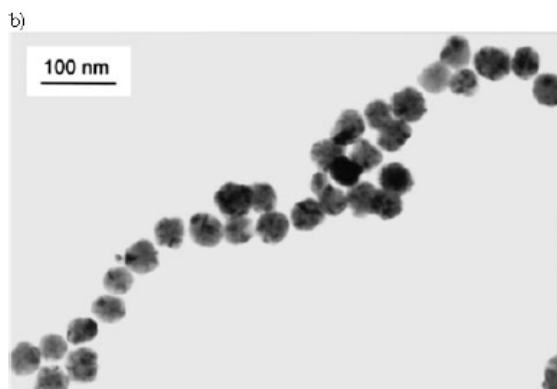
## □ Effect of Nucleating Agents

- $\text{Co}_x\text{Ni}_{1-x}$  and  $\text{Fe}_z[\text{Co}_x\text{Ni}_{1-x}]_{1-z}$  particles
- Pt or Ag ( $\text{K}_2\text{PtCl}_4$  or  $\text{AgNO}_3$ ): nucleating agents

- diameter decreases as the seeds increase



$\text{Fe}_{0.13}[\text{Co}_{50}\text{Ni}_{50}]_{0.87}$   
166 nm



Pt  
 $\text{Co}_{35}\text{Ni}_{65}$   
50 nm

Fig. 1. Powders prepared in 1,2-propanediol by heterogeneous nucleation with Pt as nucleating agent. a) SEM image of a  $\text{Fe}_{0.13}[\text{Co}_{50}\text{Ni}_{50}]_{0.87}$  powder ( $d_m = 166 \text{ nm}$ ;  $\sigma = 13 \text{ nm}$ ). b) TEM image of a  $\text{Co}_{35}\text{Ni}_{65}$  powder ( $d_m = 50 \text{ nm}$ ;  $\sigma = 5 \text{ nm}$ ).

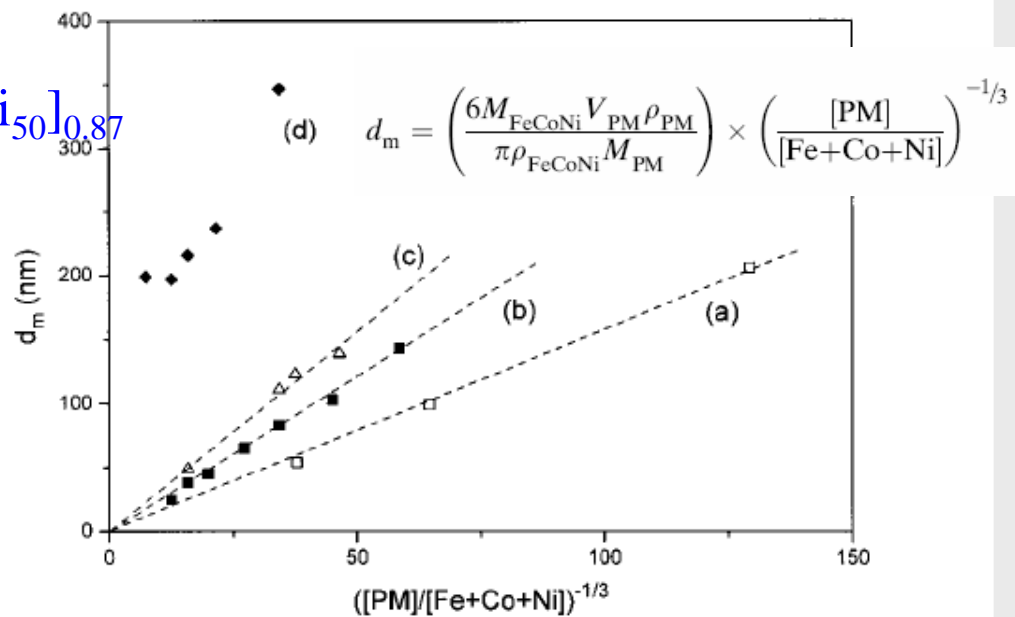
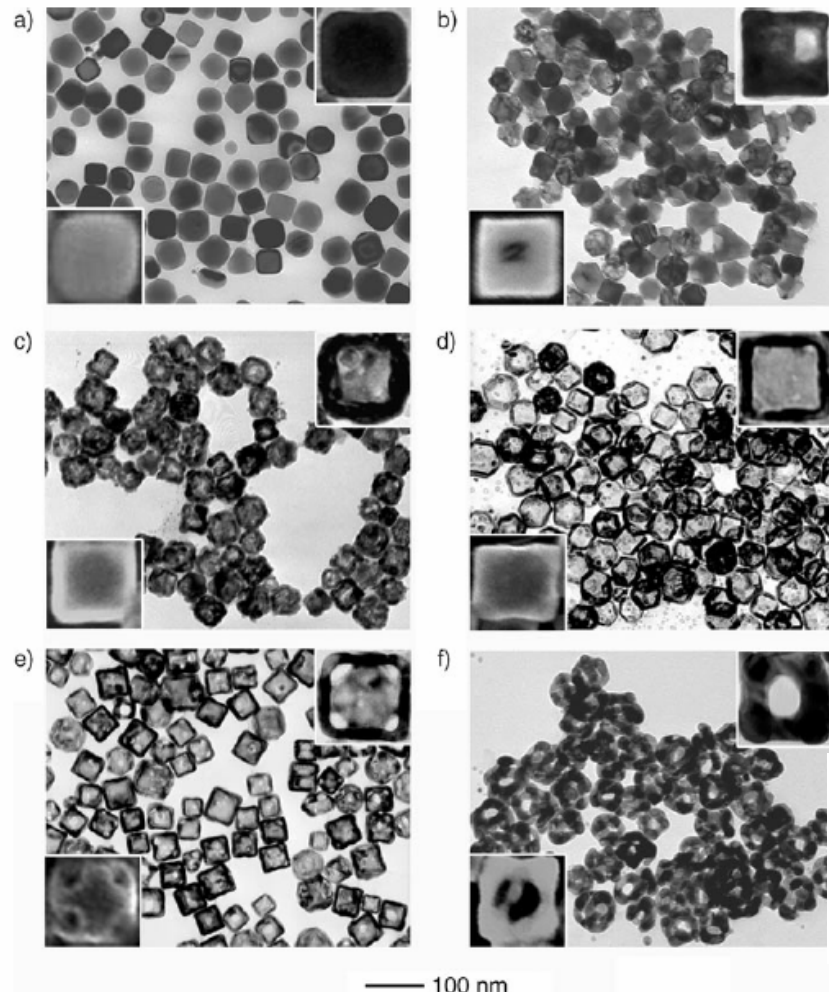


Fig. 2. Mean diameter,  $d_m$ , of particles prepared by heterogeneous nucleation versus  $([\text{PM}]/[\text{Fe}]+\text{[Co]}+\text{[Ni}])^{-1/3}$  for different compositions and different nucleating agents: a)  $[\text{Pt}]/[\text{Fe}_{0.13}(\text{Co}_{50}\text{Ni}_{50})_{0.87}]$ ; b)  $[\text{Pt}]/[\text{Co}_{80}\text{Ni}_{20}]$ ; c)  $[\text{Pt}]/[\text{Co}_{50}\text{Ni}_{50}]$ ; d)  $[\text{Ag}]/[\text{Co}_{80}\text{Ni}_{20}]$ .

# Synthesis of Nano Materials- 0D from liquid (Metal)

## □ Competitive Reaction Between Reduction and Oxidation

- Pd nanocube (box or cage)-  $\text{Na}_2\text{PdCl}_4$ , ethylene glycol, PVP, water



- up to  $t=18$  h, reduction  $\rightarrow$  nanocube
- after 20 h, etching by  $\text{O}_2$   
 $\rightarrow$  nanobox  $\rightarrow$  nanocage

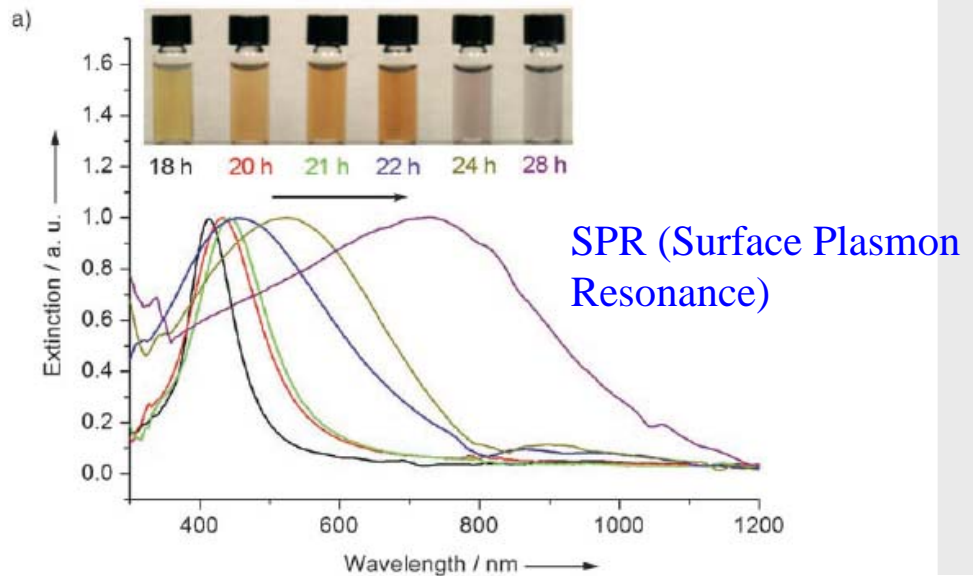


**Figure 1.** TEM images of the products at different reaction stages:  
a)  $t=18$  h; b)  $t=20$  h; c)  $t=21$  h; d)  $t=22$  h; e)  $t=24$  h; and f)  $t=28$  h.  
Note that the 100-nm bar applies to all images. The upper right and lower left insets show enlarged TEM and SEM images of an individual particle taken from each product, respectively.

Y. Xiong, Angew. Chem. Int. Ed. 44 (2005) 7915.

# Synthesis of Nano Materials- 0D from liquid (Metal)

## □ Competitive Reaction Between Reduction and Oxidation

### Simultaneous event: Reduction vs. Oxidation

- strongly depends on the existence of oxygen
- other anion can enhance the oxidation

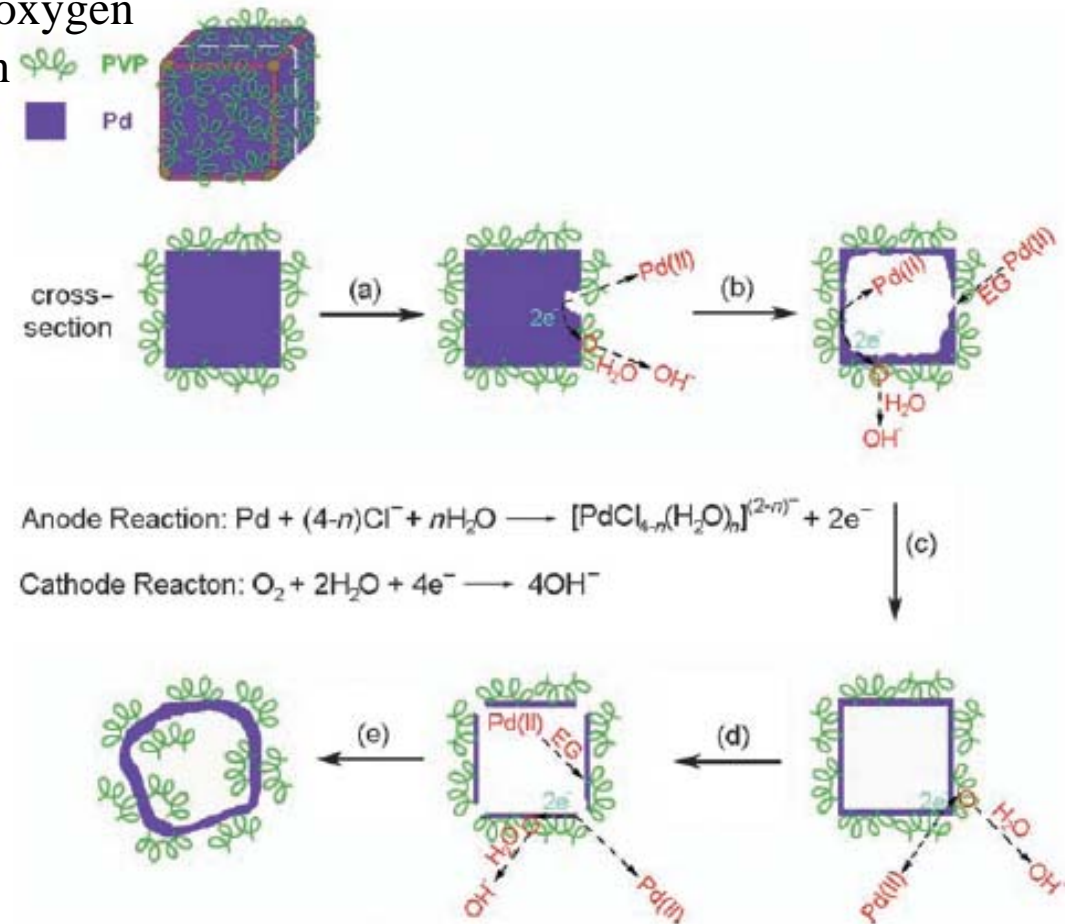


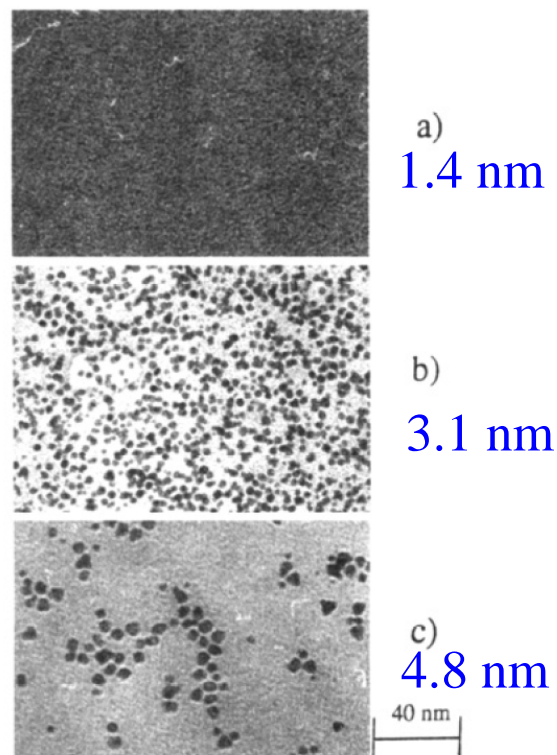
**Figure 4.** Schematic illustration summarizing all the major morphological changes involved in the synthesis of Pd nanoboxes and nanocages by corrosive etching: a) Pitting at a specific site on the surface of a nanocube where the  $O_2$  dissolved in the solvent received electrons from the cathode and generated hydroxide ions that migrated towards the anode; b) formation of hollow structures after further etching of the interior of the nanocube, and the concentration of water-substituted  $[PdCl_4]^{2-}$  increased; c) formation of a completely enclosed Pd nanobox by reducing the water-substituted  $[PdCl_4]^{2-}$  species to form Pd atoms at the edge of each hole; d) formation of nanocages by dissolving Pd from the corners of the nanobox; and e) reconstruction of the nanocage by relocating all the holes from the corners to side faces and thickening of the wall as a result of additional reduction of the water-substituted  $[PdCl_4]^{2-}$  species.

# Synthesis of Nano Materials- 0D from liquid (Metal)

## □ Heterogeneous Nucleation

### Electrochemical Deposition

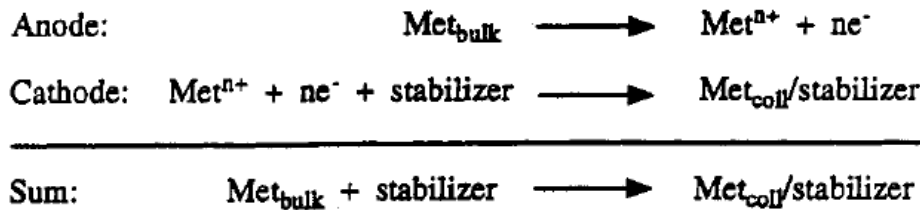
- metal sheet (Pd, Ni, Co)
- tetraalkylammonium bromide in acetonitrile/tetrahydrofuran



16

Figure 1. Transmission electron micrographs of Pd clusters prepared at current densities of (a) 5.0, (b) 0.8, and (c) 0.1  $\text{mA}/\text{cm}^2$ ; in all cases magnification of 250 000.

### Scheme 1. Electrochemical Synthesis of Stabilized Metal Clusters<sup>a</sup>



<sup>a</sup>  $\text{Met}_{\text{bulk}}$  = bulk metal sheet;  $\text{Met}_{\text{coll}}/\text{stabilizer}$  = ammonium salt stabilized colloidal metal cluster.

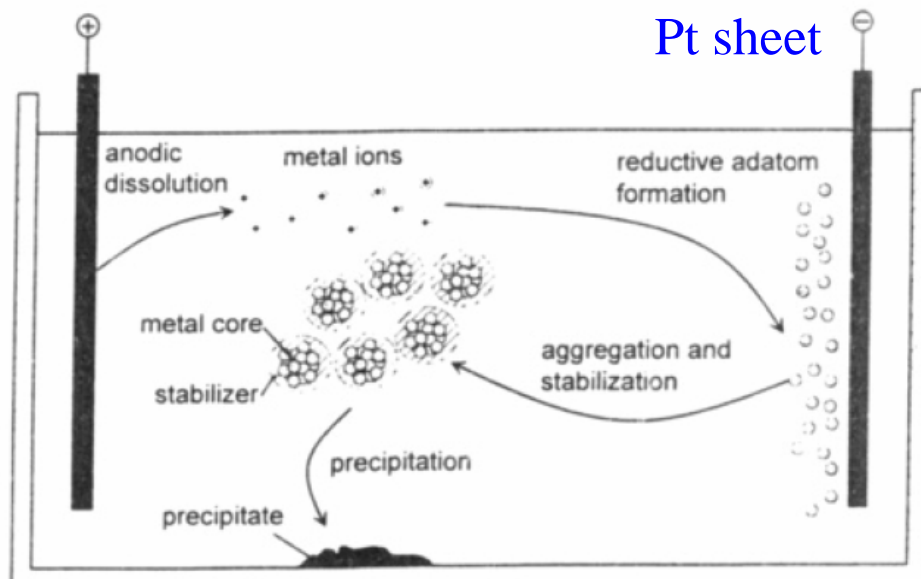


Figure 4. Formation of electrochemically produced tetraalkylammonium-stabilized metal clusters.

M.T. Reetz, J. Am. Chem. Soc. 116 (1994) 7401.  
J.A. Becker, J. Chem. Phys. 103 (1995) 2520.

# Synthesis of Nano Materials-0D from liquid (Semiconductor)

## □ Non-oxide Semiconductor Nanoparticles

- pyrolysis of organometallic precursor(s) dissolved in anhydride solvents at elevated temperature in an airless environment in the presence of polymer stabilizer or **capping materials**
- synthesis of CdX (X=S, Se, Te)  
dimethylcadmium ( $\text{Me}_2\text{Cd}$ ) as Cd source  
bis(trimethylsilyl) sulfide ((TMS)<sub>2</sub>S), trioctylphosphine selenide (TOPSe)  
trioctylphosphine telluride (TOPTe) as S, Se, Te precursors  
tri-n-octylphosphine (TOP) and tri-n-octylphosphine oxide (TOPO) as solvent and capping material
- procedures
  - injection of reagents into hot reaction vessel- sudden decrease in temperature
  - abrupt supersaturation- a short burst of homogeneous nucleation- less extent or negligible subsequent growth due to depletion of growth species
  - reheating (aging, Ostwald ripening)- further monodispersion
  - size selective precipitation

# Synthesis of Nano Materials-0D from liquid (Semiconductor)

## □ Non-oxide Semiconductor Nanoparticles

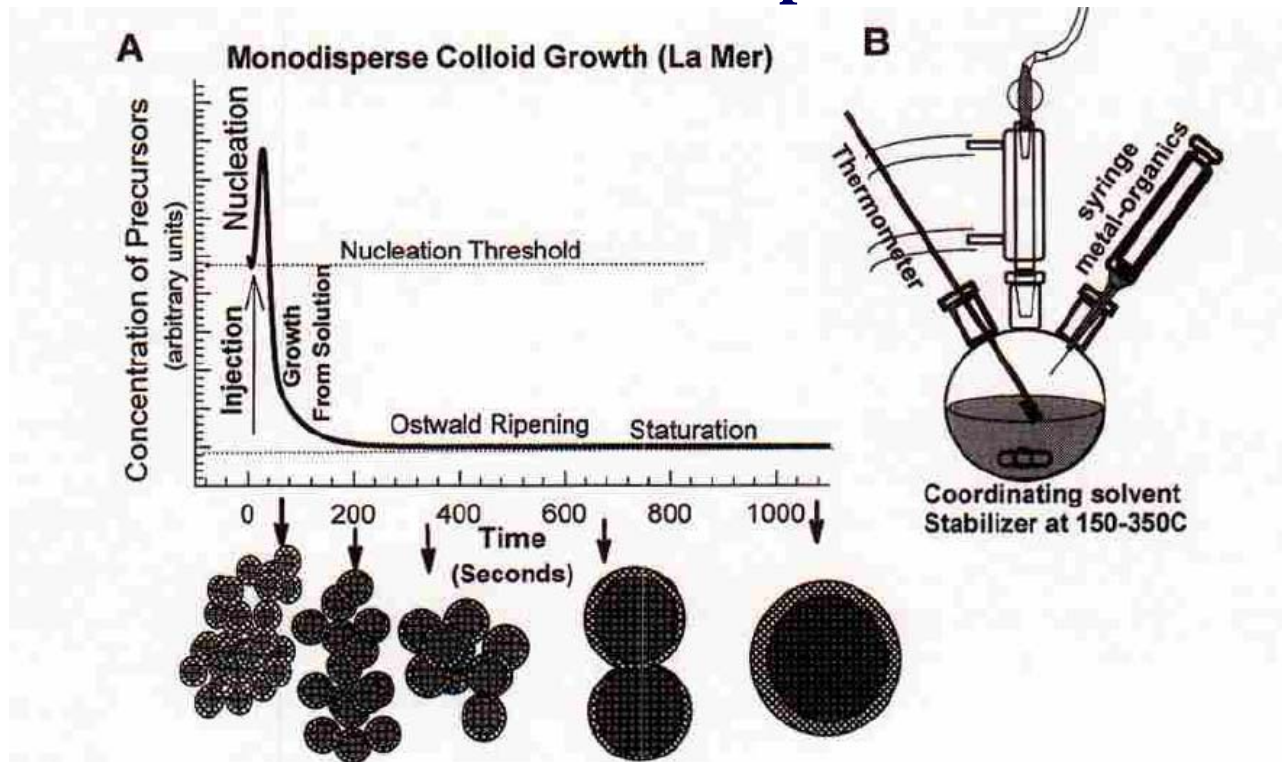


**Figure 1** (A) Cartoon depicting the stages of nucleation and growth for the preparation of monodisperse NCs in the framework of the La Mer model. As NCs grow with time, a size series of NCs may be isolated by periodically removing aliquots from the reaction vessel. (B) Representation of the simple synthetic apparatus employed in the preparation of monodisperse NC samples.

# Synthesis of Nano Materials-0D from liquid (Semiconductor)

## □ Homogeneous Nucleation & Growth

### Pyrolysis of two organometallic precursors

Ex) CdSe QD

$(\text{CH}_3)_2\text{Cd}$  in TOP+ TOPSe in TOP → TOPO at 300°C

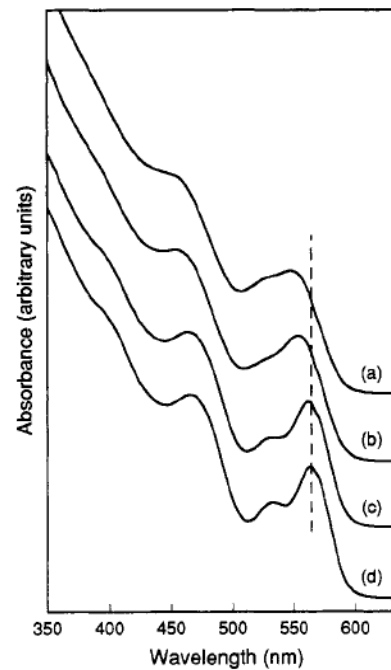
→ 180°C (kinetic control of the growth)

→ 230~260°C (aging, Ostwald ripening → increased uniformity in size)

→ isolation and purification of crystallite

→ size selective precipitation (1-butanol/methanol)

**Figure 1.** Example of the effect of size-selective precipitation on the absorption spectrum of  $\sim 37 \text{ \AA}$  diameter CdSe nanocrystallites. (a) Room temperature optical absorption spectrum of the nanocrystallites in the growth solution before size-selective precipitation. (b) Spectrum after one size-selective precipitation from the growth solution with methanol. (c) Spectrum after dispersion in 1-butanol and size-selective precipitation with methanol. (d) Spectrum after a final size-selective precipitation from 1-butanol/methanol.



# Synthesis of Nano Materials-0D from liquid (Semiconductor)

## □ Homogeneous Nucleation & Growth

Pyrolysis of two organometallic precursors

Ex) CdSe QD

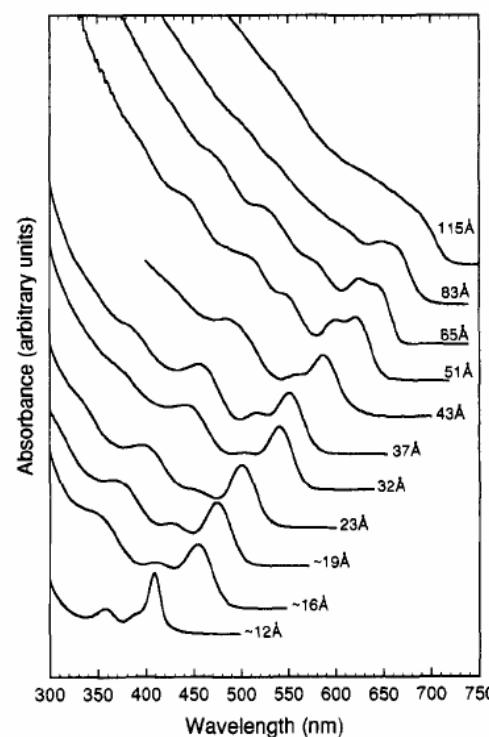


Figure 3. Room temperature optical absorption spectra of CdSe nanocrystallites dispersed in hexane and ranging in size from  $\sim 12$  to  $115$  Å.

20 Nanomaterials

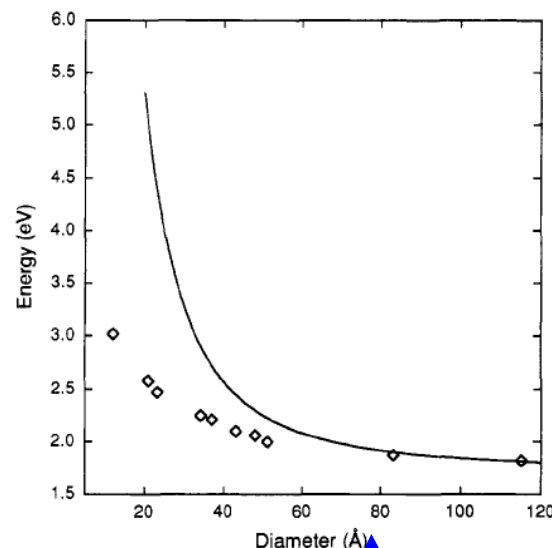


Figure 4. HOMO LUMO transition energy of CdSe crystallites as a function of size (diamonds) compared with the prediction of the effective mass approximation (solid line).

TEM, XRD

stacking fault

10 nm

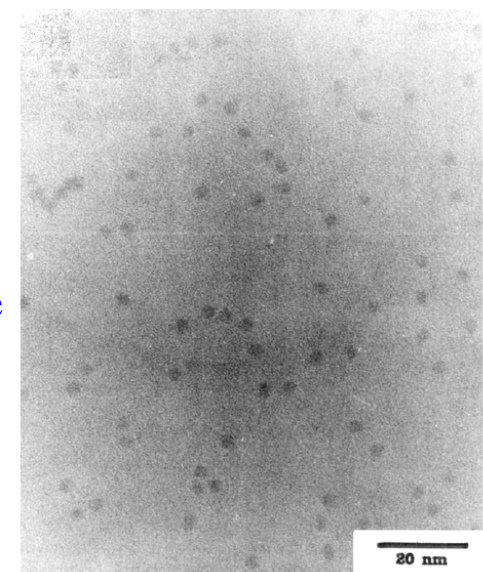


Figure 6. TEM image taken in bright field with lattice contrast shows a collection of slightly prolate particles. The elongated (002) axis measures  $35.0 \text{ \AA} \pm 5\%$  while the perpendicular axis measures  $30 \text{ \AA} \pm 6\%$ . The particles are well dispersed and not aggregated.

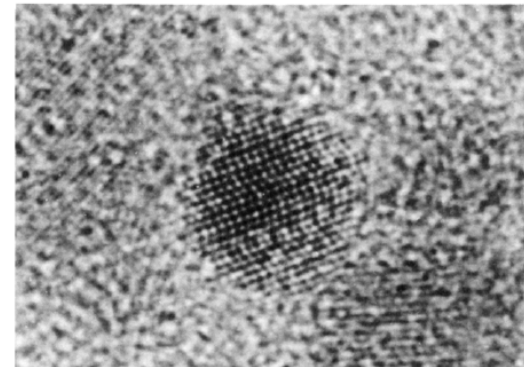


Figure 7. An  $80 \text{ \AA}$  diameter CdSe crystallite imaged in bright field with atom contrast shows the presence of stacking faults in the (002) direction.

C.B. Murray, J. Am. Chem. Soc. 115 (1993) 8706.

# Synthesis of Nano Materials-0D from liquid (Semiconductor)

## □ Homogeneous Nucleation & Growth

### Pyrolysis of two organometallic precursors

Ex) CdSe QD

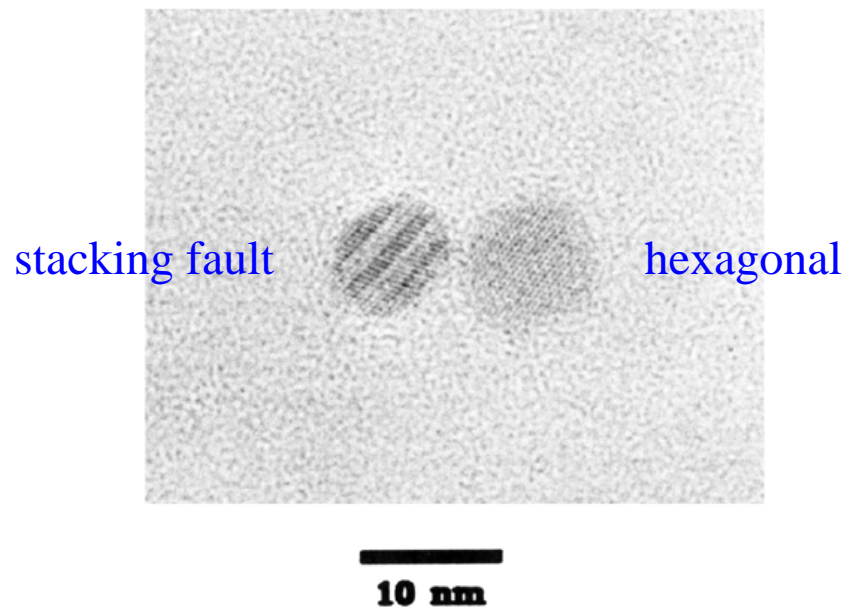


**Figure 8.** The crystallite on the left ( $\sim 110 \text{ \AA}$ ) shows a loss of lattice contrast in the (101) planes pointing to the presence of 4 stacking faults along the (002) direction. The crystallite is prolate with an aspect ratio of  $\sim 1.3$ . The crystallite on the right presents a projection perpendicular to the (002) direction and displays the hexagonal atom imaging characteristics of the wurtzite structure.

## 21 Nanomaterials

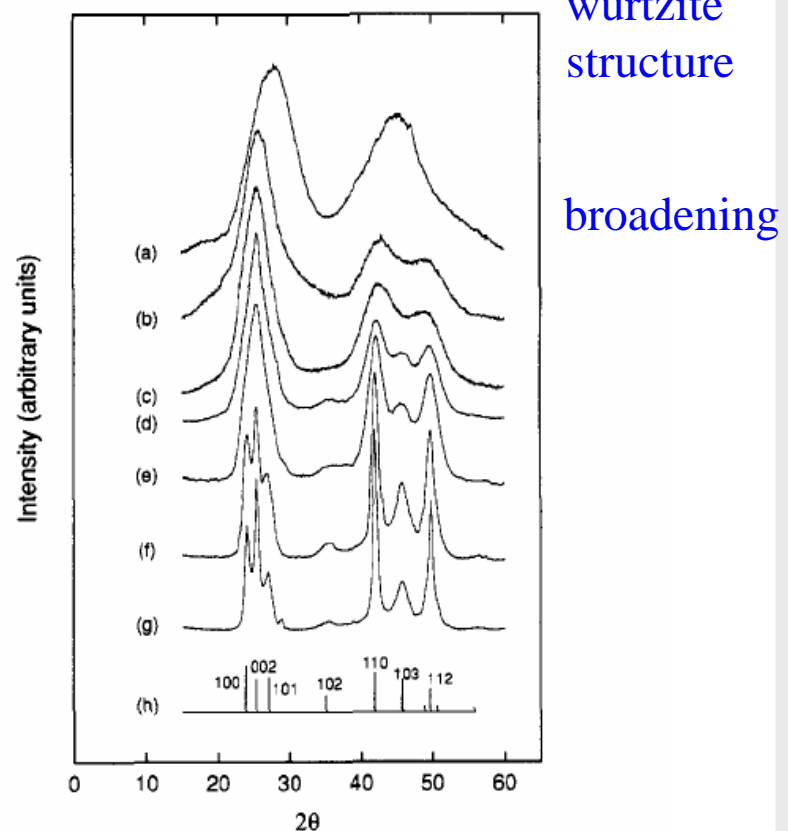


**Figure 11.** Powder X-ray diffraction spectra of (a) 12, (b) 18, (c) 20, (d) 37, (e) 42, (f) 83, and (g) 115  $\text{\AA}$  diameter CdSe nanocrystallites compared with the bulk wurtzite peak positions (h).

C.B. Murray, J. Am. Chem. Soc. 115 (1993) 8706.

# Synthesis of Nano Materials-0D from liquid (Semiconductor)

## □ Homogeneous Nucleation & Growth pyrolysis of one complex precursors

Ex 1) InP QD

Chloroindium oxalate complex and P(SiMe<sub>3</sub>)<sub>3</sub> in CH<sub>3</sub>CN (acetonitrile) at RT

→ add to a solution of TOP and TOPO

→ slowly heated to 270°C over 24 h and kept for 3-6 days

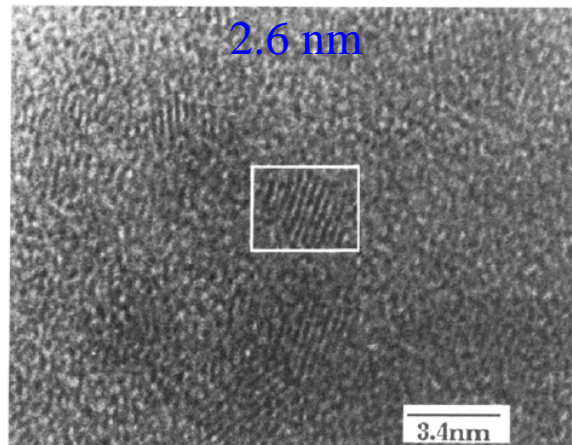
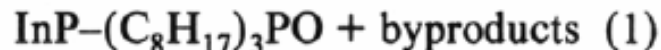
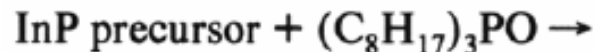


Figure 2. High-resolution transmission electron micrograph of InP QDs showing lattice fringes.

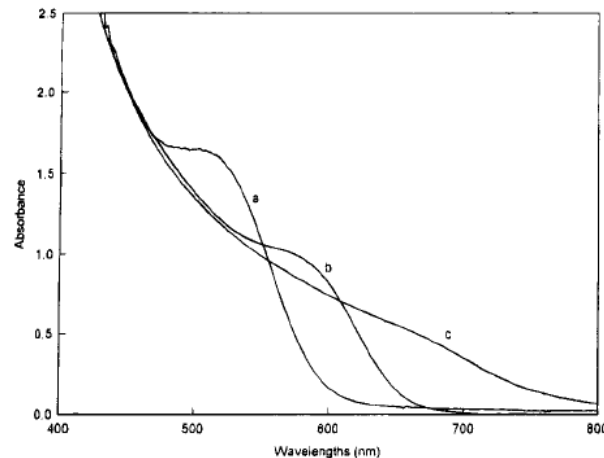


Figure 1. Absorption spectra for InP QD colloids with different diameters: (a) 26 Å; (b) 35 Å; (c) 46 Å.

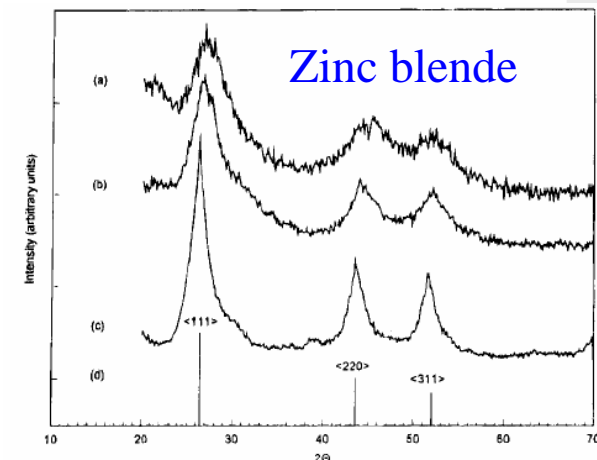


Figure 2. X-ray diffraction pattern for dried InP QDs colloids with diameters of (a) 26 Å, (b) 35 Å, and (c) 46 Å compared with the peak positions of bulk zinc blende InP (d).

# Synthesis of Nano Materials-0D from liquid (Semiconductor)

## □ Homogeneous Nucleation & Growth

**pyrolysis of one complex precursors**

Ex 2) GaAs QD

Tris(trimethylsilyl)arsine ((Me<sub>3</sub>Si)<sub>3</sub>As)+GaCl<sub>3</sub> in quinoline  
 → reflux at 240°C for 3 days

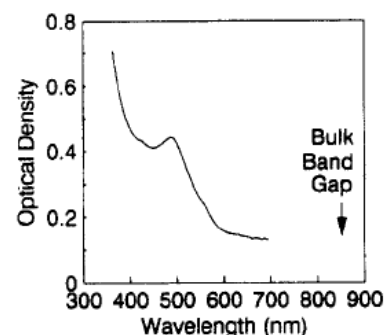
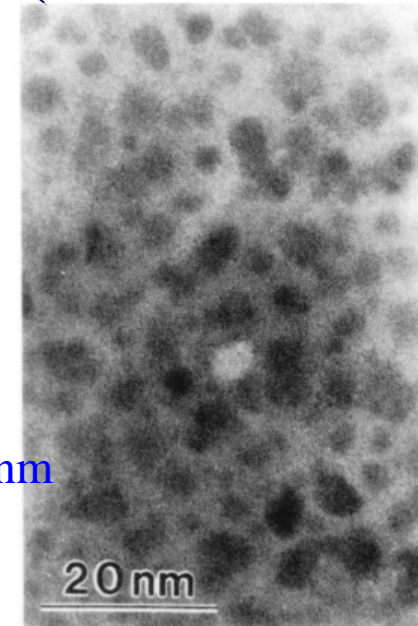
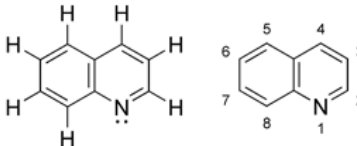


Figure 3. Optical absorption spectrum of a quinoline solution of the crystallites obtained after refluxing, but before flame annealing.

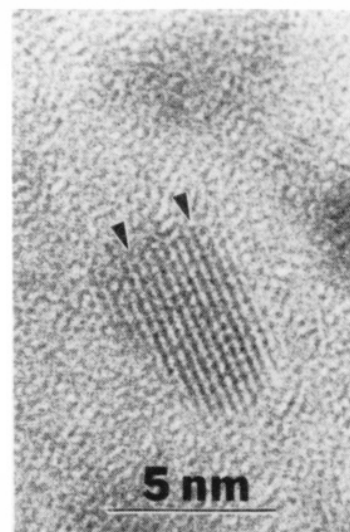


Figure 2. Transmission electron micrograph of one GaAs particle showing lattice planes.

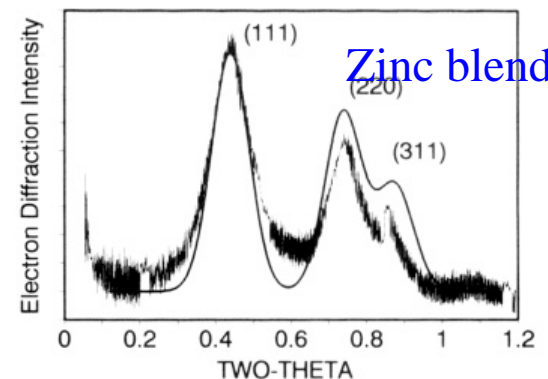


Figure 1. (a) Transmission electron micrograph from a field of GaAs particles. The bar is 20 nm. Analysis of a few hundred particles yields the average size of 45 Å by 35 Å. (b) Electron diffraction pattern from the particles. The domain size from the Debye-Scherrer formula is 24 Å.

# Synthesis of Nano Materials-0D from liquid (Semiconductor)

## □ Homogeneous Nucleation & Growth pyrolysis of one complex precursors

Ex 3) GaN QD

$\text{Ga}_2[\text{N}(\text{CH}_3)_2]_6 + \text{NH}_3$  at RT for 24 h → polymeric  $\{\text{Ga}(\text{NH})_{3/2}\}_n$   
 → slowly heated in TOA (trioctylamine) to 360 °C for 24 h and kept for 1 day  
 → TOA and HDA( hexadecylamine) added and kept 220 °C for 10 h

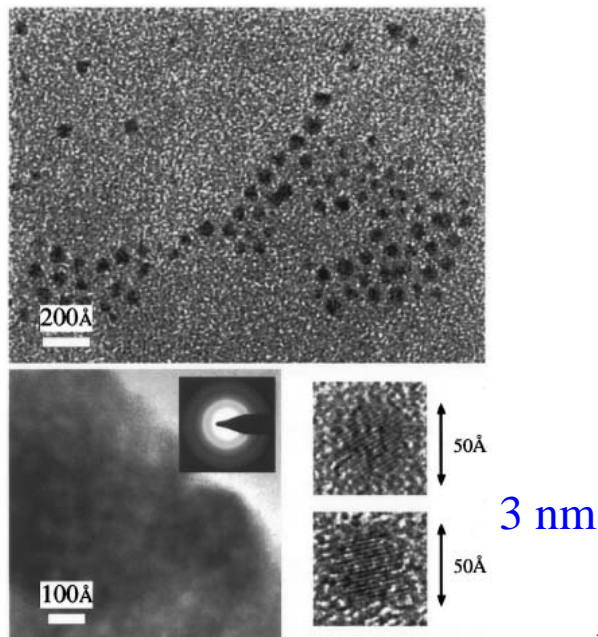


FIG. 2. TEM image of GaN QDs taken in bright field. The particles are well dispersed and not agglomerated. Top panel shows low magnification of QDs and some linear alignment. Bottom two right panels show high magnification and lattice fringes of QD oriented with the  $\langle 111 \rangle$  axis in the plane of the micrograph. Bottom left panel shows electron diffraction pattern of GaN QDs indicating zinc-blende structure.

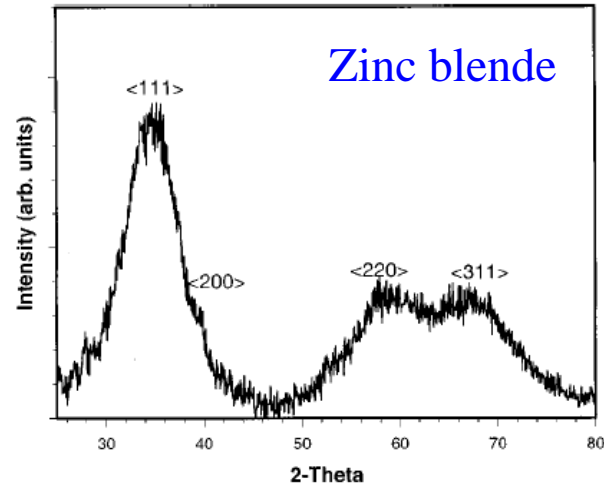


FIG. 3. X-ray diffraction pattern for dried GaN QDs colloid compare the peak positions of bulk zinc-blende InP.

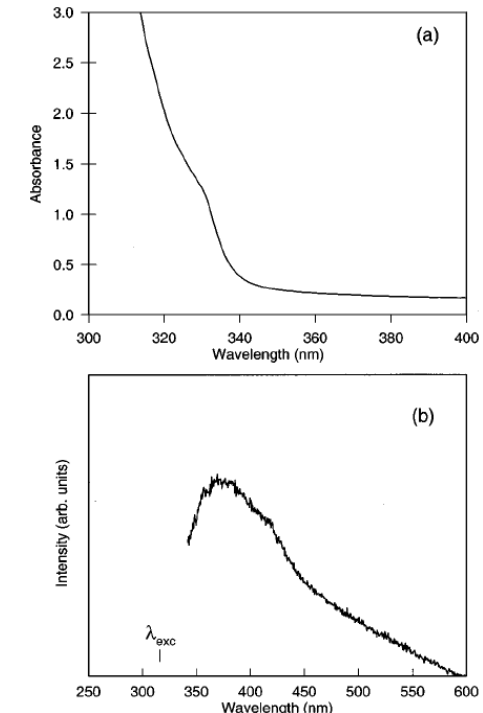


FIG. 1. Room temperature (a) absorption and (b) emission spectra for GaP QD colloids with a diameter of 30 Å.

# Synthesis of Nano Materials-0D from liquid (Semiconductor)

## □ Heterogeneous Nucleation & Growth

- quantum yield & emission life time of semiconductor nanoparticles
  - ← requires surface passivation to reduce the non-radioactive surface recombination of charge carriers
  - i) epitaxial deposition of a larger bandgap semiconductor with good lattice mismatch
  - ii) block dangling bond through adsorption Lewis bases
- i) core-shell formation using heterogeneous N & G: Epitaxial deposition ( $\text{CdSe}@\text{ZnS}$ )
- Suppressing homogeneous Nucleation

How ? →

1. control the supersaturation

(high enough for heterogeneous, but not enough for homogeneous nucleation)

- \* temperature
- \* concentration

2. control the capping agent

0.6 nm ZnS

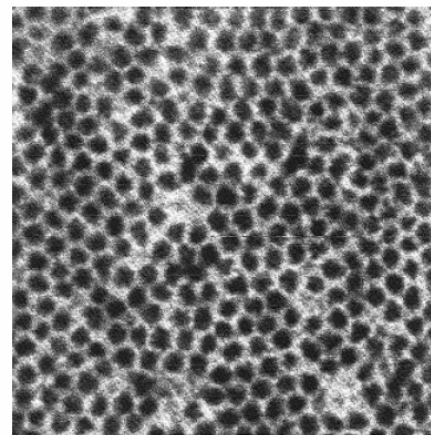


Figure 1. TEM picture of  $(\text{CdSe})\text{ZnS}$  nanocrystals. This picture is  $95 \times 95$  nm.

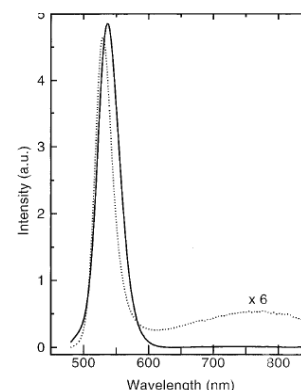
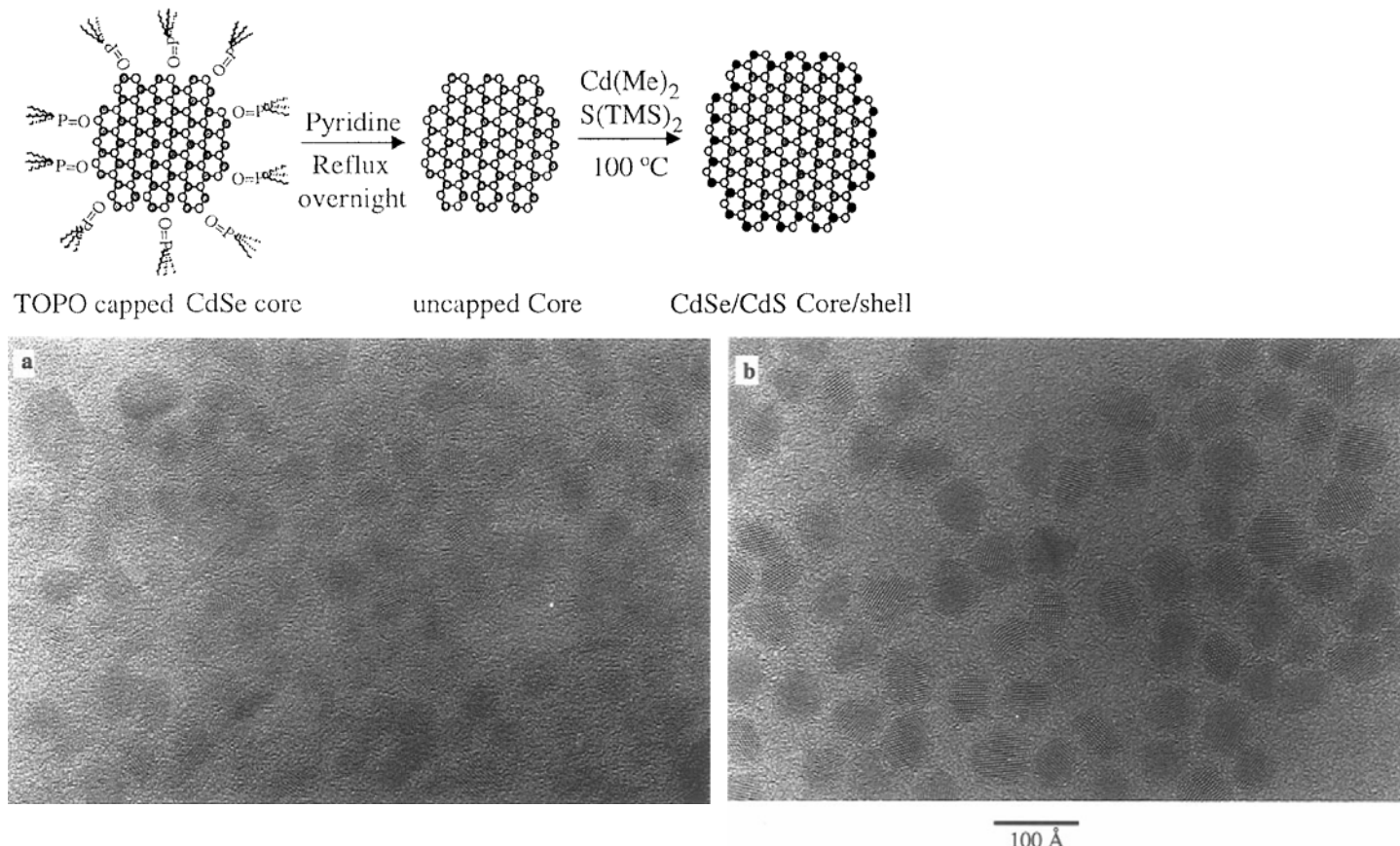


Figure 3. Fluorescence of the  $(\text{CdSe})\text{TOPO}$  (dotted line) and  $(\text{CdSe})\text{-ZnS}$  (solid line) nanocrystals normalized by their absorption at the excitation wavelength (470 nm).

two step  
single flask

# Synthesis of Nano Materials-0D from liquid (Semiconductor)

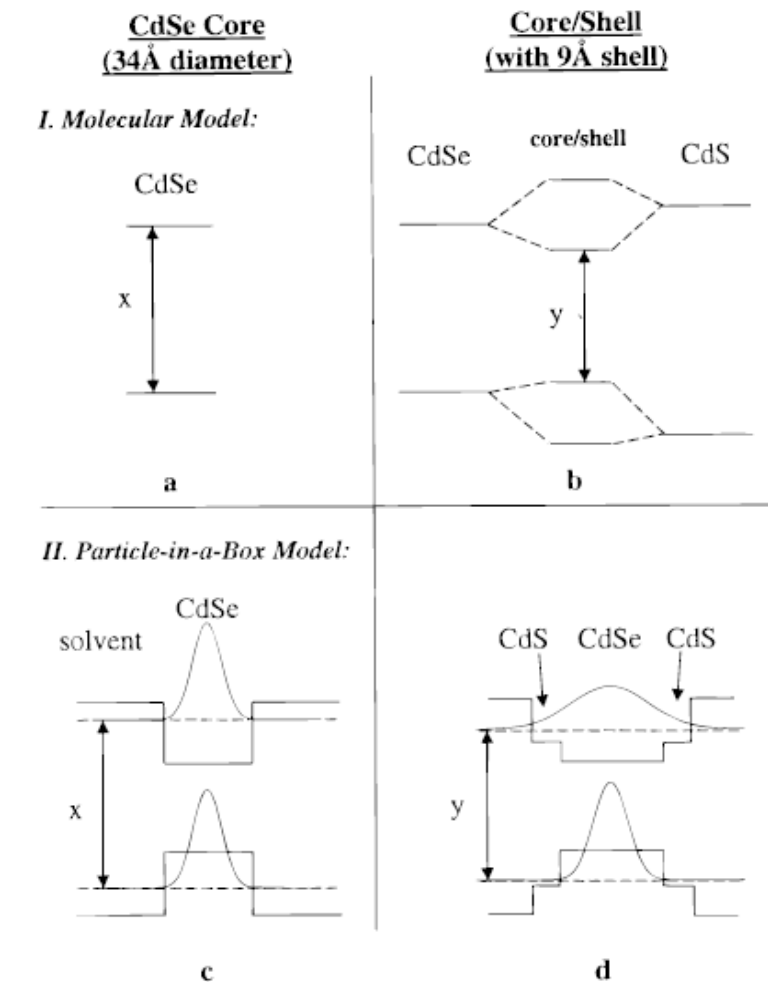
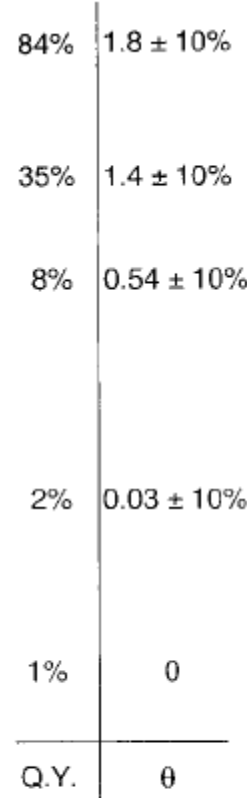
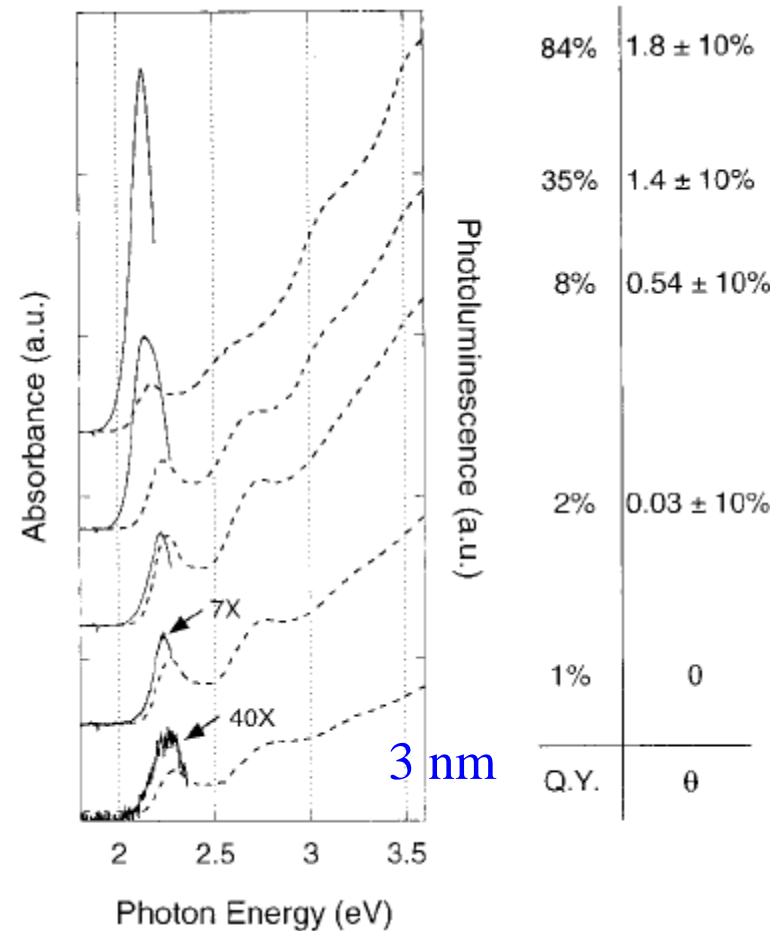
## □ Heterogeneous Nucleation & Growth – Epitaxial Growth



**Figure 11.** Wide-field HRTEMs of core (a) and core/shell (b) nanocrystals synthesized from these cores. The pictures are at the same magnification, indicated by the 100 Å length marker at the bottom. The core diameter is 34 Å and the shell thickness for the core/shell nanocrystals is 9 Å. The core/shell nanocrystals are clearly larger than the cores. Where lattice fringes are observed in the core/shells, they persist throughout the entire nanocrystal, indicating epitaxial growth. (The appearance of lattice fringes for a particular nanocrystal is a result of chance alignment.)

# Synthesis of Nano Materials-0D from liquid (Semiconductor)

## □ Heterogeneous Nucleation & Growth – Epitaxial Growth



# Synthesis of Nano Materials-0D from liquid (Semiconductor)

## □ Heterogeneous Nucleation & Growth

### ii) QD-glasses through sol-gel processing

TOP and TOPO capped CdSe and CdSe@CdS (Murray et al.)

Octylamine instead of ammonia- accelerate gelation kinetics

- passivate the surface of the QD

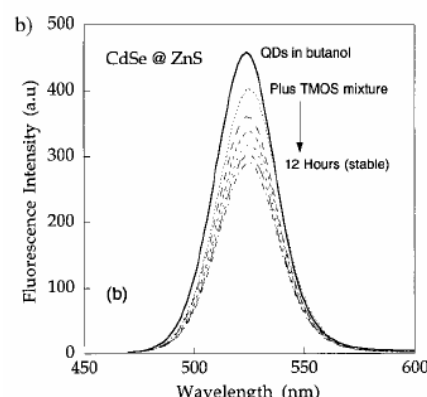
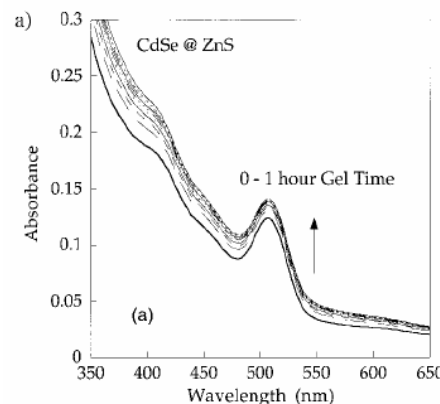


Fig. 1. a) The absorption spectra of CdSe @ ZnS QDs in butanol with octylamine (1 mM) (dark line) and over 1 h after addition of TMOS (0.4 mL to 2.0 mL of QDs). b) The emission spectra as a function of time of the solution in (a). Excitation wavelength 440 nm. There is a slight decrease immediately after addition of the TMOS due to dilution. The emission decreases over some 12 h then stabilizes.

**TMOS**  
(tetramethylorthosilicate)

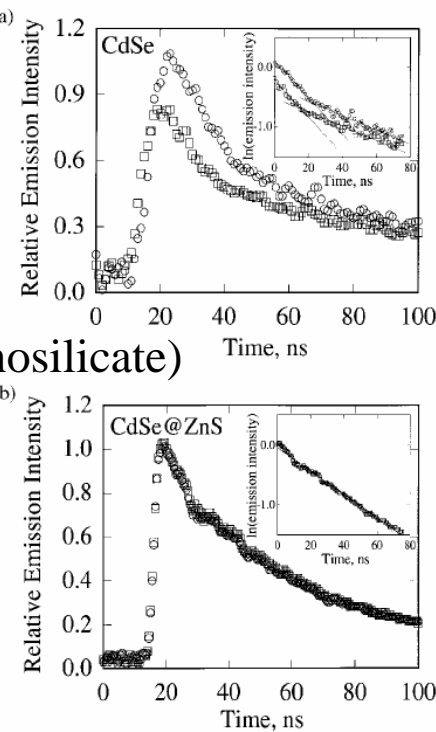


Fig. 2. a) BGL decay from CdSe before (○) and after (□) sol-gel processing. The CdSe BGL decreases during gelation by some 20 % and continues to decrease after gelation until almost gone. The decay kinetics are complex, but do not seem to change with loss of luminescence. b) Normalized BGL decay of CdSe @ ZnS QDs before gelation (○) and after the first 15 min of gelling (□). The decay is first-order and does not change during sol-gel processing, though the QY decreases slowly for the first 12 h before stabilizing. Pump source: 337 nm N<sub>2</sub> laser. Pulsewidth 2 ns



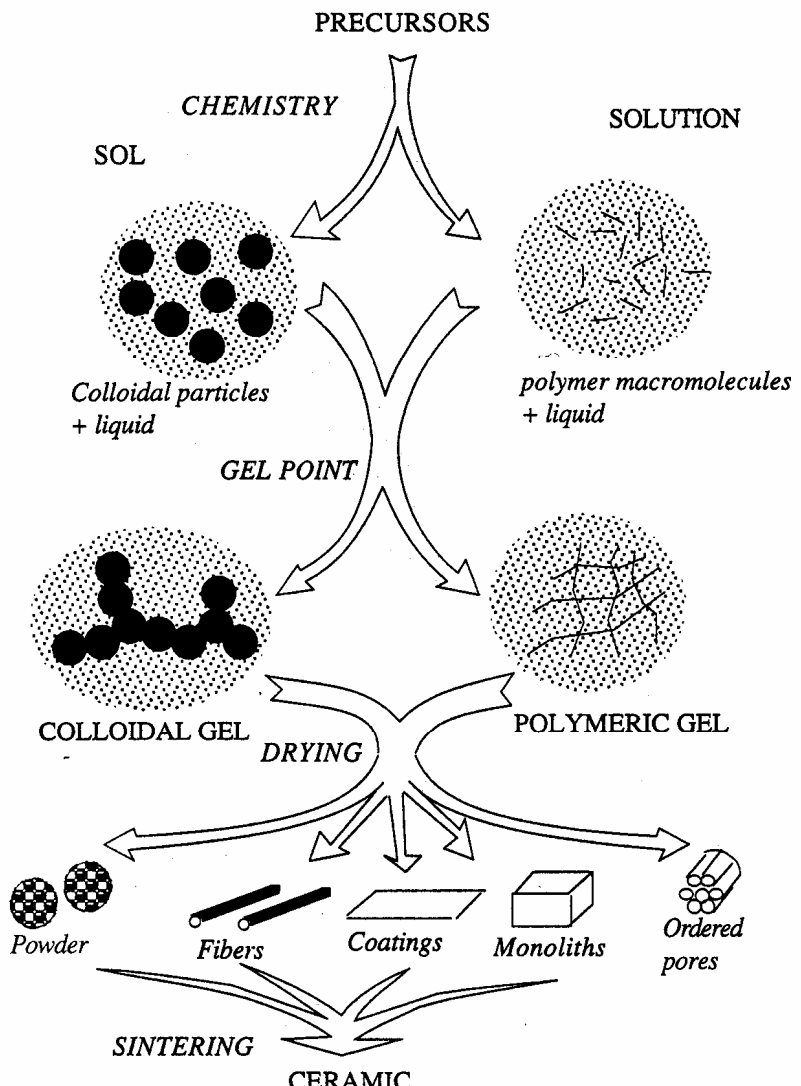
Fig. 3. Luminescence from CdSe @ ZnS QD-glasses formed from TMOS hydrolysis in the presence of octylamine. The gels were 4 days old when photographed under UV light. The QY was estimated to be 0.15 for the red TMOS glasses by comparison to rhodamine (QY = 0.92). Octylamine was used as the surface passivator and sol-gel catalyst. The orange emission was created by mixing red- and green-emitting QDs.

# Synthesis of Nano Materials-0D from liquid (Metal Oxide)

## □ Homogeneous Nucleation & Growth: Sol-Gel Process

- Sol- a stable suspension of colloidal solid particles within a liquid

Gel- an porous 3-D interconnected solid network that expands in a stable fashion throughout a liquid medium and is only limited by the size of the container



# Synthesis of Nano Materials-0D from liquid (Metal Oxide)

## □ Homogeneous Nucleation & Growth: Sol-Gel Process

- Precursors: metal alkoxides

ex)  $\text{Si(OEt)}_4$ ,  $\text{Ti(OPr}^{\text{i}}\text{)}_4$

inorganic & organic salts

ex)  $\text{AlCl}_3$

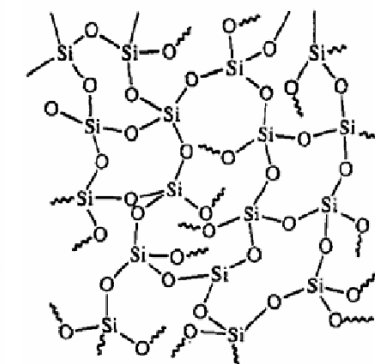
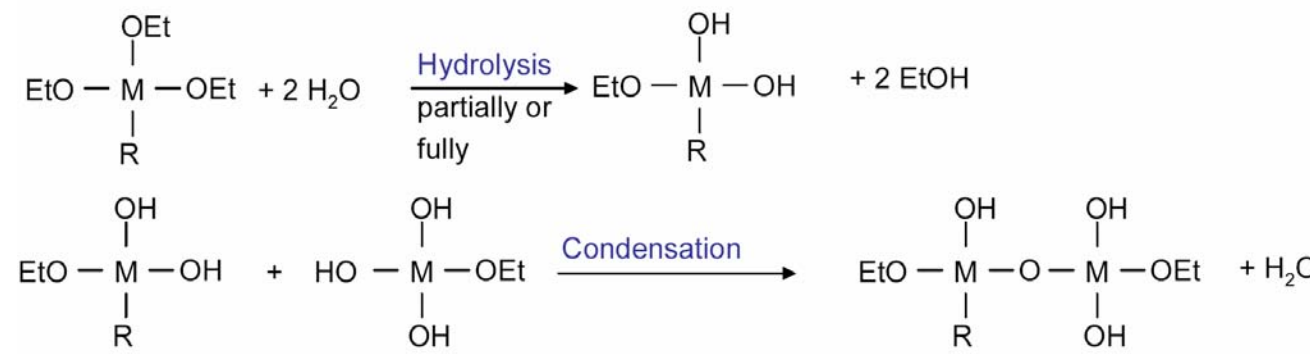
Table 2.5-1 - Nomenclature of alkoxides

alcohol R(OH)	alkoxy ligand to the metal M	alkoxide	abbrevia- tion for OR
methanol $\text{CH}_3\text{OH}$		methoxide	OMe
ethanol $\text{C}_2\text{H}_5\text{OH}$		ethoxide	OEt
1, propanol (n-propanol) $\text{C}_3\text{H}_7\text{OH}$		1-propoxide (n-propoxide)	OPr <sup>i</sup>
2, propanol $\text{C}_3\text{H}_7\text{OH}$ (iso-propanol)		2-propoxide (iso-propoxide)	OPr <sup>s</sup>
1, Butanol (n-butanol) $\text{C}_4\text{H}_9\text{OH}$		1-butoxide (n-butoxide)	OBu <sup>n</sup>
2, Butanol $\text{C}_4\text{H}_9\text{OH}$		2-butoxide (sec-butoxide)	OBu <sup>s</sup>
2, methyl- propanol (iso butanol) $\text{C}_4\text{H}_9\text{OH}$		2, methyl propoxide (iso-butoxide)	OBu <sup>i</sup>
2, methyl- prop,2,ol (tertio butanol) $\text{C}_4\text{H}_9(\text{OH})$		tertio butoxide	OBu <sup>t</sup>

# Synthesis of Nano Materials-0D from liquid (Metal Oxide)

## □ Homogeneous Nucleation & Growth: Sol-Gel Process

- Hydrolysis and condensation



- Reactivity: larger ionic radius of M → fast

**Table 3.3.** Electronegativity,  $\chi$ , partial charge,  $\delta M$ , ionic radius,  $r$ , and coordination number,  $n$ , of some tetravalent metals.<sup>77</sup>

Alkoxide	$\chi$	$\delta M$	$r(\text{\AA})$	$n$
$\text{Si}(\text{OPr}^i)_4$	1.74	+0.32	0.40	4
$\text{Ti}(\text{OPr}^i)_4$	1.32	+0.60	0.64	6
$\text{Zr}(\text{OPr}^i)_4$	1.29	+0.64	0.87	7
$\text{Ce}(\text{OPr}^i)_4$	1.17	+0.75	1.02	8

# Synthesis of Nano Materials-0D from liquid (Metal Oxide)

## □ Homogeneous Nucleation & Growth: Sol-Gel Process

- Control the reactivity: different organic ligand
  - ex)  $\text{Si}(\text{OC}_2\text{H}_5)_4$  is less reactive than  $\text{Si}(\text{OCH}_3)_4$
  - coordination state control with chelating agent such as acetylacetone
  - multistep sol-gel processing (less reactive precursors is first partially hydrolyzed)
- Organic-inorganic hybrids: co-polymerize or co-condense
  - trap organic inside inorganic network

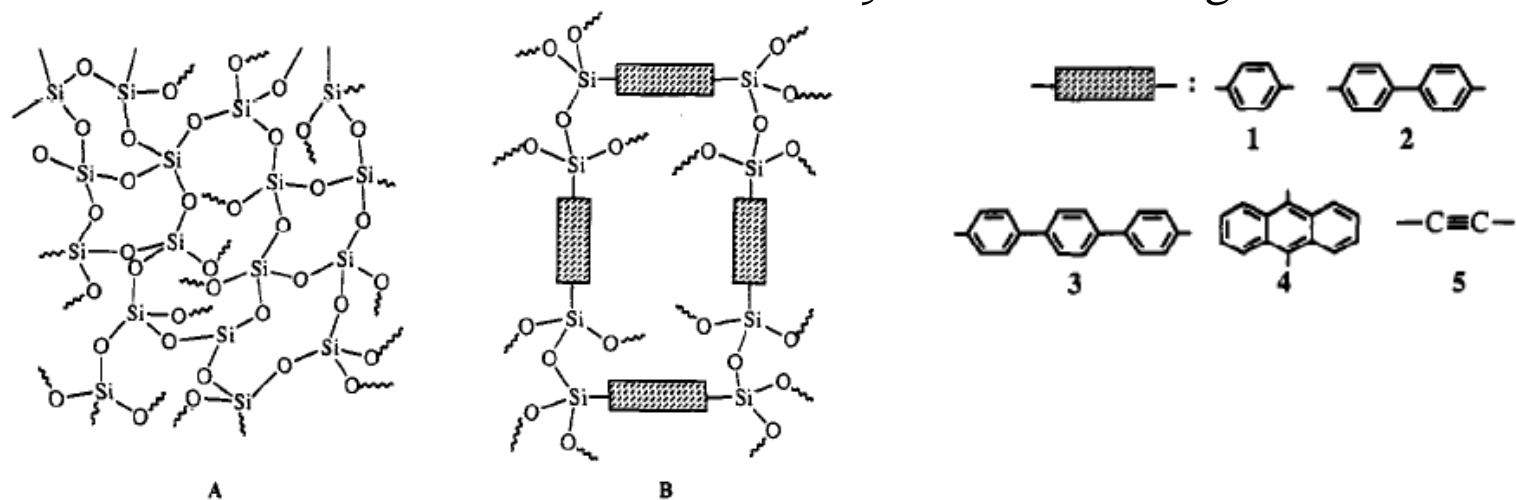


Figure 1. Amorphous silica A and bridged polysilsesquioxane B.

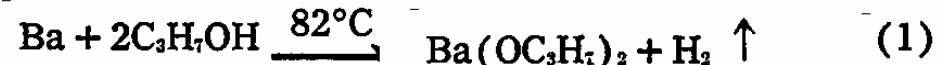
K. Shea, J. Am. Chem. Soc. 114, 6700 (1992).

# Synthesis of Nano Materials-0D from liquid (Metal Oxide)

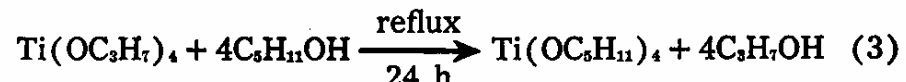
## □ Homogeneous Nucleation & Growth: Sol-Gel Process

- BaTiO<sub>3</sub>

Barium bis isopropoxide



Titanium tetrakis tertiary amyloxide



Dissolved in C<sub>3</sub>H<sub>7</sub>OH or C<sub>6</sub>H<sub>6</sub> →

Hydrolysis by adding water

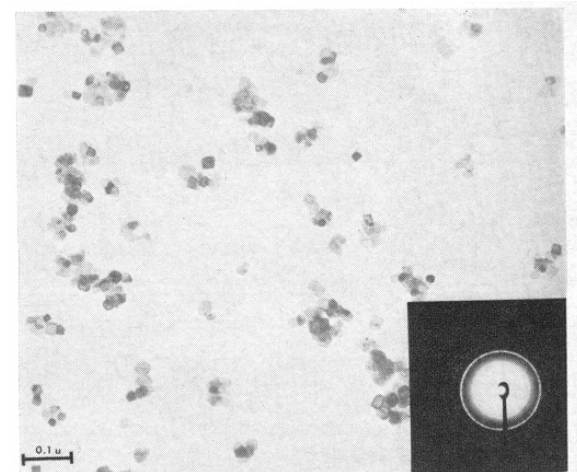
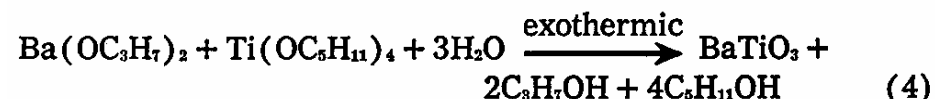


Fig. 2. Electron micrograph of BaTiO<sub>3</sub> calcined at 700°C.

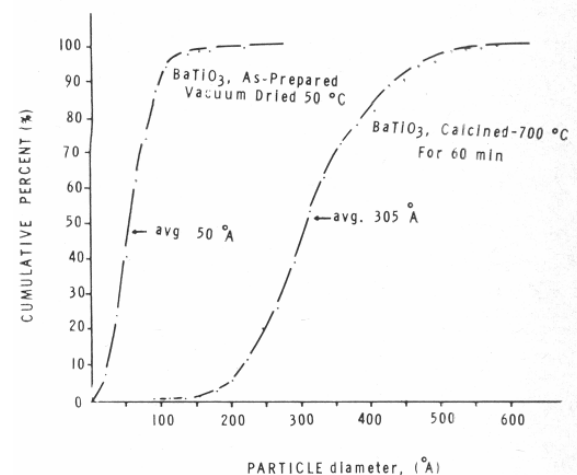


Fig. 3. Particle size distribution of high-purity BaTiO<sub>3</sub>.

## 33 Nanomaterials

K. S. Mazdiyasni, J.Am.Ceram.Soc., 52 (1969) 523

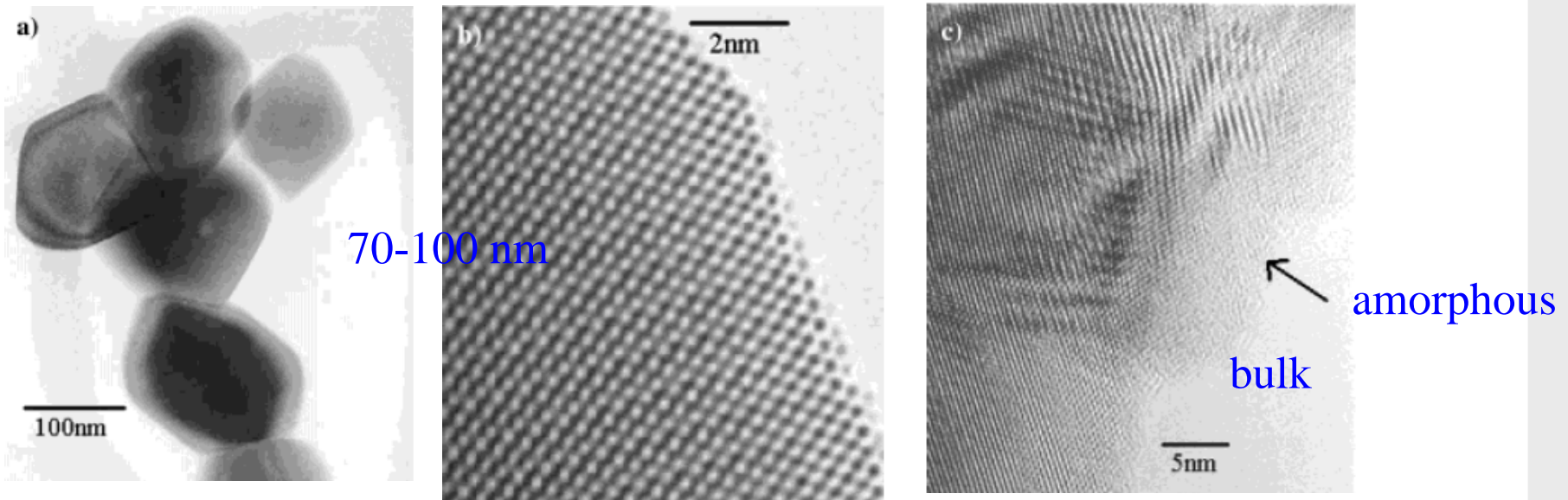
## Synthesis of Nano Materials-0D from liquid (Metal Oxide)

### □ Homogeneous Nucleation & Growth: Sol-Gel Process

- Controlled release of ions

$\text{Y}_2\text{O}_3:\text{Eu}$  (3 mol%)

yttrium and europium chlorides in water, pH~1 by HCl and KOH  
add excess of urea (15x), raise to  $> 80^\circ\text{C}$  for 2 h, pH reach  $\sim 4\sim 5$   
fire  $> 1000^\circ\text{C}$



# Synthesis of Nano Materials-0D from liquid (Metal Oxide)

## □ Homogeneous Nucleation & Growth: Sol-Gel Process

- Effect of anions on morphology

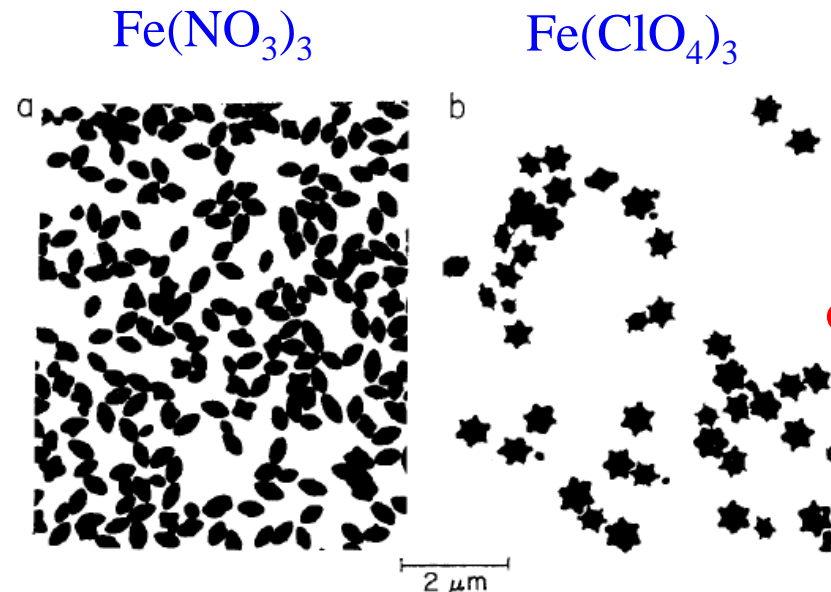


FIG. 1. Electron micrographs of particles obtained by aging two different solutions of ferric salt at 100°C for 24 hr; in both cases the original pH was 1.3–1.4 and the final pH was 1.1–1.2. Concentrations: (a) System  $\text{Fe}(\text{NO}_3)_3 + \text{HNO}_3$ :  $[\text{Fe}^{3+}]$ , 0.018 M;  $[\text{NO}_3^-]$ , 0.104 M. (b) System  $\text{Fe}(\text{ClO}_4)_3 + \text{HCl}$ :  $[\text{Fe}^{3+}]$ , 0.018 M;  $[\text{ClO}_4^-]$ , 0.104 M.

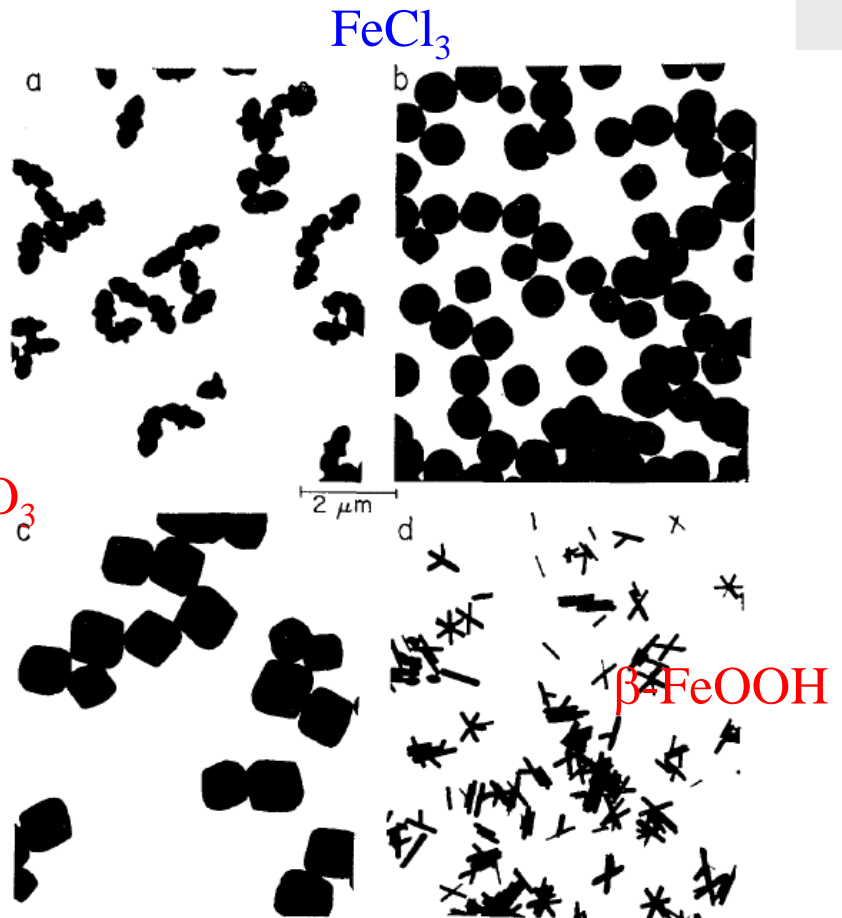


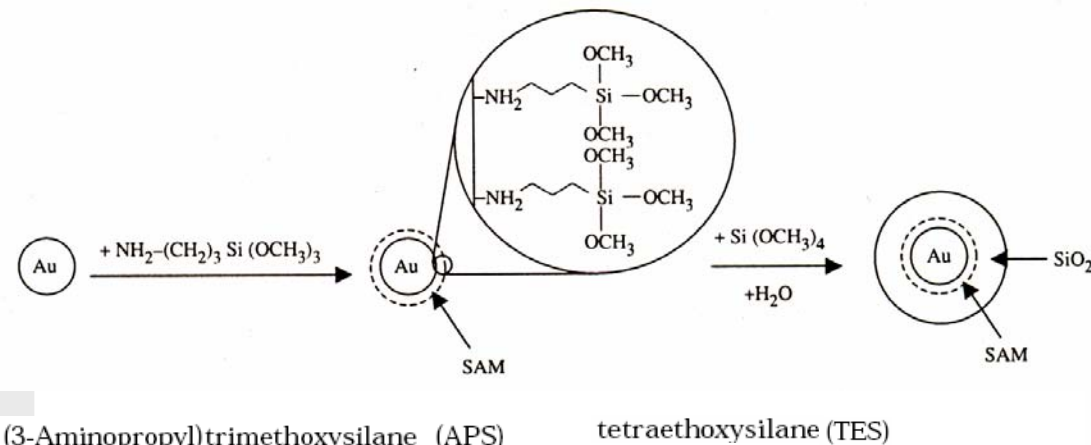
FIG. 2. Electron micrographs of particles obtained in solutions of  $\text{FeCl}_3 + \text{HCl}$  under the following conditions:

# Synthesis of Nano Materials-0D from liquid (Metal Oxide)

## □ Heterogeneous Nucleation & Growth: Sol-Gel Process

- Silica coating on other nanoparticles (metals, iron oxides, semiconductors)

Ex )  $\text{SiO}_2$  coating on Au



silane coupling agent

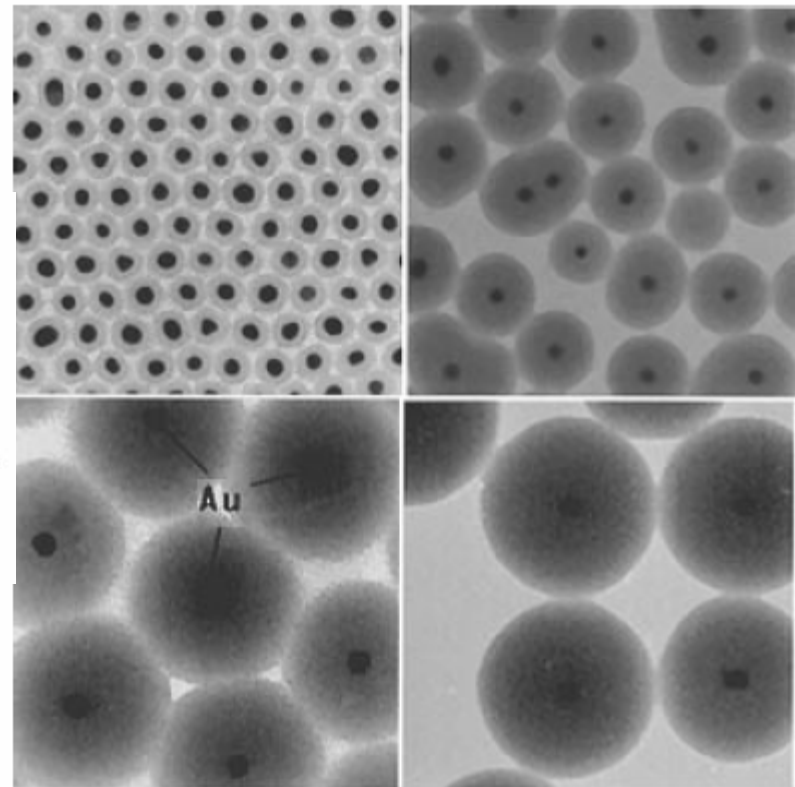


**Figure 4.** Transmission electron micrographs of silica-coated gold particles produced during the extensive growth of the silica shell around 15 nm Au particles with TES in 4:1 ethanol/water mixtures. The shell thicknesses are (a, top left) 10 nm, (b, top right) 23 nm, (c, bottom left) 58 nm, and (d, bottom right) 83 nm.

# Synthesis of Nano Materials-0D from liquid (Metal Oxide)

## □ Heterogeneous Nucleation & Growth: Sol-Gel Process

- Silica coating on Au

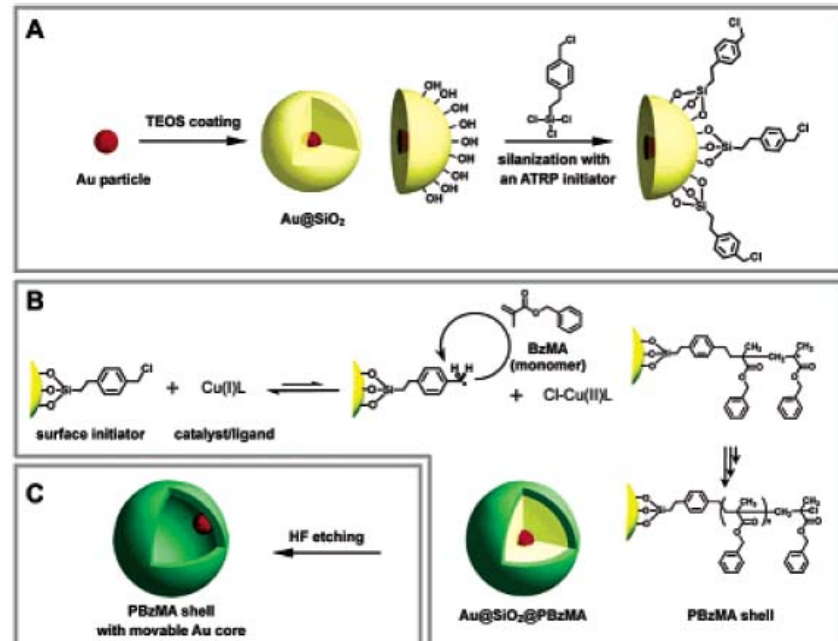


**Figure 1.** Schematic procedure used to generate PBzMA hollow beads containing movable gold cores.

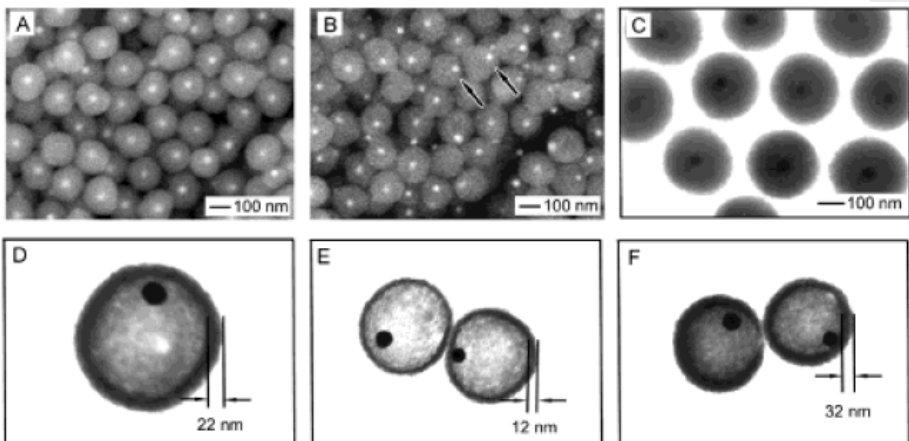


**Figure 2.** (A, B) Backscattering SEM and (C, D) TEM images of Au@SiO<sub>2</sub>@PBzMA particles before (A, C) and after (B, D) HF etching. The polymerization time was 4 h, and the polymer shell was  $\sim 22$  nm thick. (E, F) TEM images of Au@Air@PBzMA particles synthesized using different polymerization times: (E) 3 h and (F) 6 h. The polymer shells were  $\sim 12$  and  $\sim 32$  nm in thickness, respectively.

# Synthesis of Nano Materials-0D from liquid (Metal Oxide)

## □ Heterogeneous Nucleation & Growth: Sol-Gel Process

- Silica coating on  $\text{Fe}_3\text{O}_4$

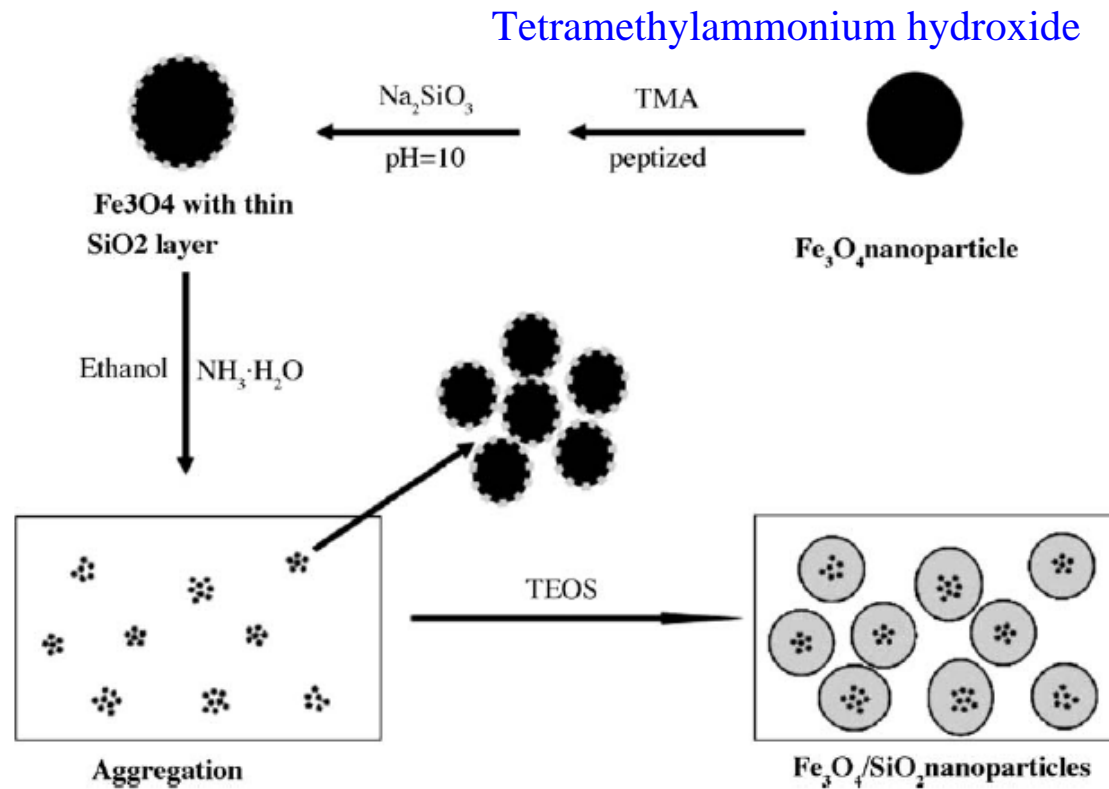
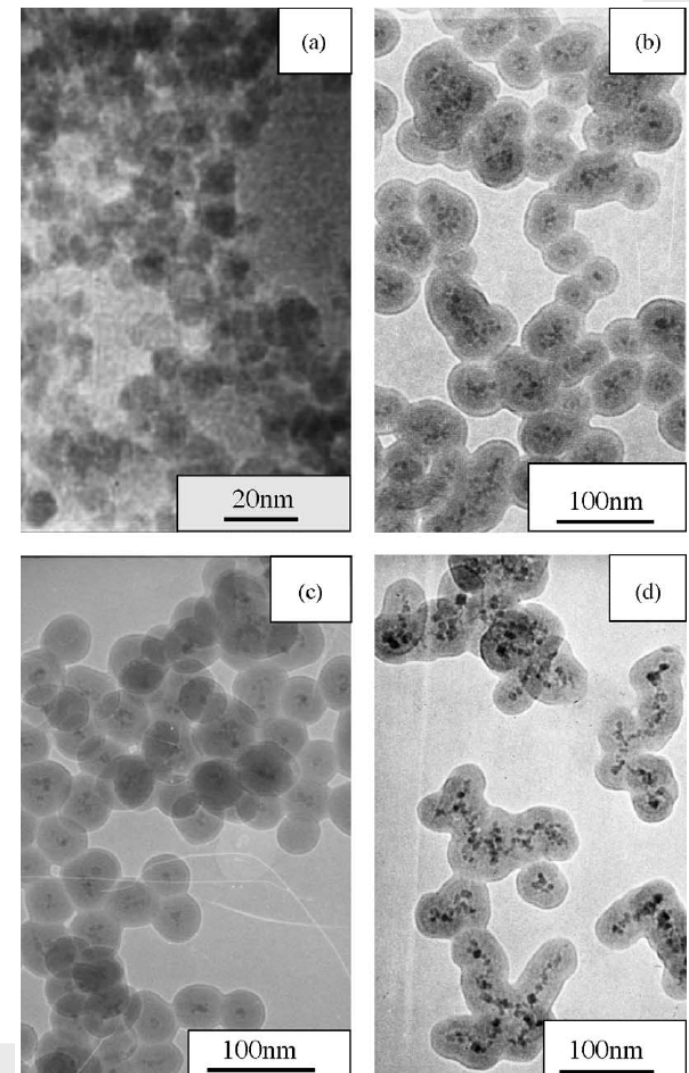


Fig. 1. Schematic illustration of the synthetic process of  $\text{Fe}_3\text{O}_4/\text{SiO}_2$  core/shell nanoparticles.

## 38 Nanomaterials

Z. Lu, Colloid and Surface 278 (2006) 140.



# Synthesis of Nano Materials-0D from liquid (Metal Oxide)

## □ Nonaqueous Sol-Gel Routes

- Surfactant-controlled Synthesis

ex)  $\gamma\text{-Fe}_2\text{O}_3$

1.  $\text{Fe}(\text{CO})_5 \rightarrow$  octyl ether+oleic acid at  $100^\circ\text{C}$ , reflux for 1h  
add  $(\text{CH}_3)_3\text{NO}$ , heated at  $130^\circ\text{C}$ , reflux for 1h
2.  $\text{Fe}(\text{CO})_5$  injected to lauric acid+octyl ether+  $(\text{CH}_3)_3\text{NO}$  at  $100^\circ\text{C}$   
reflux at  $120^\circ\text{C}$  for 1h

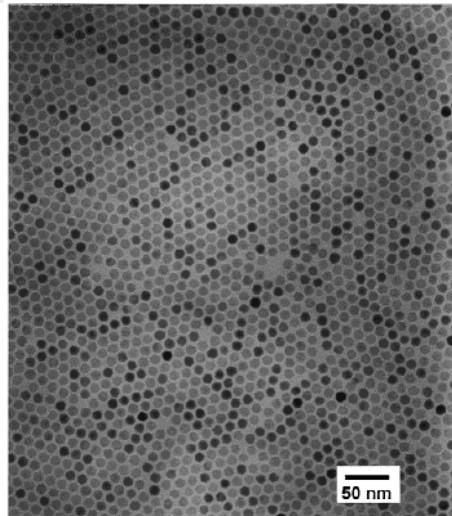


Figure 1. TEM image of a two-dimensional hexagonal assembly of 11 nm  $\gamma\text{-Fe}_2\text{O}_3$  nanocrystallites.

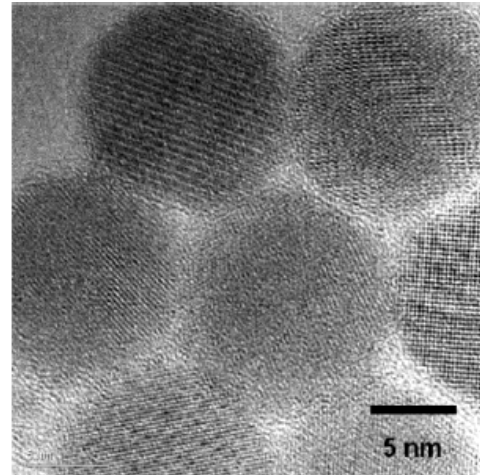


Figure 2. High-resolution TEM image of 2D hexagonally close-packed 11 nm  $\gamma\text{-Fe}_2\text{O}_3$  nanocrystallites.

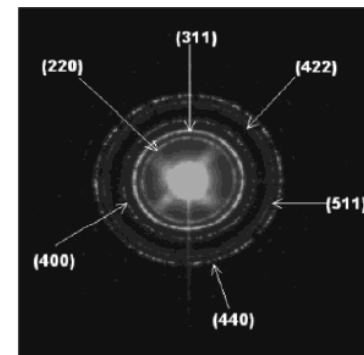


Figure 3. Electron diffraction pattern of 11 nm  $\gamma\text{-Fe}_2\text{O}_3$  nanocrystallites.

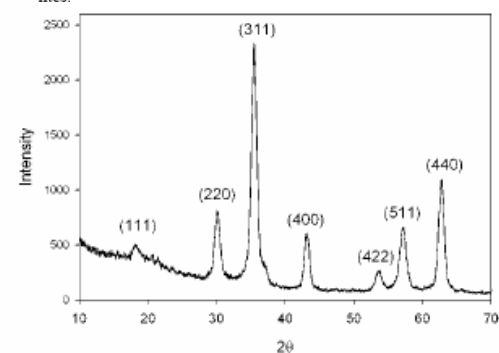
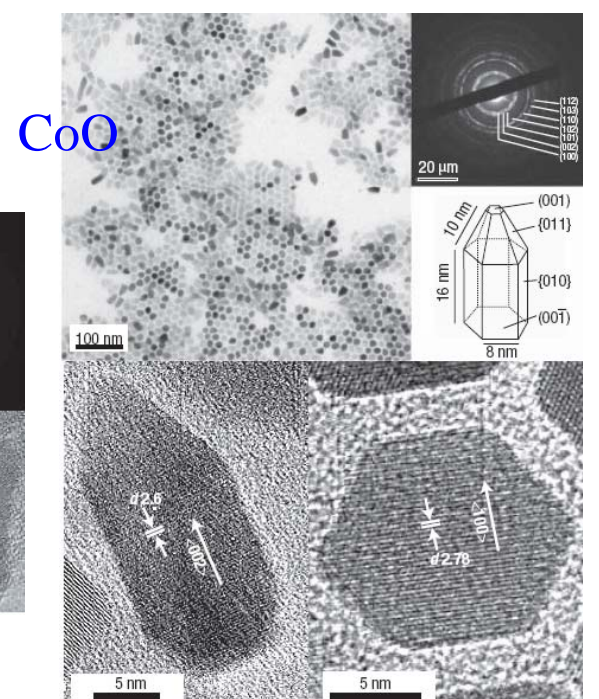
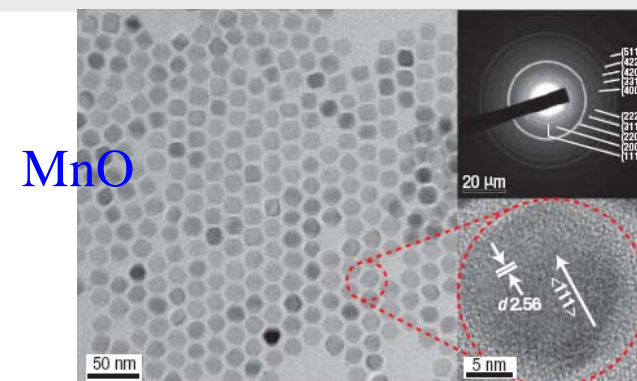
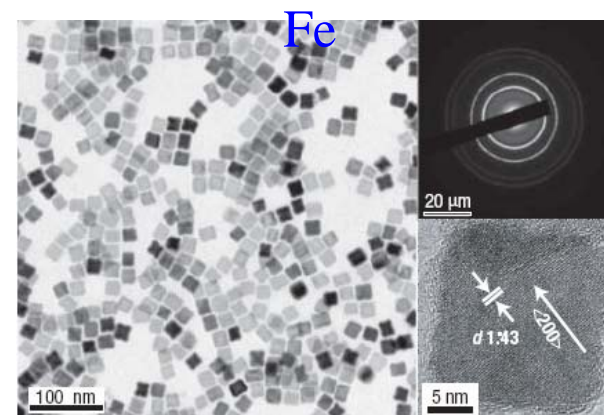
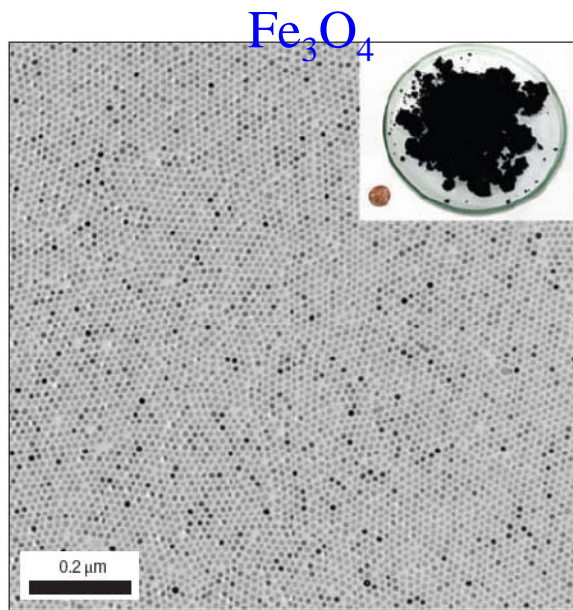
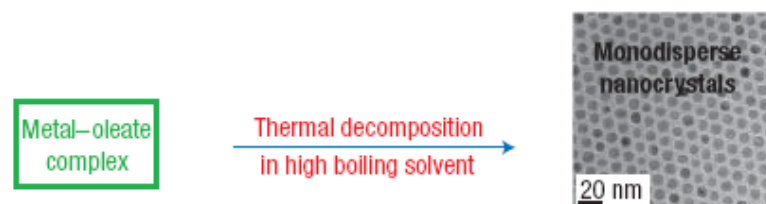


Figure 4. X-ray diffraction pattern of 11 nm  $\gamma\text{-Fe}_2\text{O}_3$  nanocrystallites.

# Synthesis of Nano Materials-0D from liquid (Metal Oxide)

## □ Nonaqueous Sol-Gel Routes

- Surfactant-controlled Synthesis



# Synthesis of Nano Materials-0D from liquid (Metal Oxide)

## □ Nonaqueous Sol-Gel Routes

### - Surfactant-controlled Synthesis

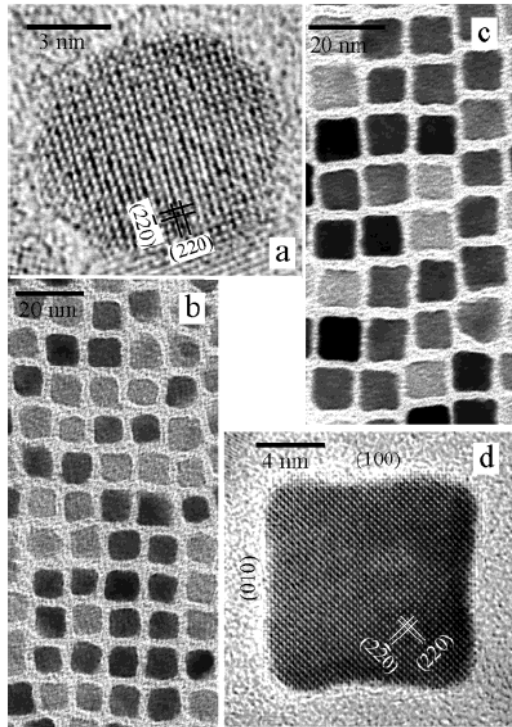


**Figure 2.** HRTEM micrographs. Panel (a) is a  $\sim 8$  nm spherical  $\text{CoFe}_2\text{O}_4$  nanocrystal. Panels (b) and (c) display the short-range order in  $\sim 9$  and  $\sim 11$  nm nanocube assemblies. Panel (d) shows a  $\sim 12$  nm cubic  $\text{CoFe}_2\text{O}_4$  nanocrystal. The spacing of atomic lattice plane (220) in panels (a) and (d) is  $2.994 \text{ \AA}$ , and the zone-axis is [001].

### 41 Nanomaterials

Q. Song, J. Am. Chem. Soc. 126 (2004) 6164.

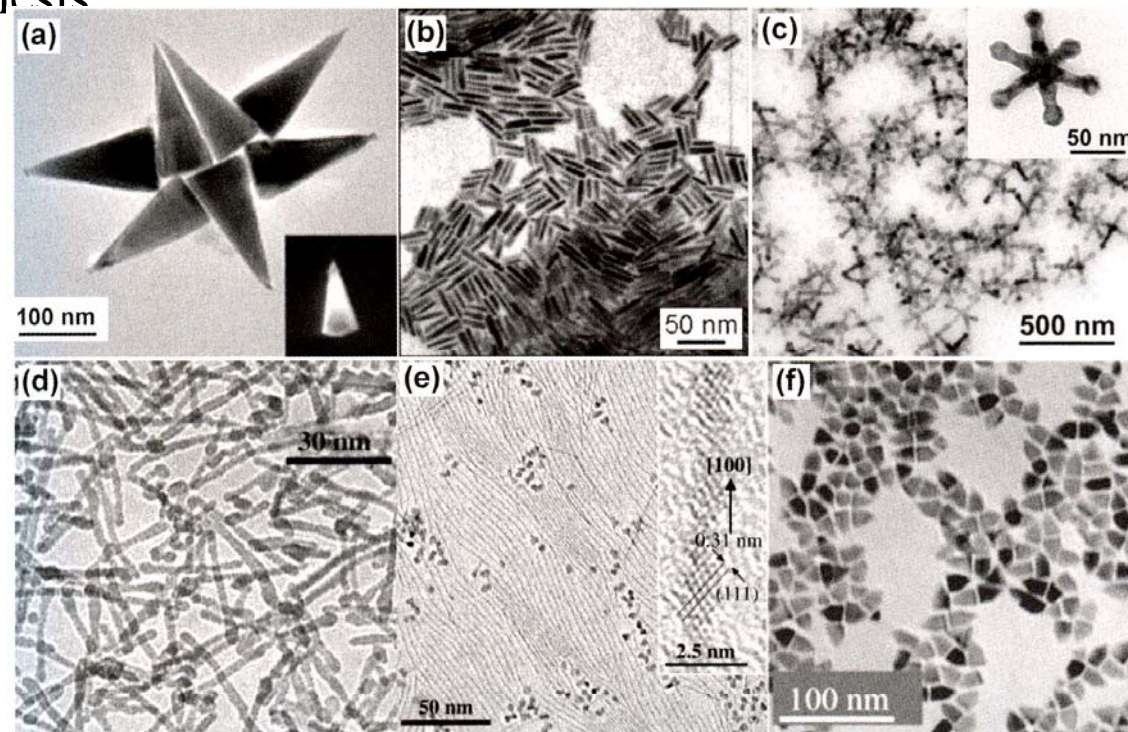


**Fig. 3.3** (a) TEM image of cone-like  $\text{ZnO}$  nanocrystals (inset: dark field TEM image of one crystal). Image taken from Ref. [38] with permission of Wiley-VCH. (b) TEM image of tungsten oxide nanorods. Image taken from Ref. [39] with permission of the American Chemical Society. (c) TEM image of  $\text{MnO}$  multipods (inset: hexapod). Images taken from Ref. [40] with permission of the

American Chemical Society. (d) TEM image of  $\text{TiO}_2$  nanorods. Image taken from Ref. [42] with permission of Wiley-VCH. (e) TEM image of ceria nanowires (inset: HRTEM image of one nanowire). Image taken from Ref. [43] with permission of Wiley-VCH. (f) TEM image of  $\text{Co}_3\text{O}_4$  nanocrystals. Image taken from Ref. [44] with permission of the American Chemical Society.

C.N.R.Rao, Nanomaterials Chemistry, 2007.

Table 3.1 Selected examples of metal oxide nanoparticles synthesized via nonaqueous and surfactant-controlled processes.

Metal Oxide	Precursors	Solvents and surfactants	Temperature	Product morphology	Reference
Cu <sub>2</sub> O	copper acetate	OLA, TOA	270 °C	spherical	47
γ-Fe <sub>2</sub> O <sub>3</sub>	M(Cup) <sub>3</sub>	OA	300 °C	spherical	48
γ-Fe <sub>2</sub> O <sub>3</sub>	Fe(CO) <sub>5</sub>	octyl ether, OLA or LA	300 °C	spherical	32
Fe <sub>3</sub> O <sub>4</sub>	Fe(acac) <sub>3</sub>	2-pyrrolidone	reflux	spherical	49
Fe <sub>3</sub> O <sub>4</sub> , MFe <sub>2</sub> O <sub>4</sub> (M = Fe, Co, Mn)	Fe(acac) <sub>3</sub> M(acac) <sub>2</sub>	polyalcohols, OLA, OA	305 °C	spherical	50
HfO <sub>2</sub>	Hf(OiPr) <sub>4</sub> and HfCl <sub>4</sub>	TOPO	360 °C	spherical and nanorods	51
In <sub>2</sub> O <sub>3</sub>	In(acac) <sub>3</sub>	OA	250 °C	spherical	52
MnO, Mn <sub>3</sub> O <sub>4</sub>	Mn(acac) <sub>2</sub>	OA	180 °C	spherical	53
SnO <sub>2</sub> , ZnO	tin or zinc 2-ethylhexanoate	diphenyl ether and various amines	230–250 °C	spherical	54
TiO <sub>2</sub>	TiCl <sub>4</sub> and Ti(OiPr) <sub>4</sub>	diethyl ether TOPO, LA	300 °C	bullet-shaped to nanorods	55
TiO <sub>2</sub>	Ti(COT) <sub>2</sub>	DMSO, TBP or TBPO or TOPO	120 °C	spherical	56
TiO <sub>2</sub>	Ti(OiPr) <sub>4</sub>	1-octadecene, OLA and OA	260 °C	nanorods	57
W <sub>18</sub> O <sub>49</sub>	W(CO) <sub>6</sub>	OA	270 °C	nanorods	58
ZnO	diethyl zinc	decane, octylamine, TOPO	200 °C	spherical	59
ZnO	zinc acetate	various alkylamines, <i>tert</i> -butylphosphonic acid	220–300 °C	spherical	60
ZrO <sub>2</sub>	Zr(OiPr) <sub>4</sub> and ZrCl <sub>4</sub>	TOPO	340 °C	spherical	61

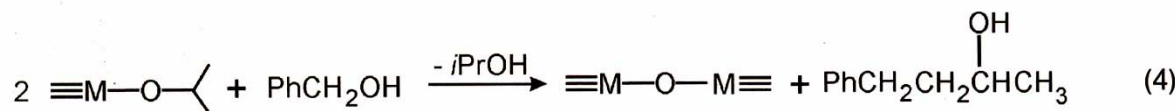
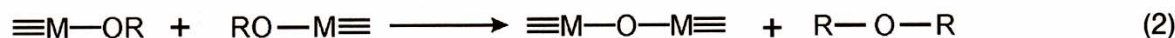
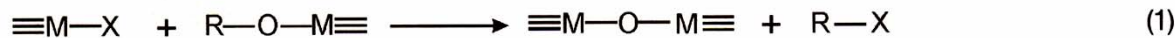
Abbreviations: TOPO: Trioctylphosphine oxide; LA: lauric acid; COT: cyclooctatetraene; DMSO: dimethyl sulfoxide; TBP: tributylphosphine; TBPO: tributylphosphine oxide; OLA: oleic acid; OA: oleylamine; acac: acetylacetone; Cup: N-nitrosophenylhydroxylamine; TOA: trioctylamine.

# Synthesis of Nano Materials-0D from liquid (Metal Oxide)

## □ Nonaqueous Sol-Gel Routes

- Solvent-controlled Synthesis

- i) metal halides with alcohols
- ii) metal alkoxides with alcohols
- iii) metal alkoxides with ketones and aldehydes
- iv) metal acetylacetonates with organic solvents



**Scheme 3.1** Selected reaction pathways to metal oxide formation in nonaqueous systems. Eq. (1): Alkyl halide elimination, Eq. (2): ether elimination, Eq. (3): ester elimination, Eq. (4): C-C bond formation between benzylic alcohols and alkoxides, Eq. (5): aldol-like condensation reactions.

# Synthesis of Nano Materials-0D from liquid (Metal Oxide)

## □ Nonaqueous Sol-Gel Routes

i) metal halides with alcohols

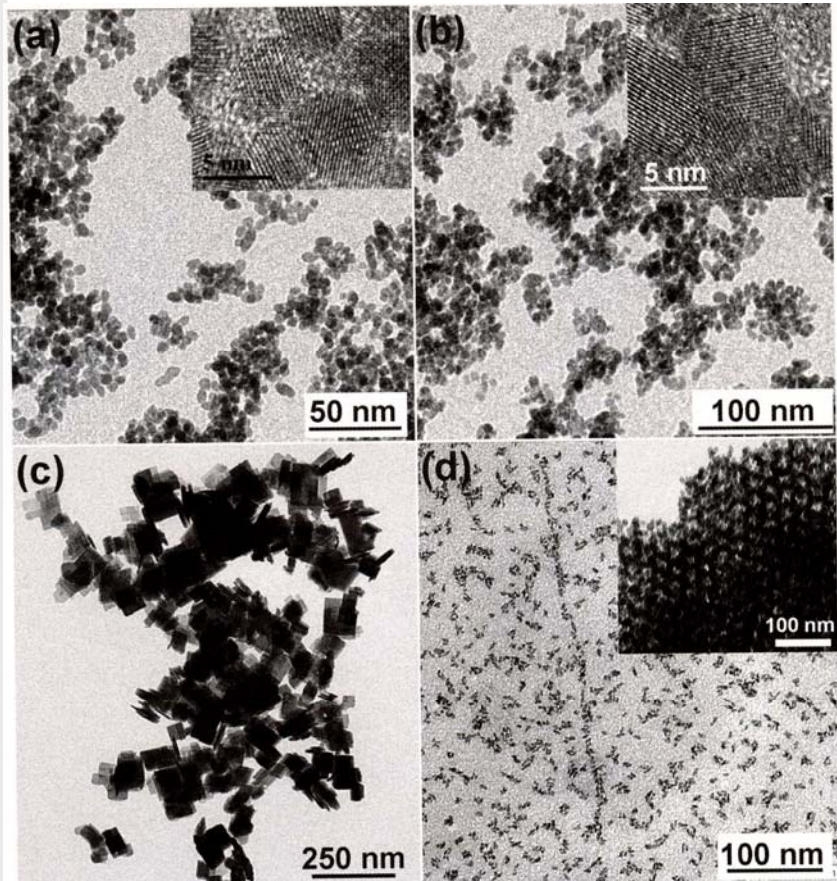


**Fig. 3.4** TEM images of various metal oxide nanoparticles prepared from the corresponding metal chlorides in benzyl alcohol. (a)  $\text{HfO}_2$ , inset: HRTEM image; (b)  $\text{Ta}_2\text{O}_5$ , inset: HRTEM image; (c)  $\text{WO}_3 \cdot \text{H}_2\text{O}$ ; (d)  $\text{SnO}_2$ , inset:  $\text{SnO}_2$  nanoparticles assembled into mesoporous materials after calcination.

ii) metal alkoxides with alcohols

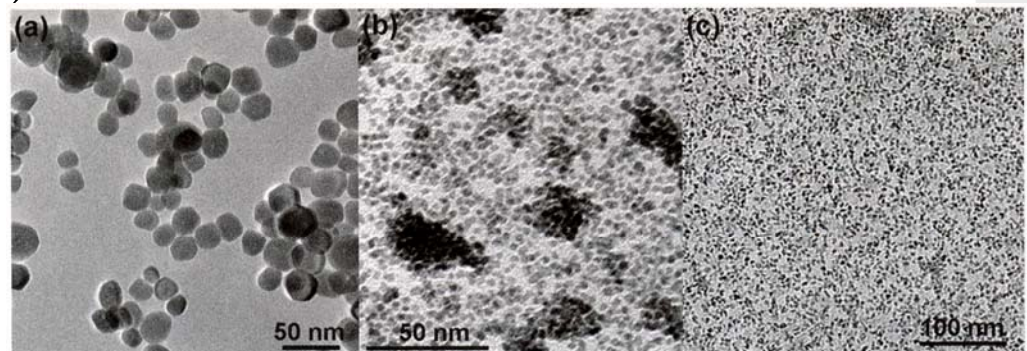


**Fig. 3.6** TEM overview images of (a)  $\text{In}_2\text{O}_3$ , (b)  $\text{CeO}_2$ , and (c)  $\text{BaTiO}_3$  nanocrystals obtained from the reaction of the metal alkoxides with benzyl alcohol.

iv) metal acetylacetones with organic solvents

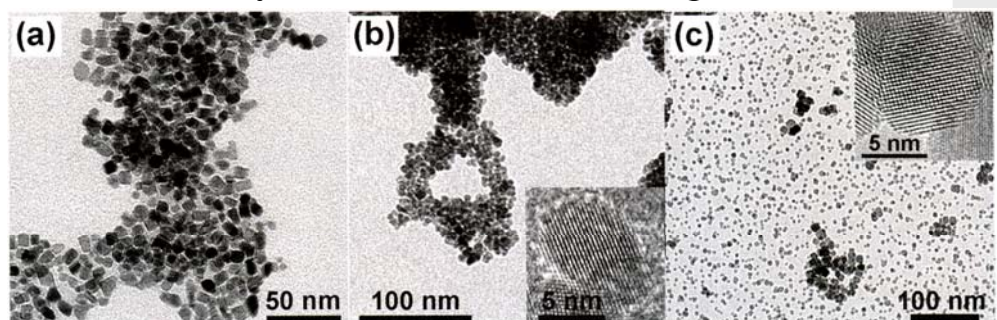
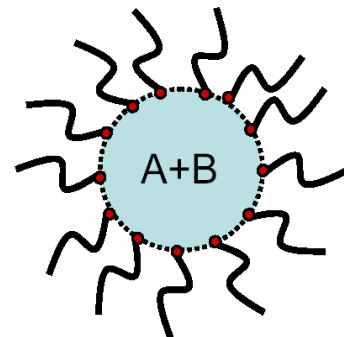


**Fig. 3.8** TEM overview images of (a)  $\text{In}_2\text{O}_3$  nanoparticles obtained from indium acetylacetonate and benzylamine, (b)  $\text{In}_2\text{O}_3$  synthesized from indium acetylacetonate and acetonitrile, inset: HRTEM of one particle, (c)  $\text{SnO}_2$ -doped  $\text{In}_2\text{O}_3$  (10 wt%  $\text{SnO}_2$ ), inset: HRTEM of one particle.

# Synthesis of Nano Materials-0D from liquid (Polymer)

## □ Suspension Polymerization

Intense Mechanical Stirring with Homogenizers or Ultrasonication



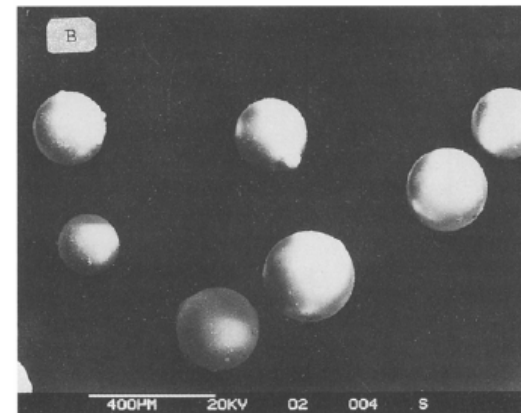
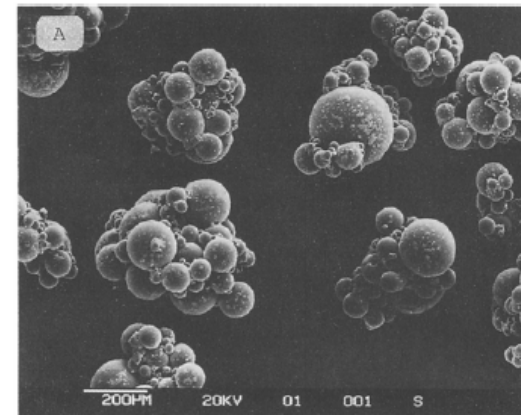
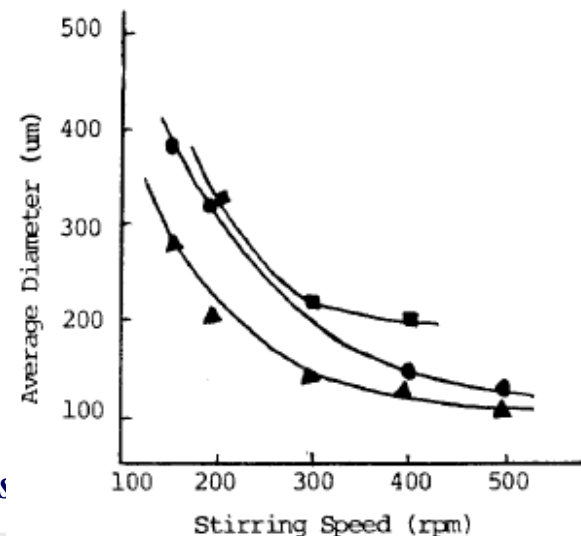
Initiator: soluble in monomer

Initiator, Monomer:

insoluble in the solvent

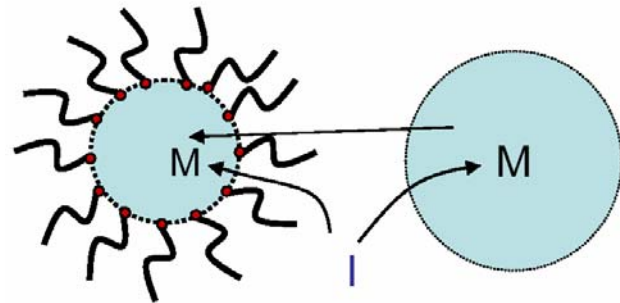
Surfactant used for stabilization

→ Polydisperse colloids obtained



# Synthesis of Nano Materials-0D from liquid (Polymer)

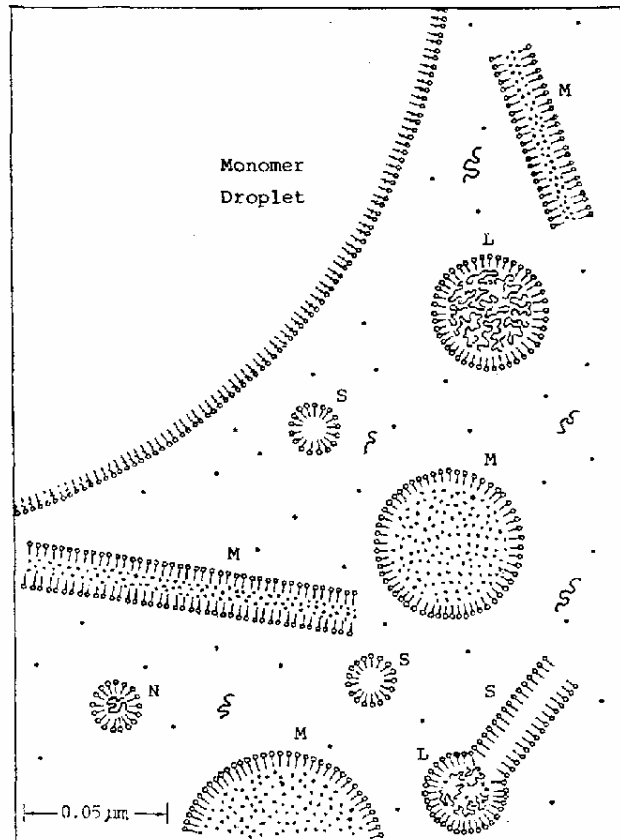
## □ Emulsion Polymerization



Initiator: soluble in the solvent

Monomer: insoluble in the solvent  
existing in emulsifiers

→ Uniform colloids obtainable



• = Monomer molecule, M = Monomer containing micelle  
S = Soap micelle, L = Growing latex particle  
N = Polymer nucleus, S = Growing macroradicals

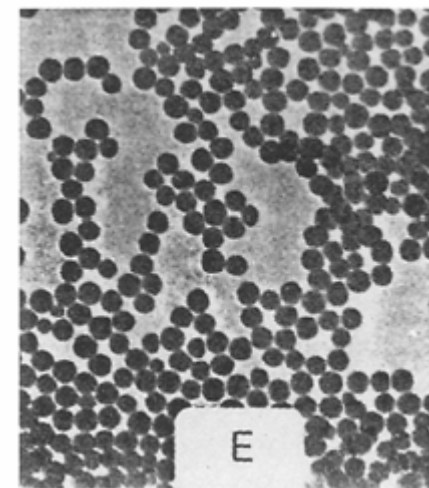
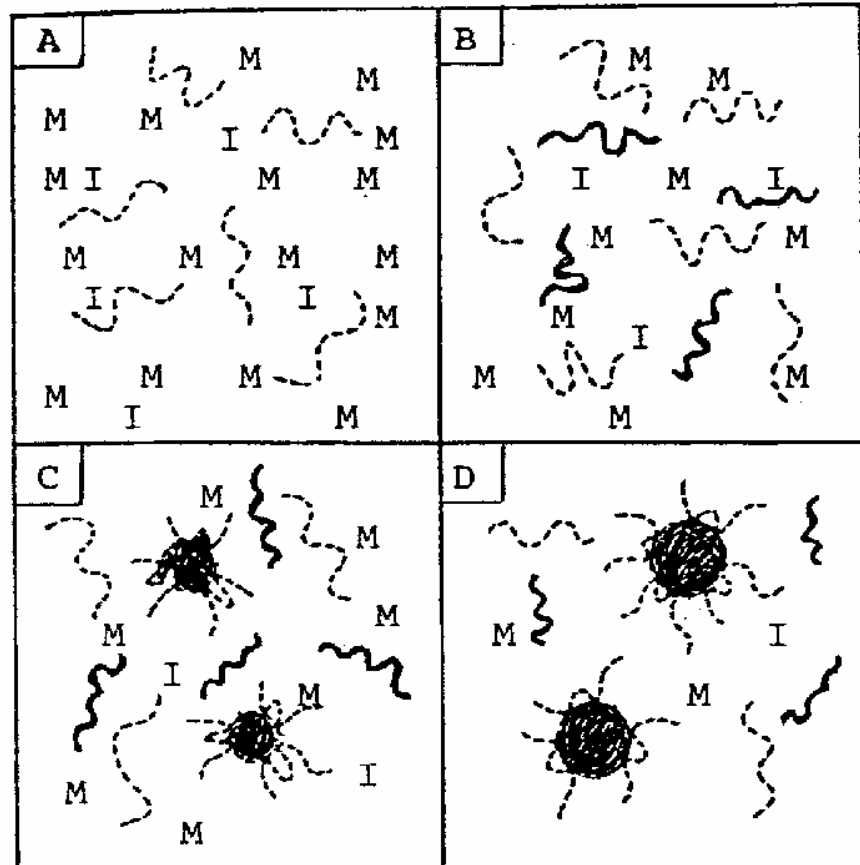


Fig. 8. Polyvinyltoluene particles produced by emulsion polymerization at 23 °C (A), 50 °C (B), 70 °C (D), and 80 °C (E) [84]

## Synthesis of Nano Materials-0D from liquid (Polymer)

### □ Dispersion Polymerization



Initiator, Monomer: soluble in the solvent  
, but polymers are insoluble

Surfactant used

→ Uniform colloids obtainable

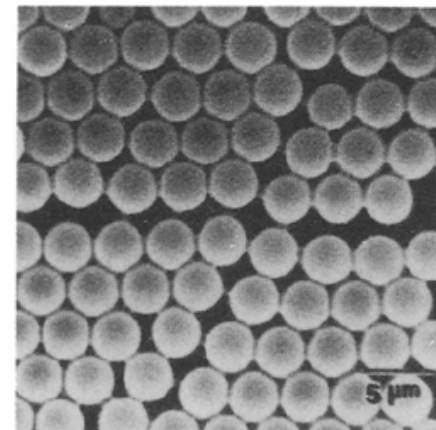
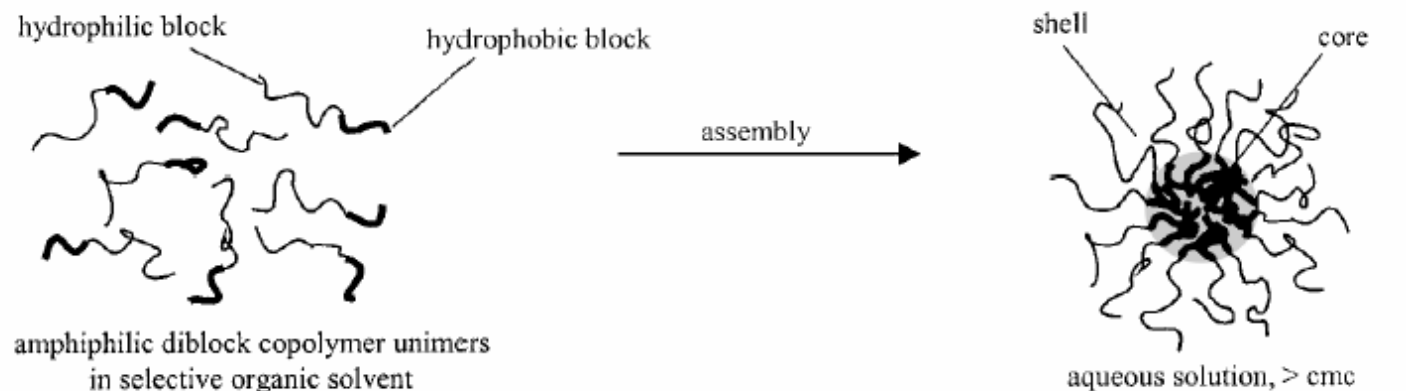


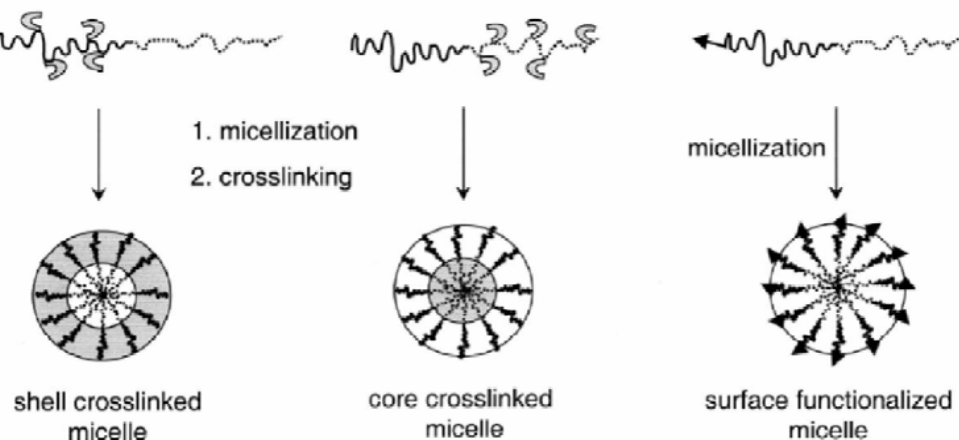
Fig. 11. Polystyrene particles produced by dispersion polymerization in ethanol in the presence of polyvinylpyrrolidone (PVP) and different costabilizers (AOT, aerosol OT) (from [42])

# Synthesis of Nano Materials-0D from liquid (Polymer)

## □ Amphiphilic Block Copolymer Colloids

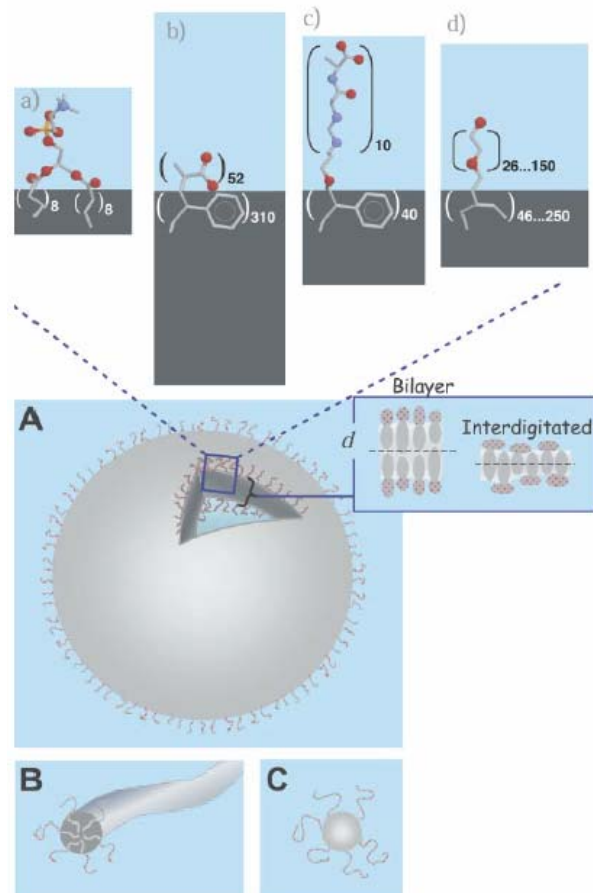


Self-assembly of amphiphilic block copolymers and their functionalization



# Synthesis of Nano Materials-0D from liquid (Polymer)

## □ Vesicles from Amphiphilic Block Copolymers

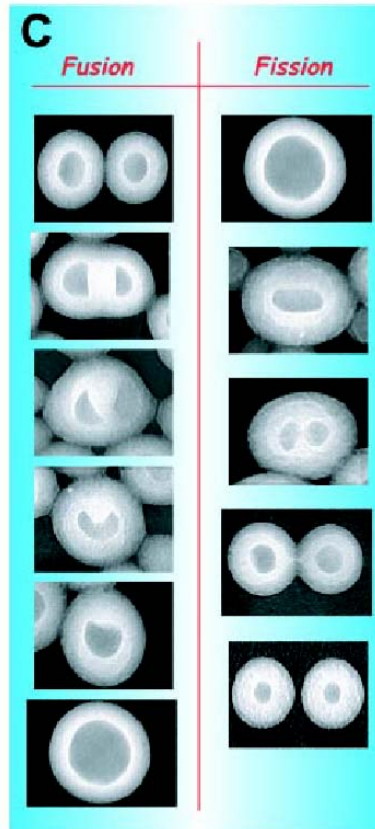
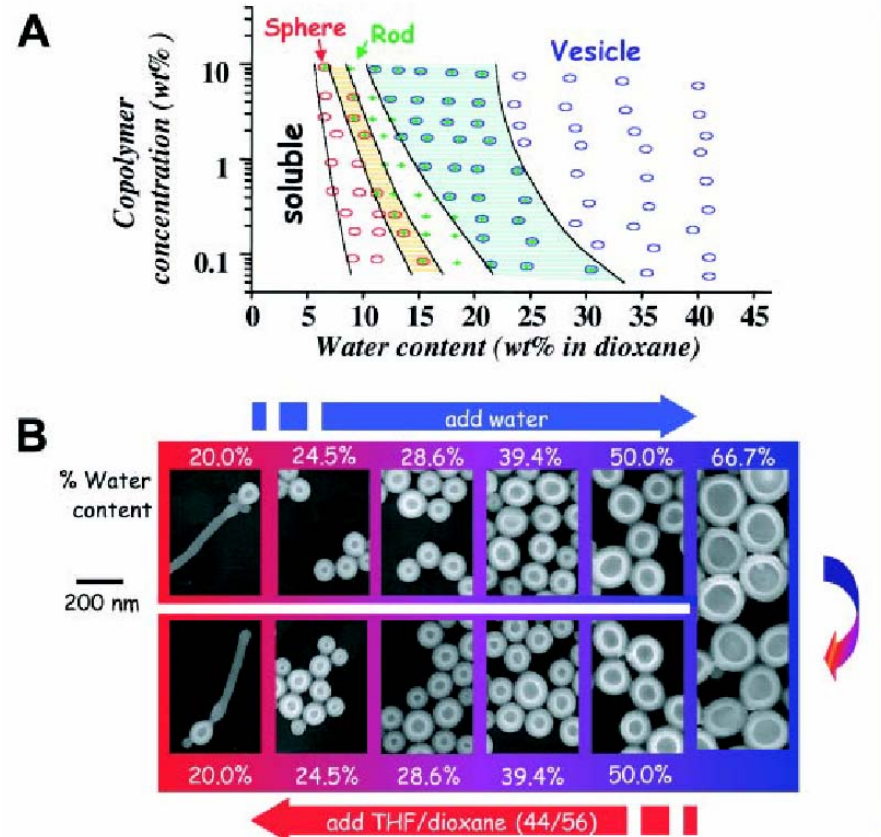


**Vesicles:** Self-directed assembly of lipids to form sacs that enclose a volume with a molecularly thin membrane

**Fig. 1.** Schematic of a vesicle and related micellar aggregates plus vesicle-forming lipid and diblock copolymers. (A) Vesicle with a section removed to reveal the membrane thickness  $d$ , schematically represented by the dark gray regions for (a) a phosphatidylcholine lipid as a typical, natural liposome former; (b) a diblock copolymer of polyacrylic acid-polystyrene (PAA-PS), which precipitates as a vesicle when water is added to solvent (24); (c) PS-poly(isocyanoo-L-alanine-L-alanine), which makes vesicles in coexistence with rods under acidic conditions (30); and (d) a molecular weight series of nonionic polyethyleneoxide-polybutadiene (PEO-PBD), which makes robust vesicles in pure aqueous solutions (31–38). In these physical representations of amphiphile structure, gray is hydrocarbon, red is oxygen, blue is nitrogen, and yellow is phosphorus. Detailed chemical structures are given in the references; note that the numbers of monomer units indicated for the block copolymers are just average numbers. As sketched in cross section, a vesicle membrane can be a bilayer with a well-defined midplane, as is typical of phospholipid membranes, or it can be a more interdigitated structure. Polydispersity in molecular size that is intrinsic to polymer amphiphiles would tend to give a more intermediate membrane structure. (B and C) A worm- or rod-like micelle and a spherical micelle, respectively, formed from block copolymers and related amphiphiles.

# Synthesis of Nano Materials-0D from liquid (Polymer)

## □ Vesicles Transformations

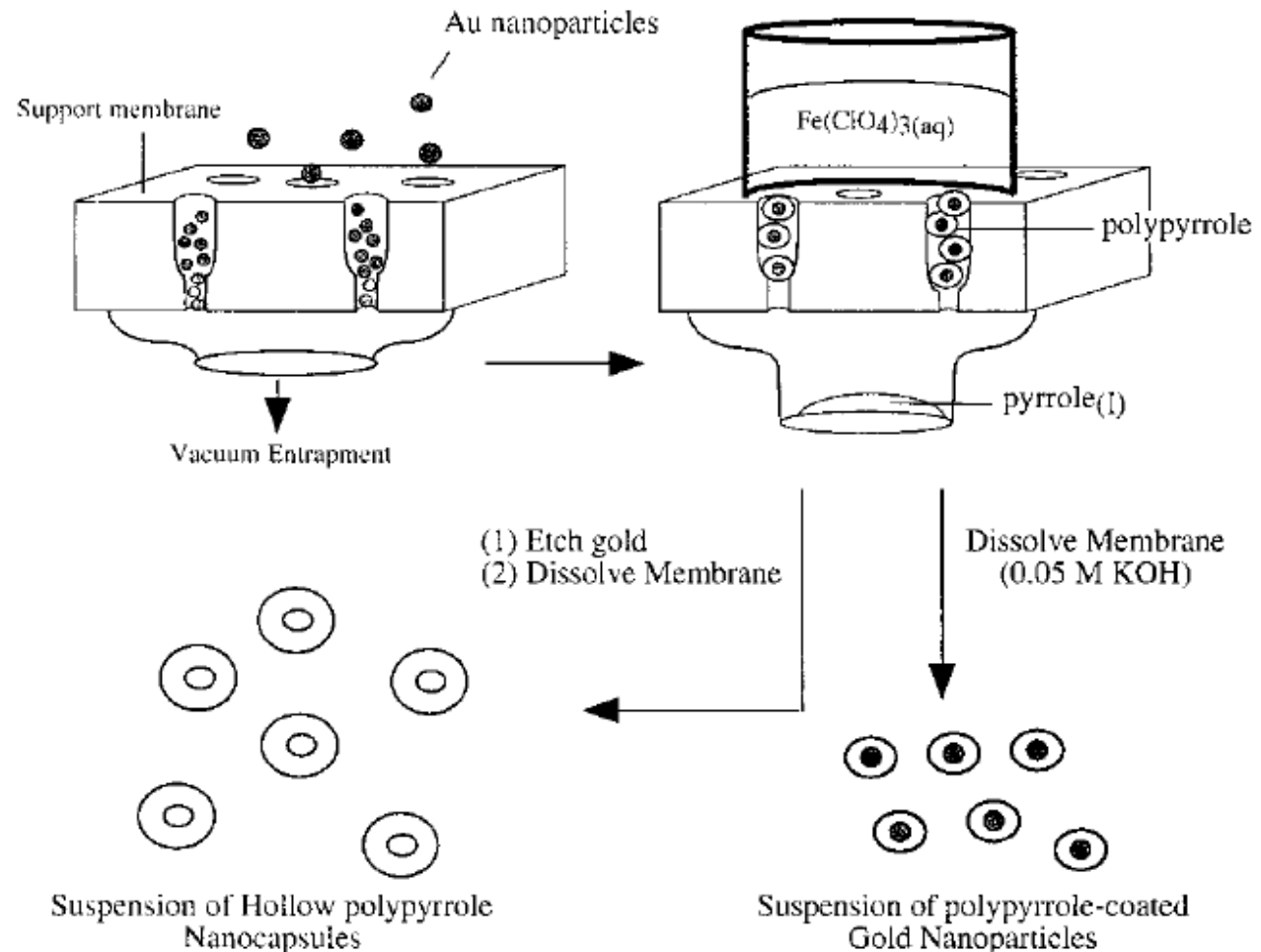
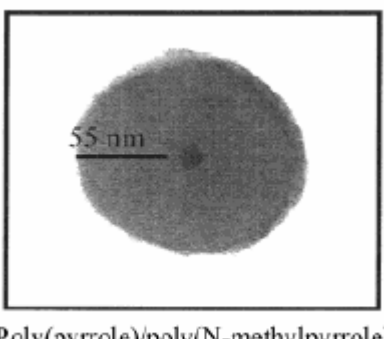
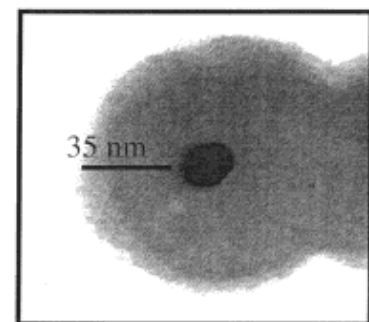


$\text{PS}_{310}\text{-PAA}_{52}$  in a mixture of dioxane and water

**Fig. 2.** Morphological phases and vesicle transformations in dilute solutions. (A) Phase diagram of  $\text{PS}_{310}\text{-PAA}_{52}$  in dioxane plus water; the full ternary phase diagram with separate water, dioxane, and copolymer axes looks similar (24). The colored regions between sphere and rod phases and between rod and vesicle phases correspond to coexistence regions. (B) Reversibility of the vesicle formation and growth process for  $\text{PS}_{300}\text{-PAA}_{44}$  (28), presumably based in part on fusion and fission processes illustrated in (C).

# Synthesis of Nano Materials-0D from liquid (Polymer)

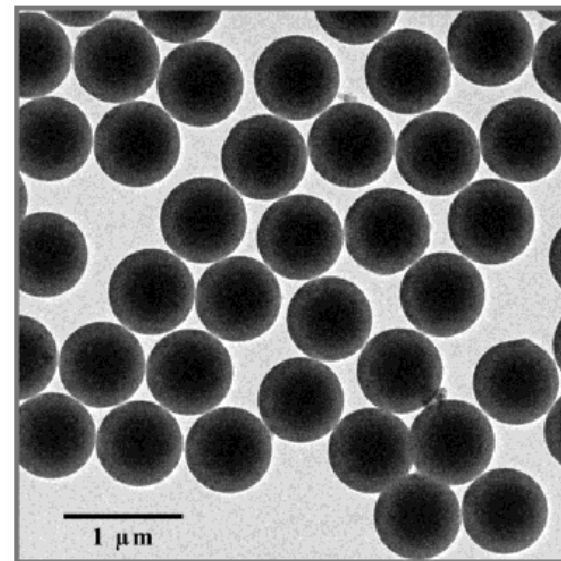
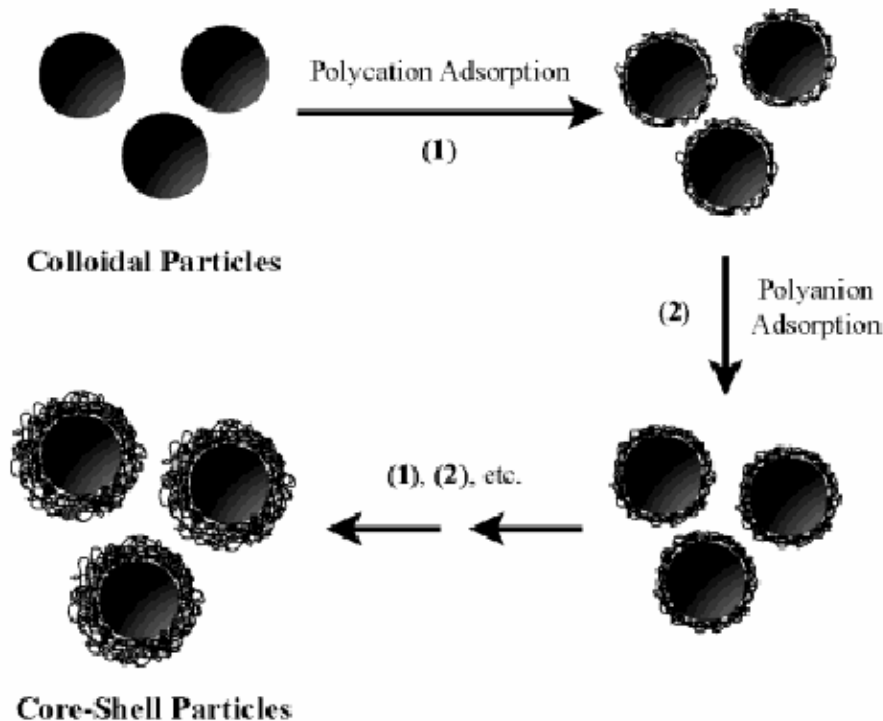
## □ Polymer coating - membrane-based



## Synthesis of Nano Materials-0D from liquid (Polymer)

### □ Polymer coating

- layer by layer process- polyelectrolyte, electrostatic interaction



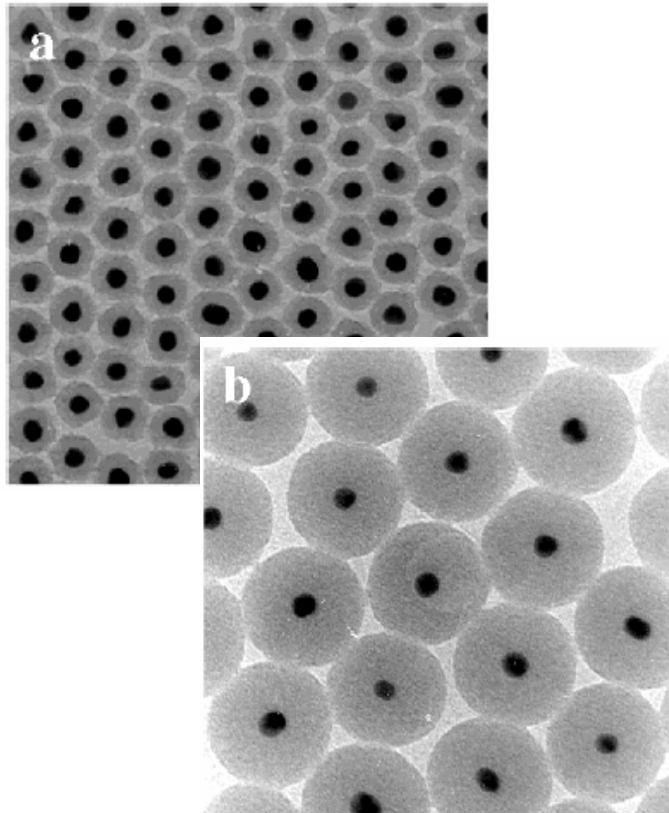
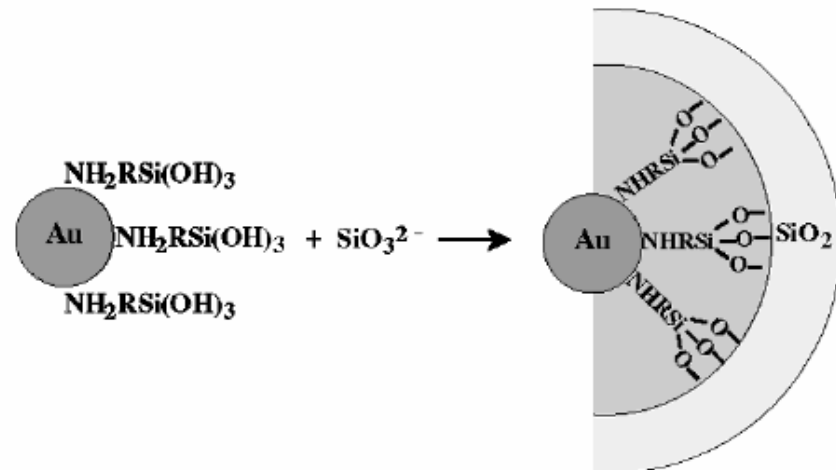
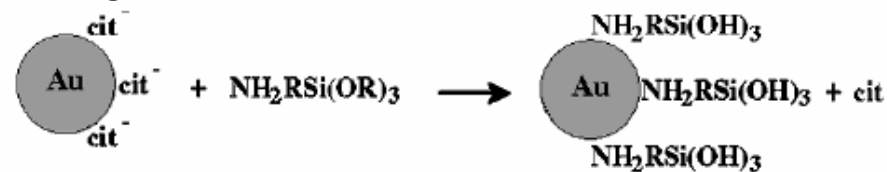
640 nm/ 34 nm/710 nm

Polystyrene (negatively charged) coated with 21 alternating layers of poly(allylamine hydrochloride) (PAH) and poly(styrenesulfonate) (PSS)

# Synthesis of Nano Materials-0D from liquid (Polymer)

## □ Polymer coating

- sol-gel

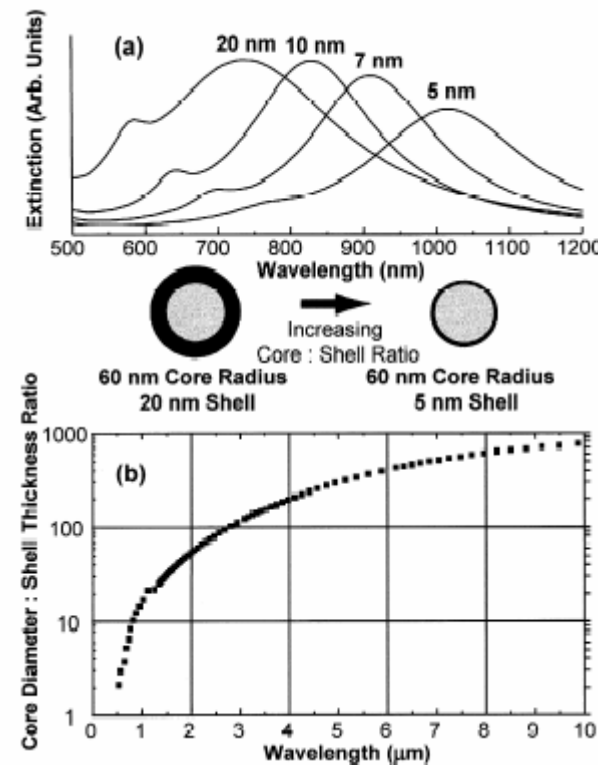
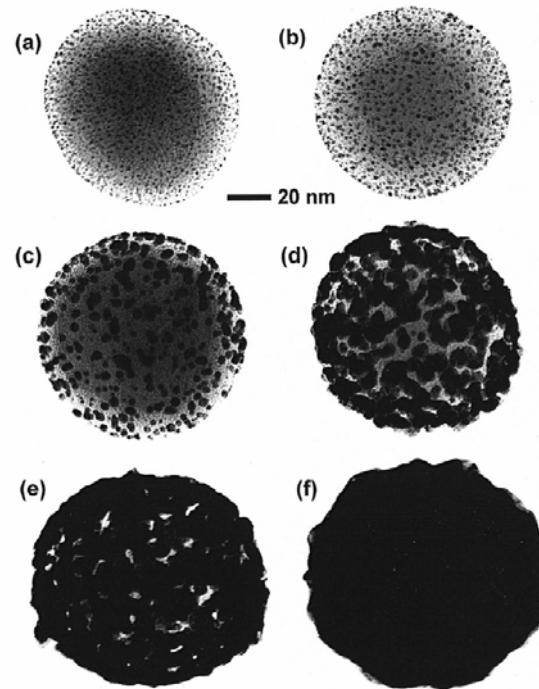


Scheme 3. Schematic diagram of the surface reactions occurring in the process of forming a thin silica shell on citrate-stabilized gold particles. The first step involves reaction with (3-aminopropyl)trimethoxysilane, thereby making the gold surface vitreophilic. Secondly, sodium silicate solution (pH 10–11) is added and the silica polymerizes onto the gold particle surface.

# Synthesis of Nano Materials-0D from liquid (Polymer)

## □ Polymer coating

- self-assembly and chemical reduction

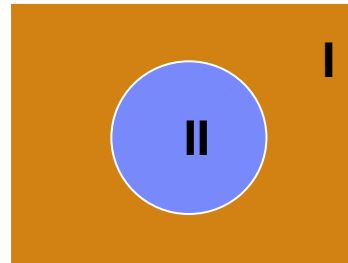


- Au nanoshell growth on 120 nm diameter silica nanoparticle  
1-2 nm diameter gold colloids onto 3-aminopropyltriethoxysilane-modified silica  
chloroauric acid+potassium carbonate/sodium borohydride

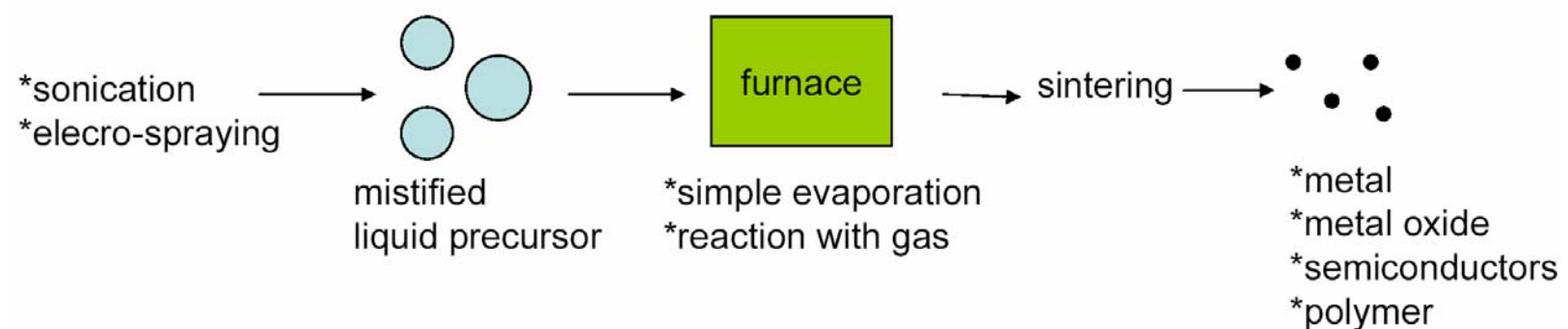
# Synthesis of Nanoparticles – 0D Kinetic Confinement

## □ Kinetically Confined Synthesis

- i) liquid droplets in gas phase including aerosol synthesis and spray pyrolysis
- ii) liquid droplets in liquid such as micelle and microemulsion synthesis
- iii) template-based synthesis
- iv) self-terminating



- i) Vapor (I) & Liquid (II): aerosol synthesis, spray pyrolysis



# Synthesis of Nanoparticles – 0D Kinetic Confinement

## □ Kinetically Confined Synthesis

i) ex)  $\text{TiO}_2$

Ti alkoxide (ethoxide, isopropoxide),  $\text{TiCl}_4$

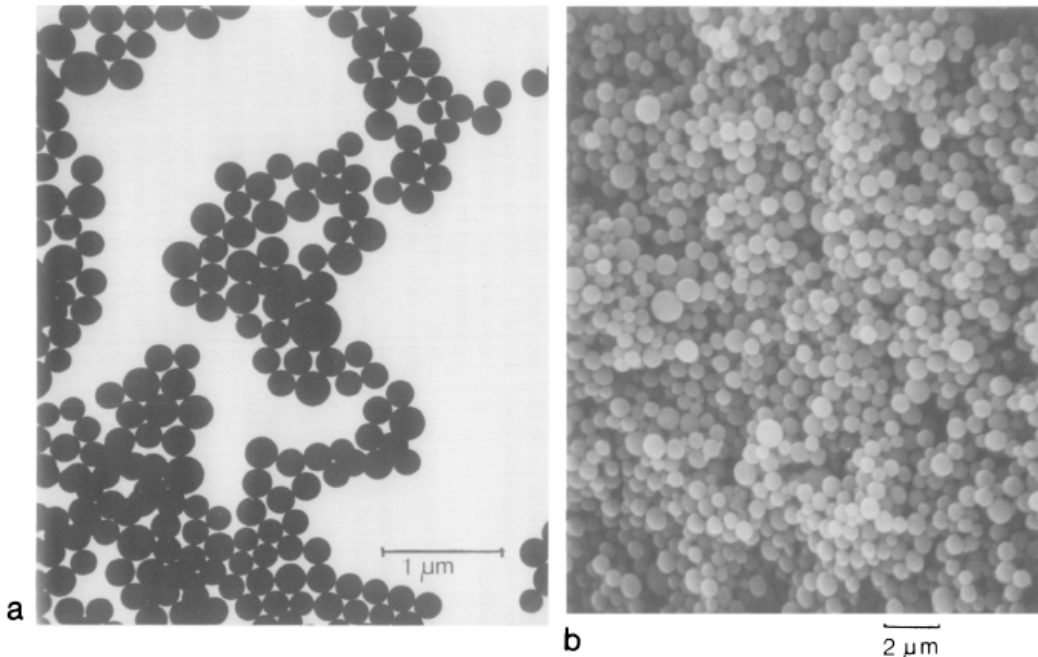


FIG. 3. (a) Transmission electron micrograph of titanium dioxide particles prepared by hydrolysis of an aerosol of titanium(IV) ethoxide. Helium flow rate, 800 ml/min; generator temperature, 96.5°C; nuclei oven temperature, 620°C. (b) Scanning electron micrograph of titanium dioxide particles prepared by hydrolysis of an aerosol of titanium(IV) isopropoxide. Nitrogen flow rate, 500 ml/min; generator temperature, 58.5°C; nuclei oven temperature, 620°C.

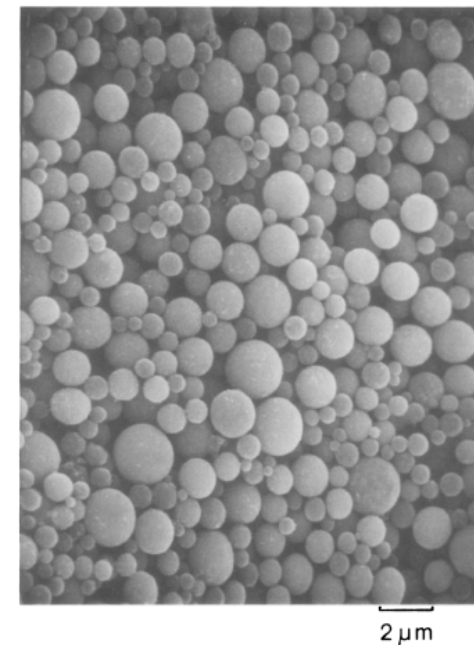
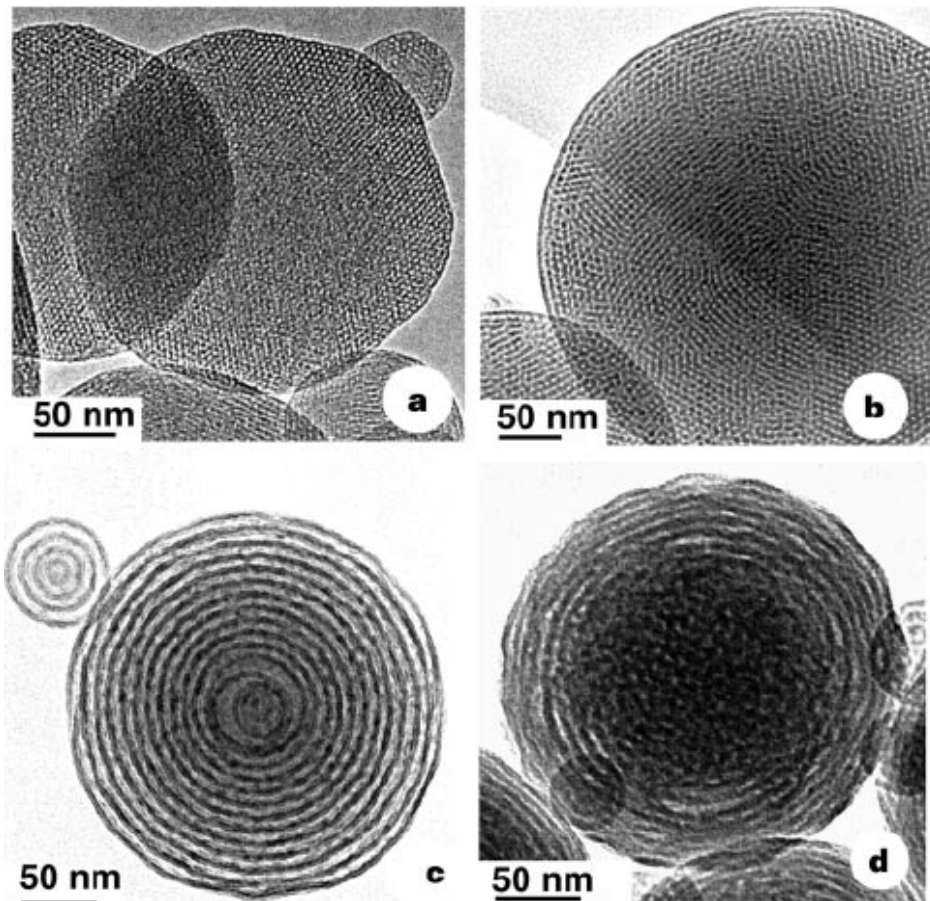
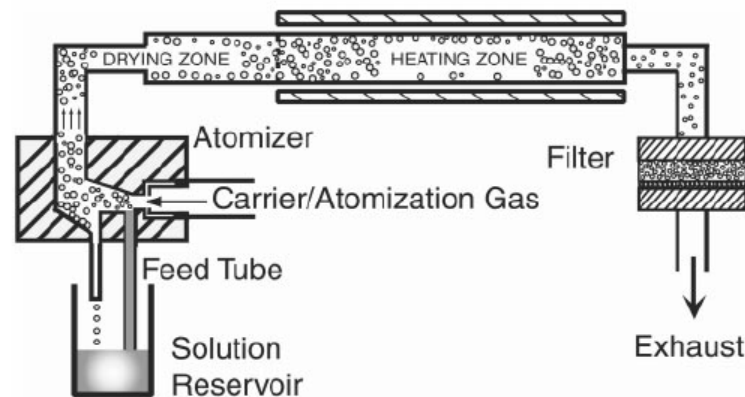


FIG. 6. Scanning electron micrograph of titanium dioxide particles prepared by hydrolysis of a  $\text{TiCl}_4$  aerosol. Nitrogen flow rate 90 ml/min; generator temperature 25°C.

# Synthesis of Nanoparticles – 0D Kinetic Confinement

## □ Kinetically Confined Synthesis

i) ex2) aerosol-assisted self-assemble of mesostructured spherical nanoparticle  $\text{SiO}_2$

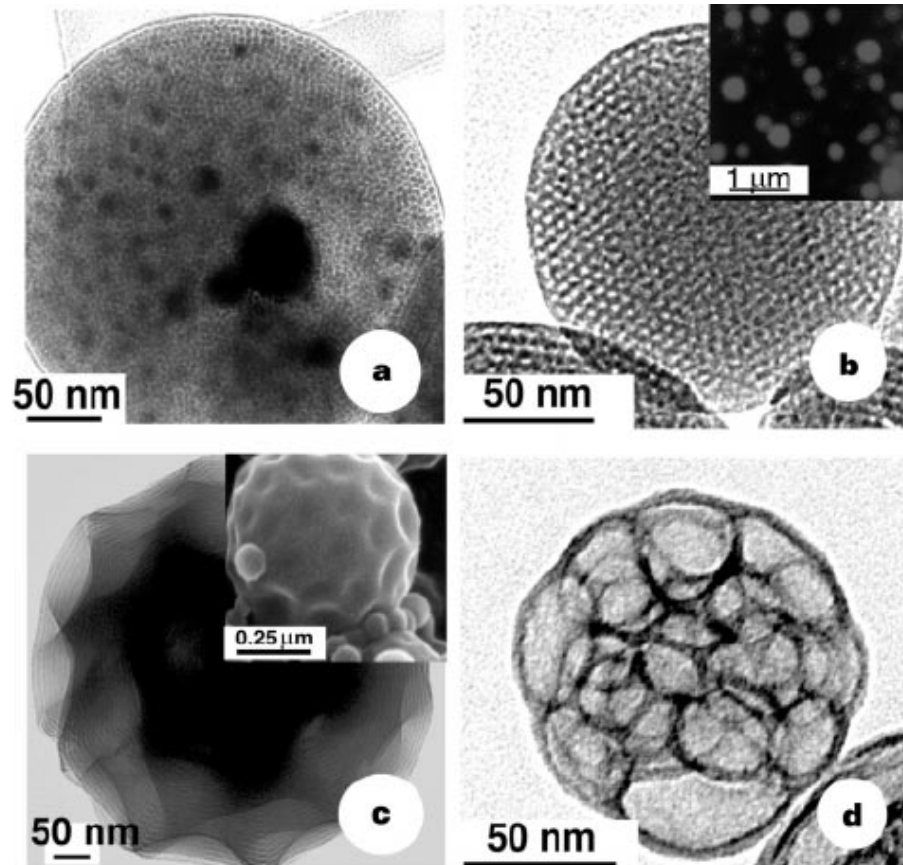


TEOS:EtOH:water:HCl:surfactant  
CTAB (a)  
Brij-56 (b)  
P123 (c)  
Brij-57 (d)

# Synthesis of Nanoparticles – 0D Kinetic Confinement

## □ Kinetically Confined Synthesis

i) ex2) aerosol-assisted self-assemble of mesostructured spherical nanoparticle  $\text{SiO}_2$

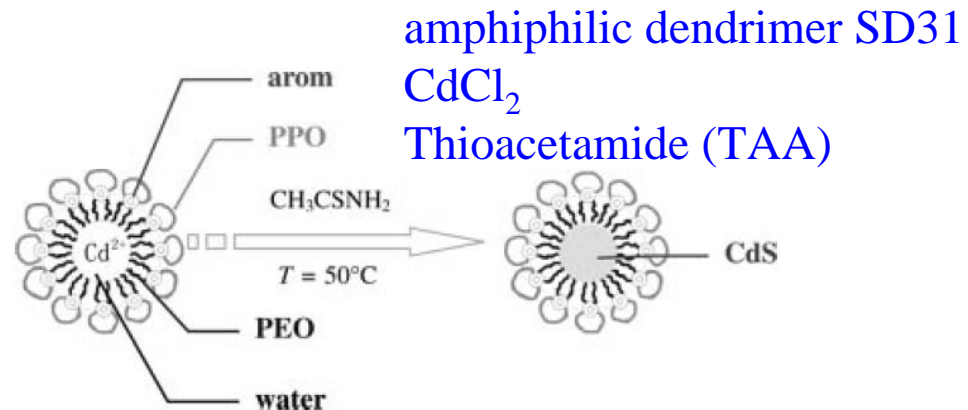


- (a) silica/gold nanocomposite
- (b) Silica/rhodamine B
- (c) Silica/polymer
- (d) Silica/polymer

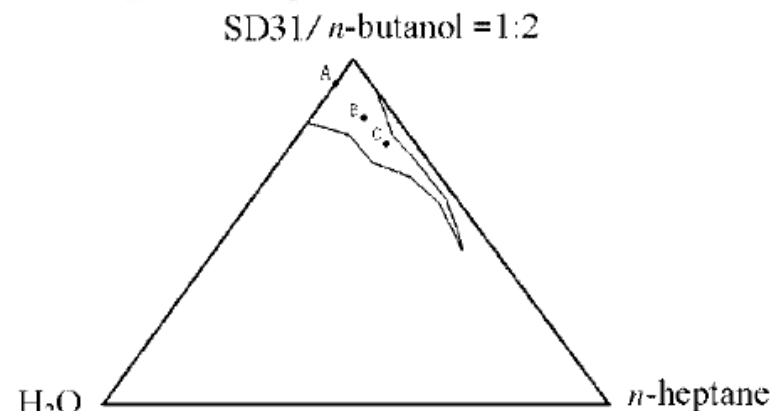
# Synthesis of Nanoparticles – 0D Kinetic Confinement

## □ Kinetically Confined Synthesis

- ii) Liquid (I) & Liquid (II): micelles, microemulsions, inverse microemulsion  
 ex) ZnS in inverse microemulsion



Scheme 1. Proposed mechanism for the formation of monodisperse CdS nanospheres; PEO = poly(ethylene oxide), PPO = poly(propylene oxide), arom = bisphenol A.<sup>[48]</sup>



spherical  
 size  $\uparrow$  w  $\uparrow$

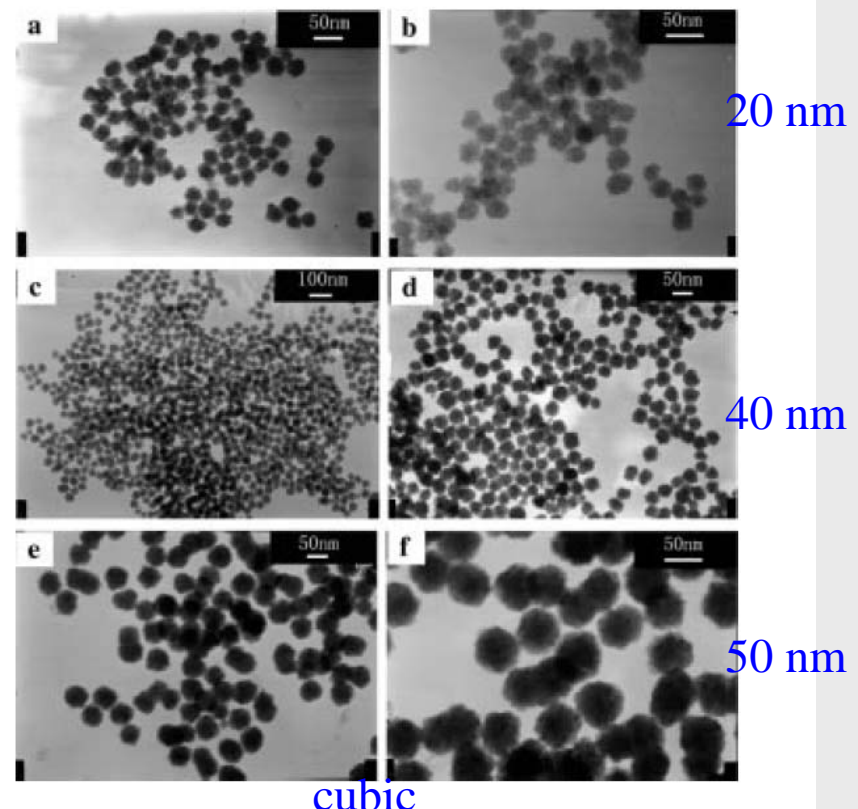
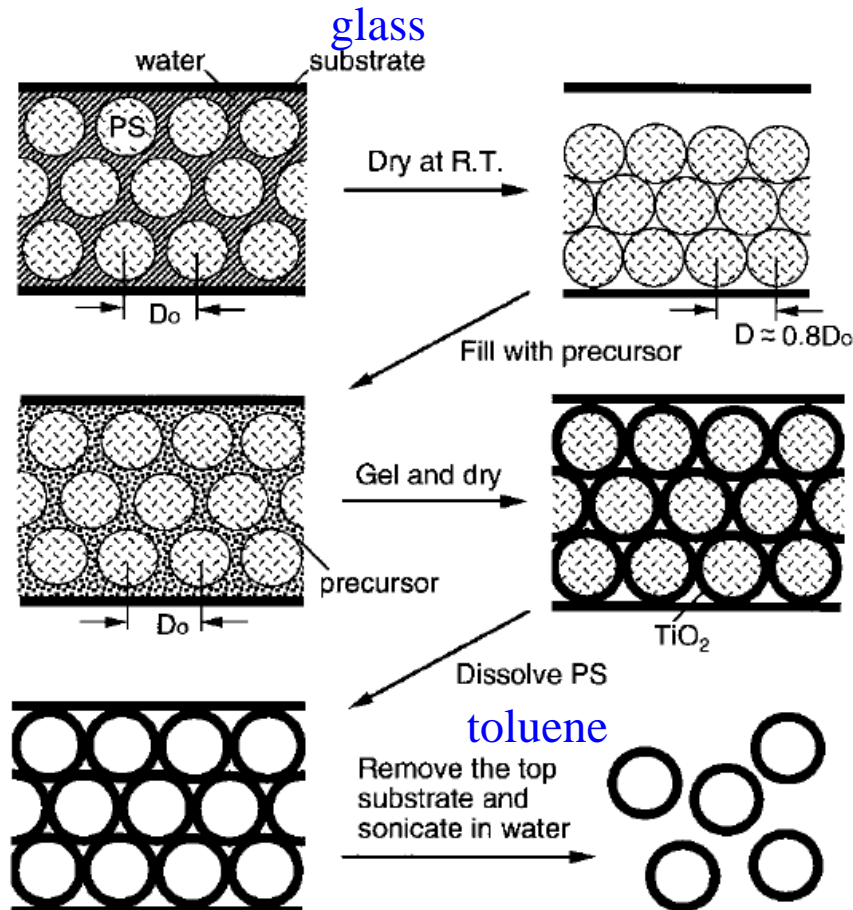


Figure 1. TEM images of CdS spheres obtained in three microemulsions with different [water]/[dendrimer] mass ratios ( $\omega$ ): (a and b) products from microemulsion A ( $\omega = 0.19$ ); (c and d) products from microemulsion B ( $\omega = 0.21$ ); (e and f) products from microemulsion C ( $\omega = 0.24$ ). F. Wang, Eur. J. Inorg. Chem. 109 (2006).

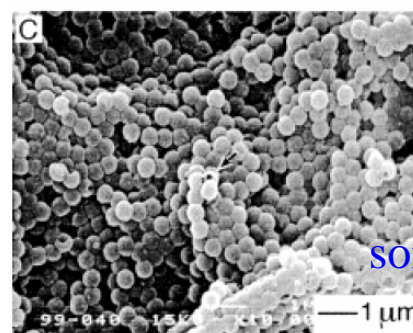
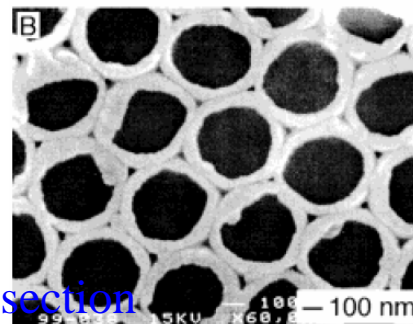
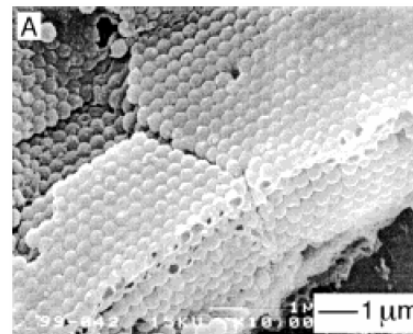
# Synthesis of Nanoparticles – 0D Kinetic Confinement

## □ Kinetically Confined Synthesis

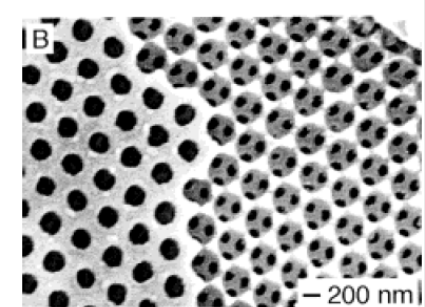
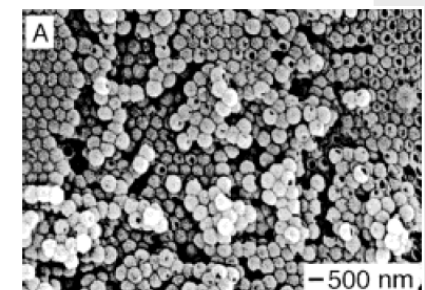
### iii) Template-based synthesis



TiO<sub>2</sub> Ti isopropoxide



tetraisopropyl  
tin isopropylalanol  
SnO<sub>2</sub>



SiO<sub>2</sub>  
sonication tetraethyl  
orthosilicate

Fig. 1. Schematic outline of the experimental procedure. A cross-section view of the cell is shown here.

Z. Zhong, Adv. Mater. 12 26 (2000).

# Synthesis of Nanoparticles – 0D Kinetic Confinement

## □ Kinetically Confined Synthesis

### iv) Growth Termination

Ex) ZnS

cadmium acetate dissolved in methanol,  $[Cd]=0.1\text{ M}$

sodium sulfide in water and methanol (1:1),  $[S^{2-}]=0.1\text{M}$

thiophenol in methanol,  $[PhSH]=0.2\text{ M}$

- increase of amount of capping molecules reduces particle size

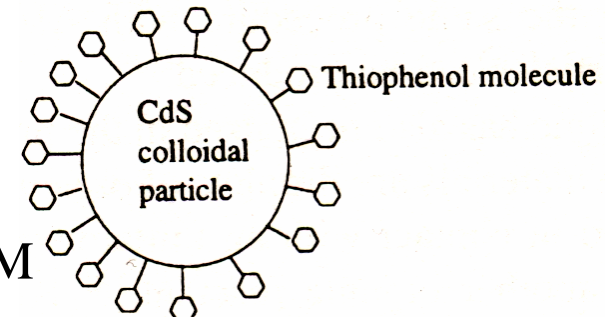


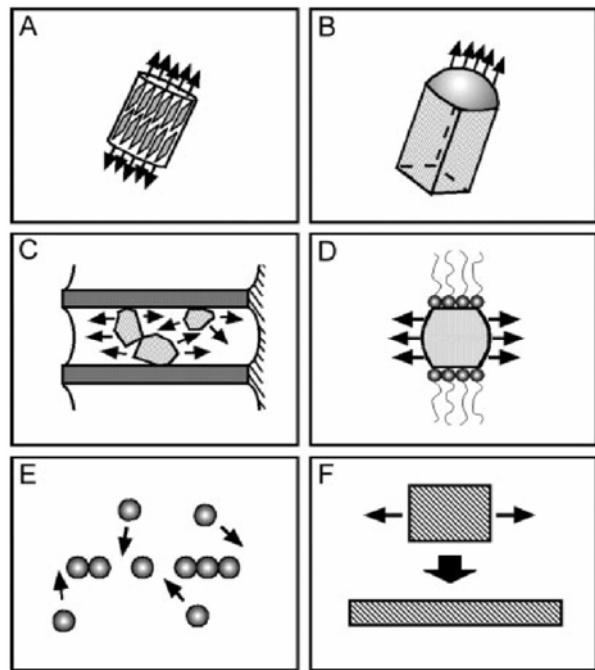
**Table I.** Analytical Results for CdS/SPh Clusters Isolated as Powders

S/SPh used	Cd, %	S, %	C, %	H, %	empirical formula	Cd:S:C <sub>6</sub> H <sub>5</sub>	S/SPh calc	X-ray diam, Å
0.33 <sup>a</sup>	39.25	20.02	38.62	2.60	CdS <sub>0.26</sub> (SPh) <sub>1.48</sub> (HSPh) <sub>0.06</sub>	1:1.80:1.54	0.17	<15
0.5 <sup>a</sup>	42.29	9.90	35.53	2.52	CdS <sub>0.34</sub> (SPh) <sub>1.31</sub> (HSPh) <sub>0.00</sub>	1:1.65:1.31	0.26	<15
0.75 <sup>a</sup>	47.68	20.40	29.31	2.19	CdS <sub>0.54</sub> (SPh) <sub>0.92</sub> (HSPh) <sub>0.04</sub>	1:1.50:0.96	0.56	~20
1.17 <sup>a</sup>	58.92	21.23	18.06	1.43	CdS <sub>0.78</sub> (SPh) <sub>0.44</sub> (HSPh) <sub>0.04</sub>	1:1.26:0.48	1.62	~25
2.0 <sup>a</sup>	61.38	21.45	15.22	1.20	CdS <sub>0.84</sub> (SPh) <sub>0.32</sub> (HSPh) <sub>0.07</sub>	1:1.23:0.39	2.15	~30
4.5 <sup>a</sup>	66.45	22.18	9.68	0.85	CdS <sub>0.92</sub> (SPh) <sub>0.16</sub> (HSPh) <sub>0.09</sub>	1:1.17:0.25	3.70	~35
0.5 <sup>b</sup>	45.89	21.80	26.94	2.04	CdS <sub>0.75</sub> (SPh) <sub>0.50</sub> (HSPh) <sub>0.42</sub>	1:1.67:0.92	0.81	<15
0.75 <sup>b</sup>	50.65	23.03	24.04	1.97	CdS <sub>0.86</sub> (SPh) <sub>0.28</sub> (HSPh) <sub>0.46</sub>	1:1.60:0.74	1.16	~20

<sup>a</sup> Materials prepared in methanol solvent. <sup>b</sup> Materials prepared in mixed solvent with acetonitrile.

# Synthesis of Nano Materials-1D

## □ Strategies toward 1-D Nanostructures

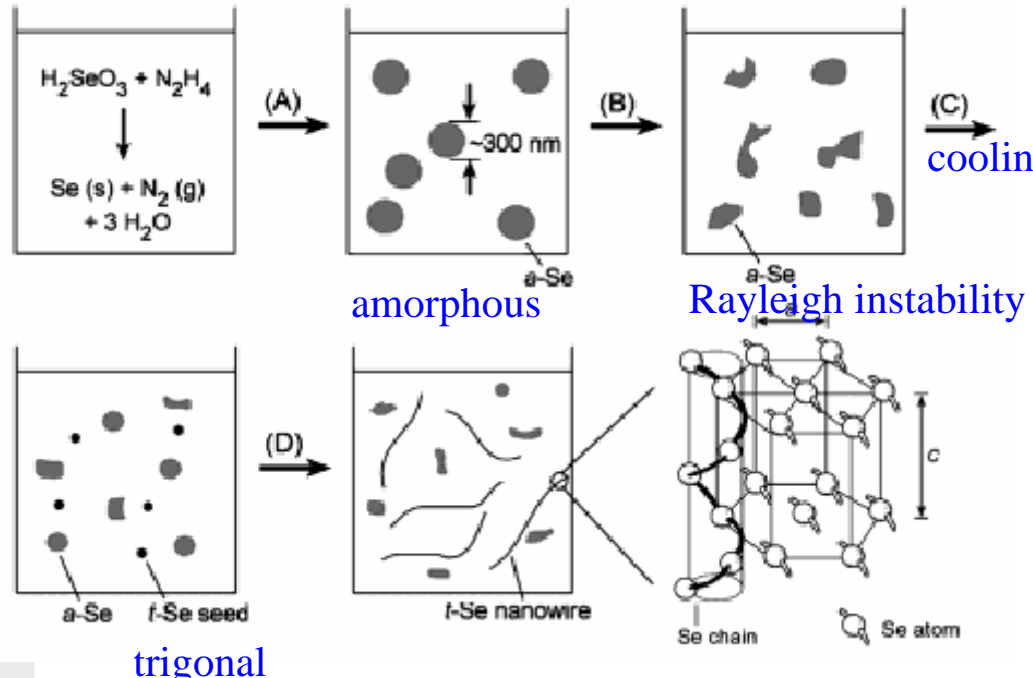
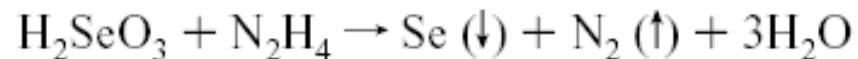


- A. Spontaneous Anisotropic Crystal Structures (homogeneous)
- B. Seed-initiated growth (heterogeneous)
- C. Templating (filling)
- D. Kinetic control by organic surfactants (homogeneous)
- E. Self-assembly
- F. Size reduction
- G. Templating (coating)
- H. Transforming via chemical reaction
- I. Electrospinning

# Synthesis of Nano Materials-1D from liquid

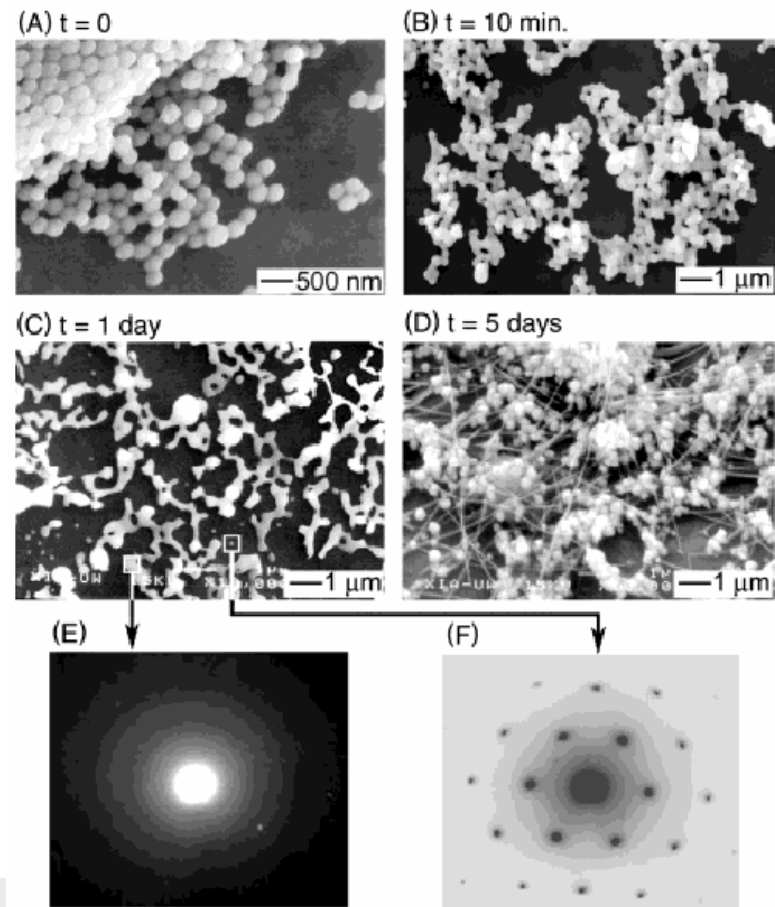
## □ Dissolution and Condensation (Intrinsically Anisotropic)

- Chalcogens (Se, Te): polymeric, helical crystal structure
- ex) Se



63 Nanomaterials

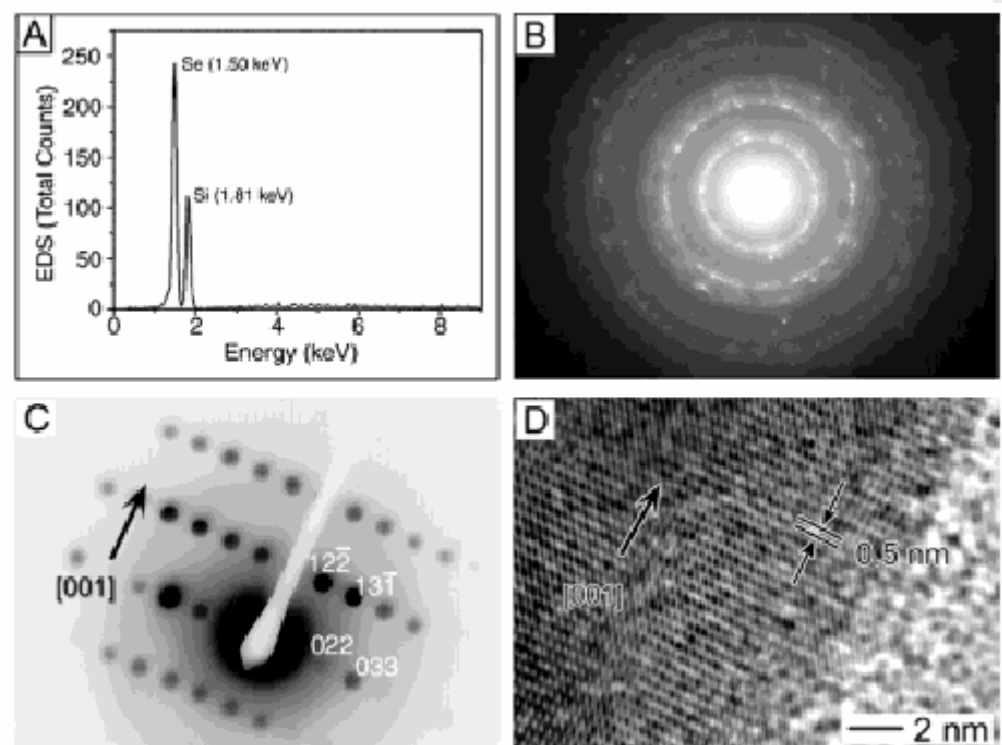
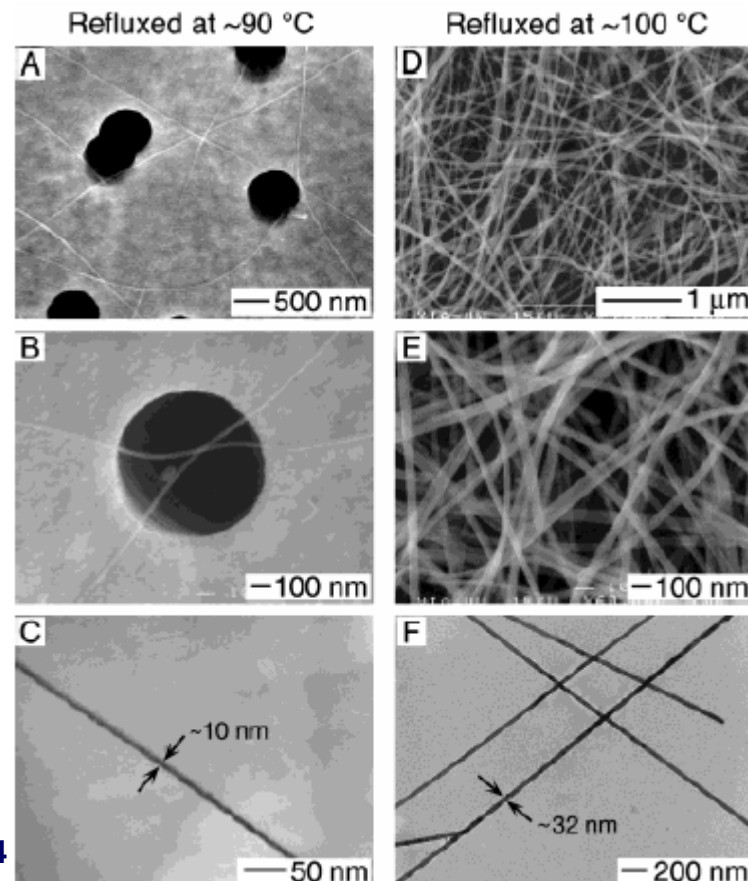
B.Gate, Adv. Funct. Mater. 12 (2002) 219.



# Synthesis of Nano Materials-1D from liquid

## □ Dissolution and Condensation (Intrinsically Anisotropic)

ex) Se

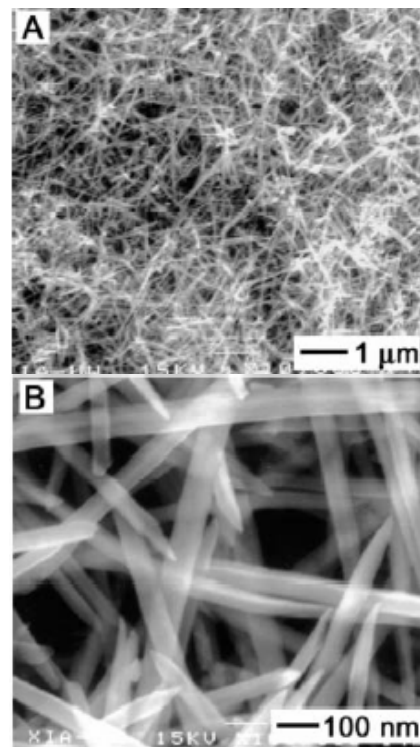
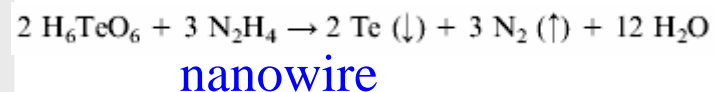


# Synthesis of Nano Materials-1D from liquid

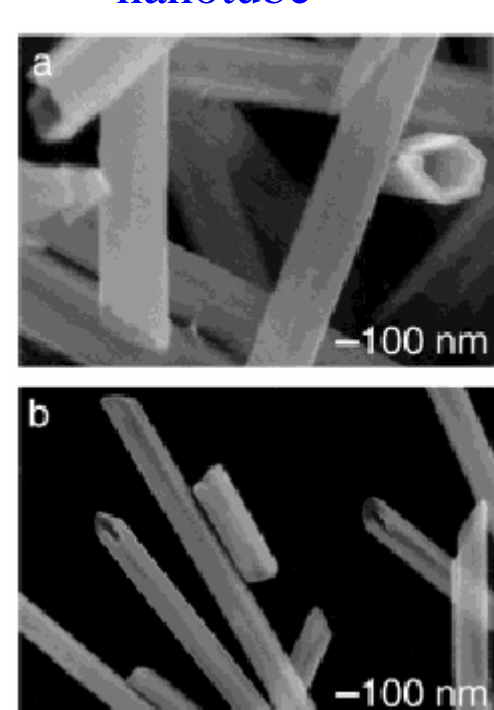
## □ Dissolution and Condensation (Intrinsically Anisotropic)

ex) Te

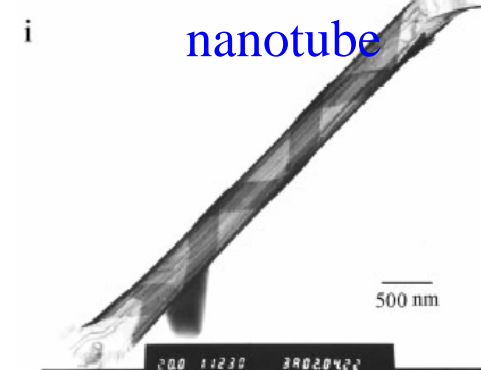
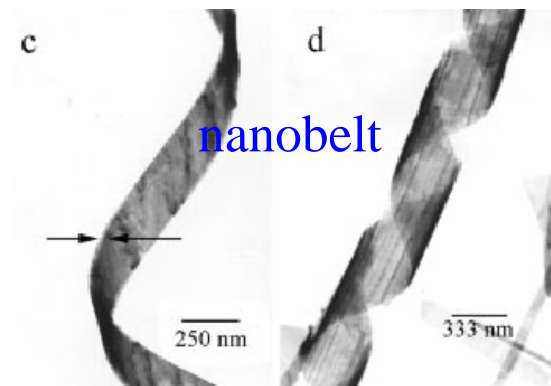
i) water



ii) ethylene glycol



iii) hydrothermal

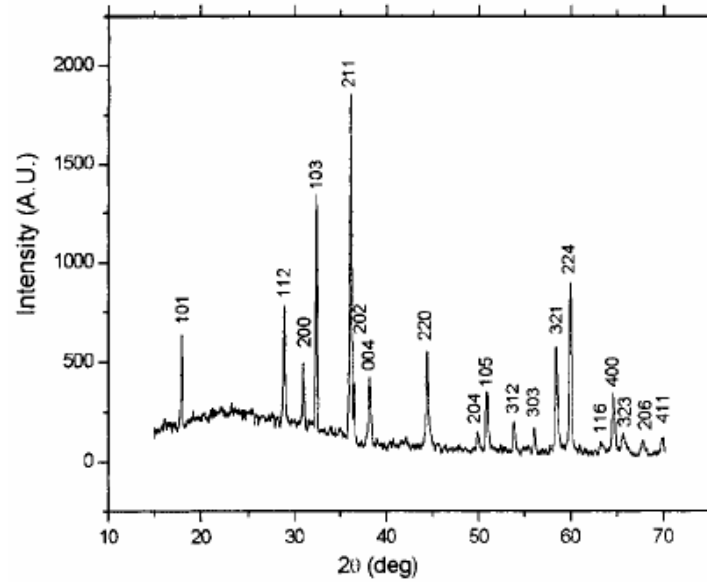


# Synthesis of Nano Materials-1D from liquid

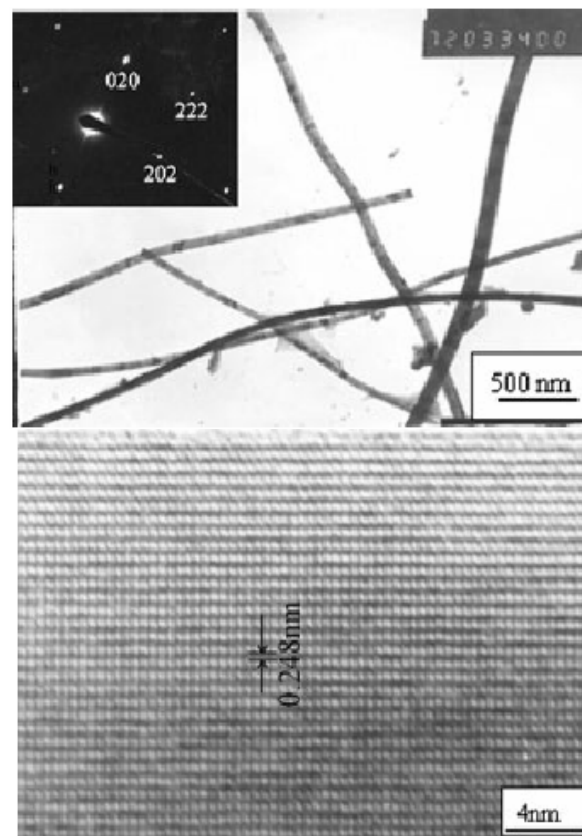
## □ Dissolution and Condensation (Flux)

ex)  $\text{Mn}_3\text{O}_4$

- $\text{MnCl}_2 + \text{Na}_2\text{CO}_3 + \text{NaCl}$  (flux) + nonyphenyl ether (NP-9)
- heated to 850 °C
- cooling and washing



{211}

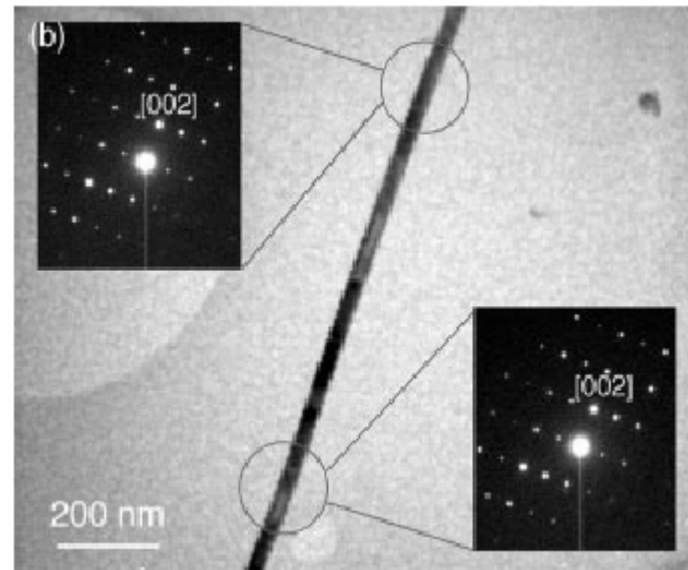
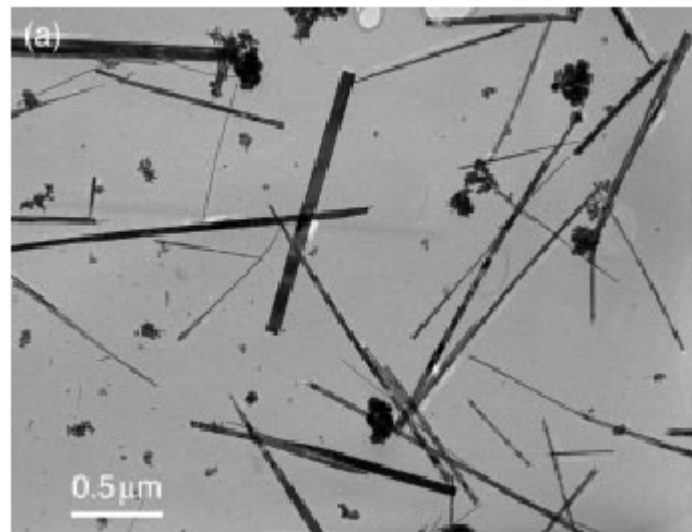


# Synthesis of Nano Materials-1D from liquid

## □ Dissolution and Condensation (Thermal Decomposition)

ex) BaTiO<sub>3</sub>

- an excess of 30% H<sub>2</sub>O<sub>2</sub> was added at 100°C to a heptadecane solution containing a 10:1 molar ratio of BaTi[OCH(CH<sub>3</sub>)<sub>2</sub>]<sub>6</sub> to oleic acid
- heated to 280 °C for 6 hrs

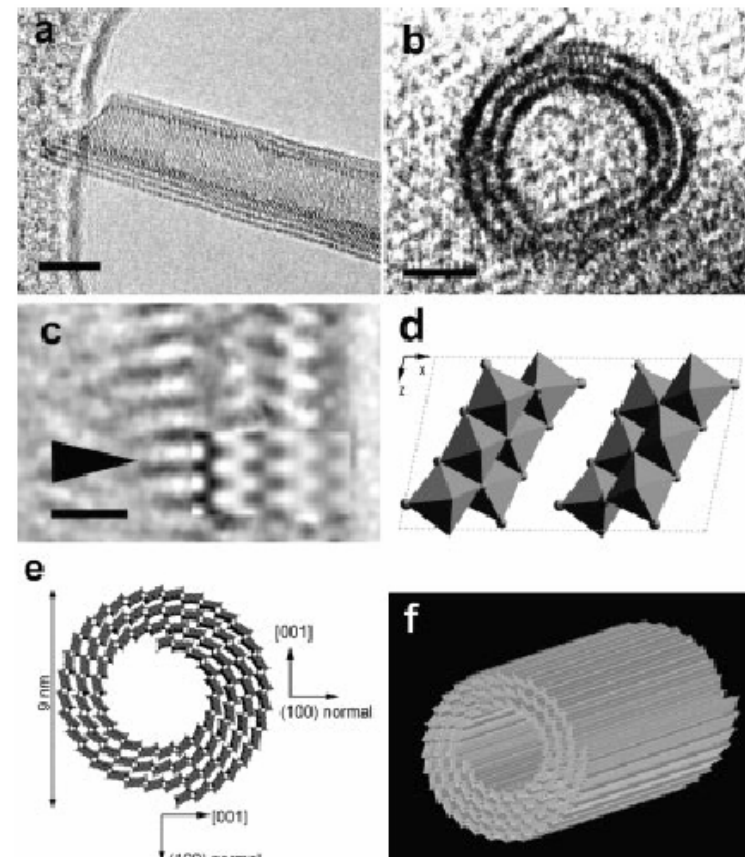
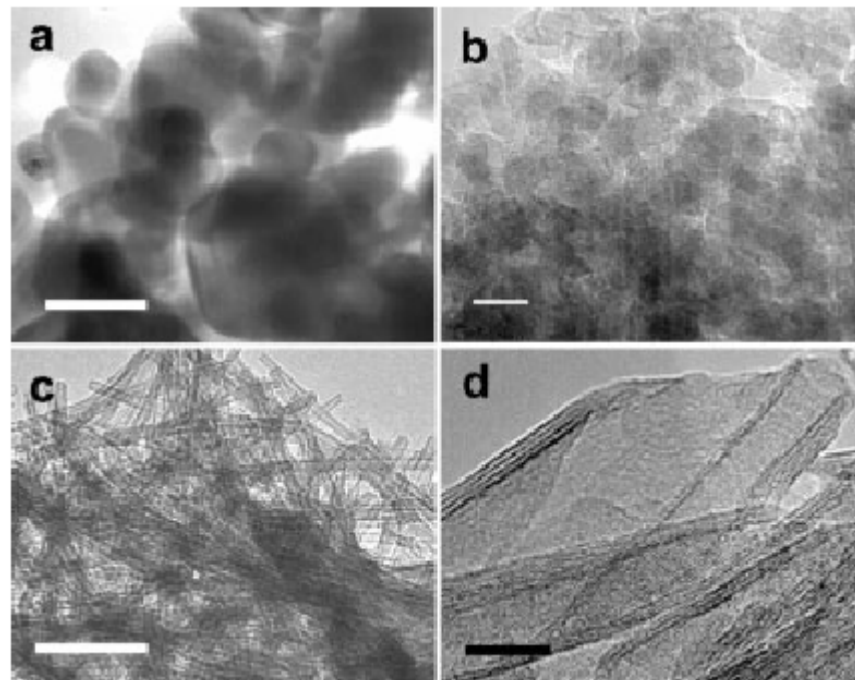


# Synthesis of Nano Materials-1D from liquid

## □ Dissolution and Condensation (Hydrothermal)

ex)  $\text{H}_2\text{Ti}_3\text{O}_7$  nanotube

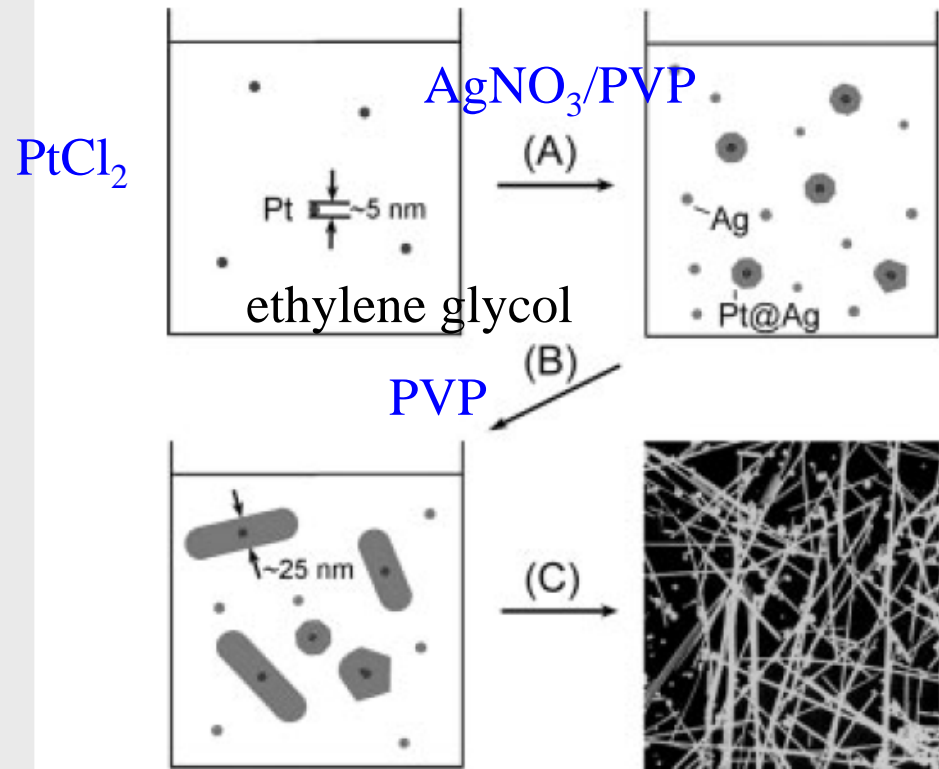
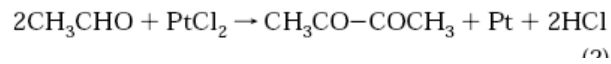
- Anatase  $\text{TiO}_2$  in 10 M NaOH → hydrothermal treatment at 130°C for 72 h



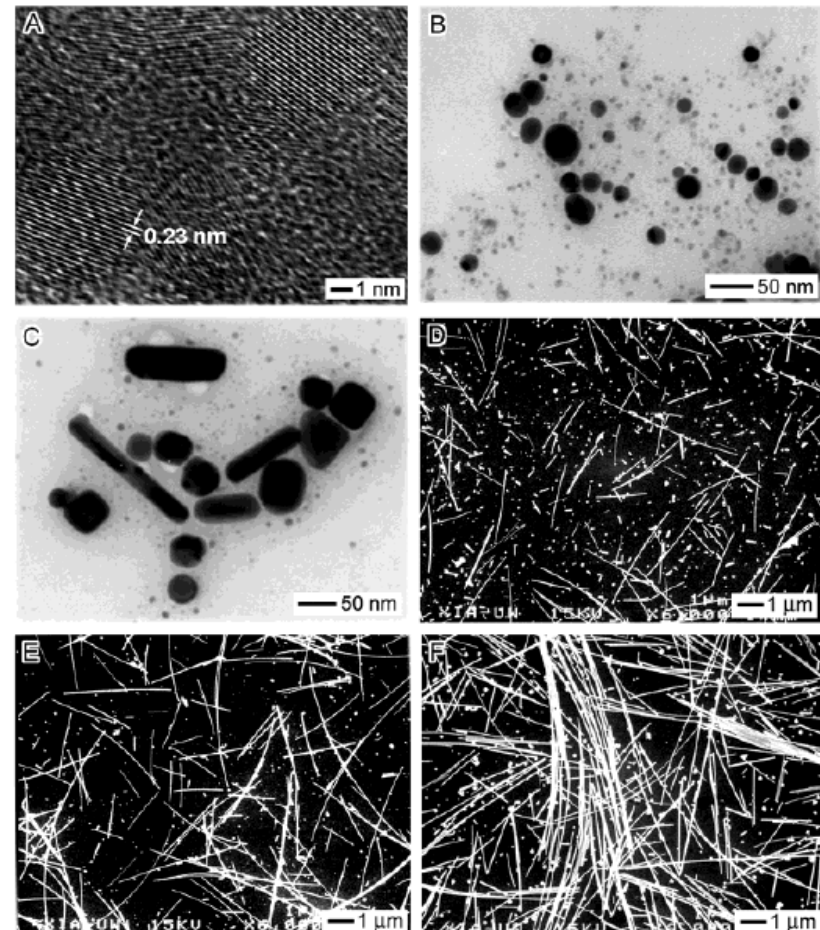
# Synthesis of Nano Materials-1D from liquid

## □ Dissolution and Condensation (Seeding, Capping agent)

ex) Ag nanowire



69 poly(vinyl pyrrolidone) (PVP,  $M_w \approx 55\,000$ )



# Synthesis of Nano Materials-1D from liquid

## □ Dissolution and Condensation (Seeding, Capping agent)

ex) Ag nanowire

